



從蛋白質微陣列晶片至單一分子奈米陣 列-應用於癌症篩檢

From Protein Micro Array to Protein Single Molecule Array-for early cancer detection

Prof. Fan-Gang Tseng

曾繁根 教授

**Engineering and System Science Dept./
Institute of NEMS**

National Tsing Hua University, Taiwan

國立清華大學 工科系/奈微所

Institute of Applied Science, Academia Sinica, Taiwan

中研院應科中心

03.27.2008



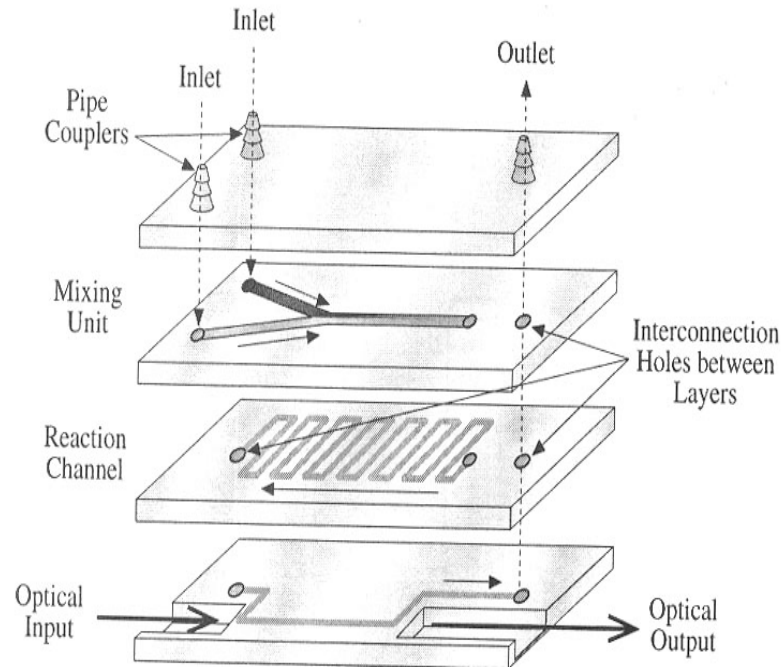
Outline

- Surface tension dominate Micro/
Nano Fluidic Systems
- 3-in-1 Protein Chip
 - Micro filling chip
 - Micro stamper chip
 - Micro bio-reaction chip
- Single Protein Molecule Array



微奈米流體系統 Micro/Nano fluidic systems

類比(連續)式微流體系統 Continuous Fluidic Systems



μ Transducers sourcebook, 98

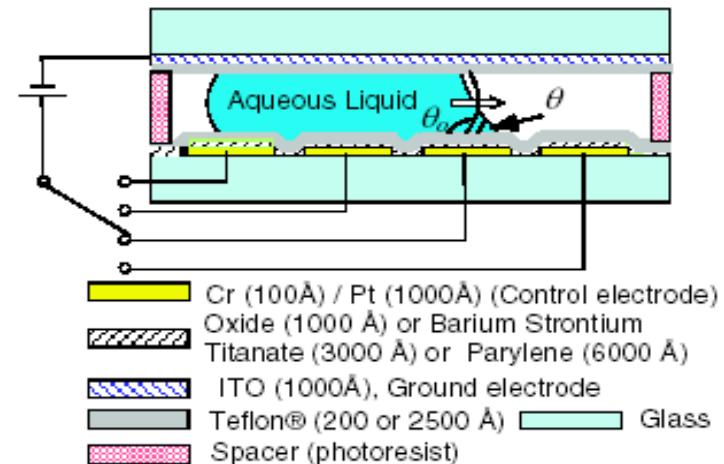
液珠控制系統 \Leftrightarrow 連續流體系統

1. 計量精確控制 (metering issue)
2. 較少因接觸所產生之摩擦阻力、表面反應、及氣泡阻塞問題 (surface tension, friction, surface interaction issues)
3. 較簡單之流體系統 (System integration)



μ -Nano Bio & fluidic Systems Lab

數位式微流體系統 Digital Fluidic Systems

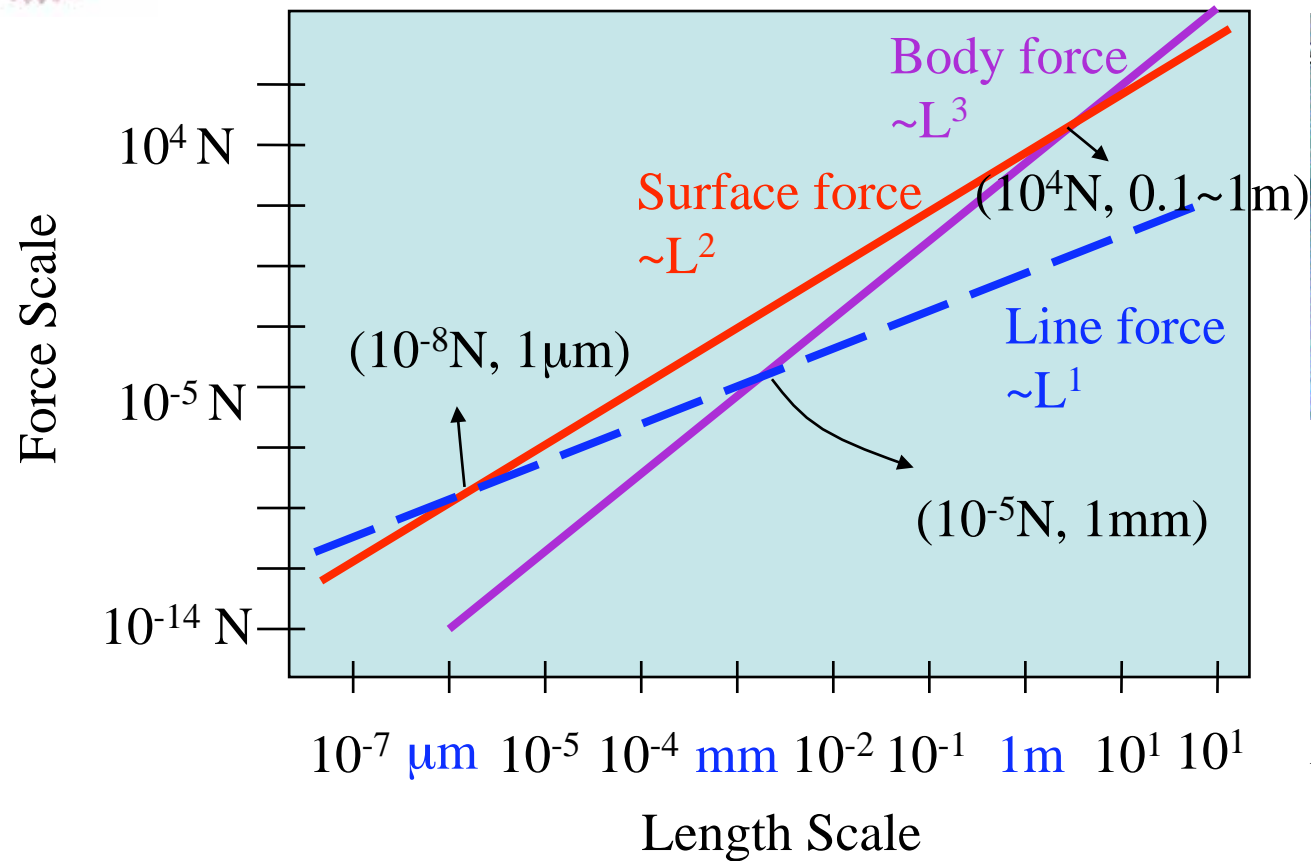


EWOD, CJ Kim, UCLA

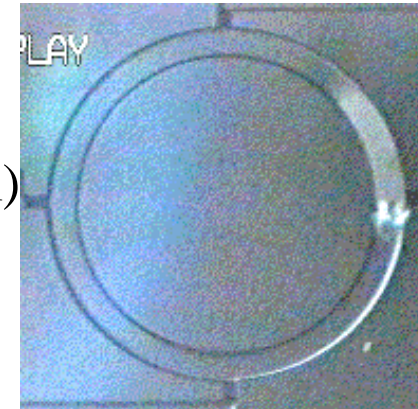
Prof. Fan-Gang Tseng



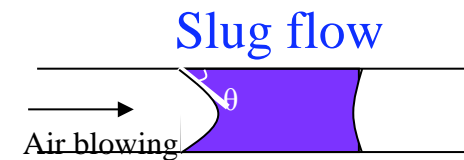
Introduction



Mercury motor



J. Lee, and C.-J. Kim,
J of MEMS, June 2000



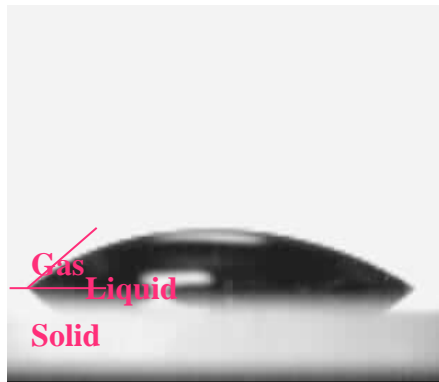
Surface tension force (line force) is dominate in nano scale and important in micro scale!!

F. Tseng, Nanomechanics 04, ACPOT'06



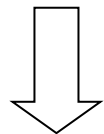
Role of Surface Tension in Micro/nano Scale

Line force/body force



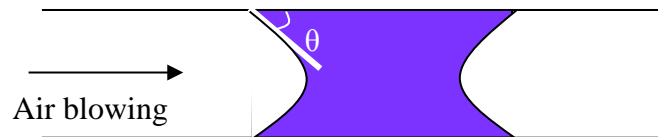
$$F_s = \sigma(\pi D) \sin \theta$$

$$F_b \sim \pi D^3$$



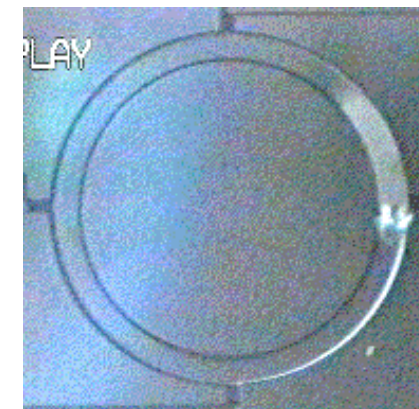
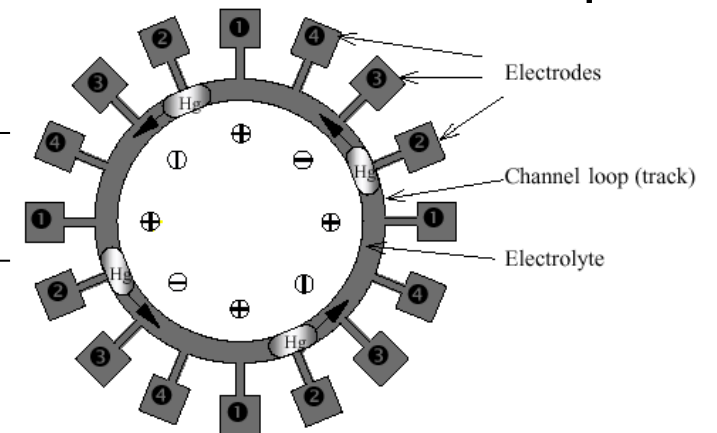
$$F_s/F_b = 1/D^2$$

Drug delivery or bio-sample transportation



1. Air blowing to provide clean actuation
2. Precise dosage control
3. Less distance limitation
4. Surface tension is one of the dominate forces
5. Dynamic contact angle between liquid and channel wall

Surface Tension Driven Hg slug



J. Lee, and C.-J. Kim,
J of MEMS, June 2000



數位微流體系統 (Digital Micro Fluidic Systems)

1. 液珠產生

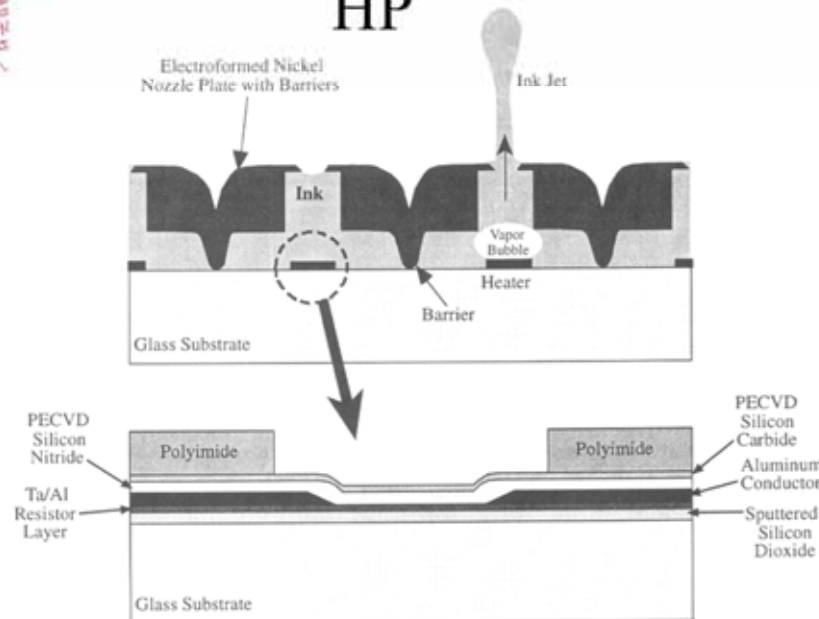
2. 液珠懸浮控制

3. 液珠平面控制

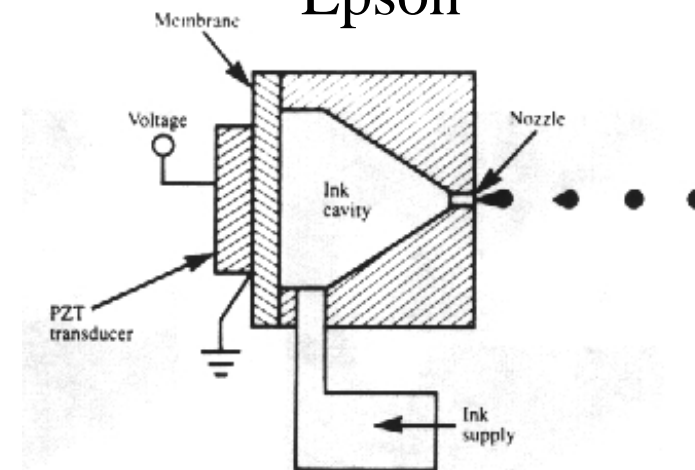


Droplet generators

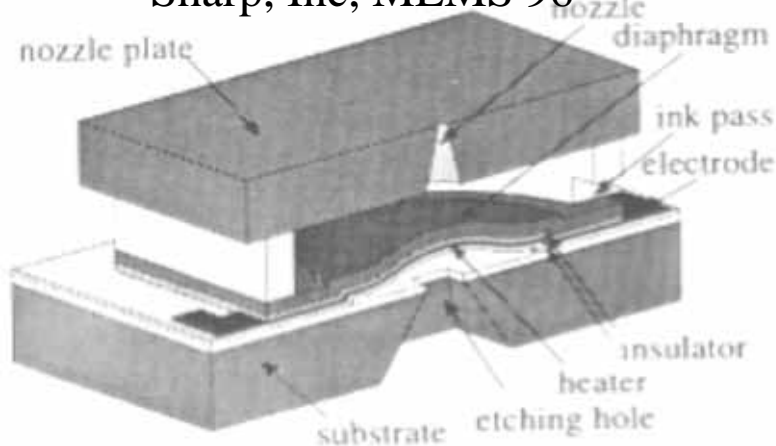
HP



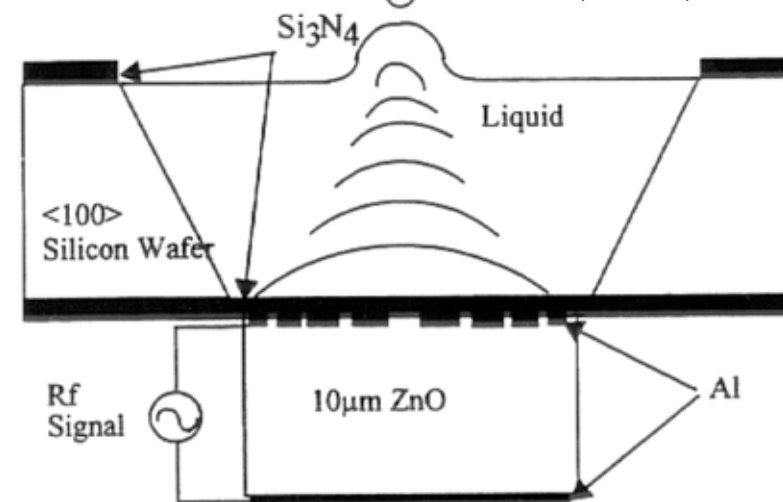
Epson



Sharp, Inc, MEMS 96



E.S. Kim, USC, MEMS98

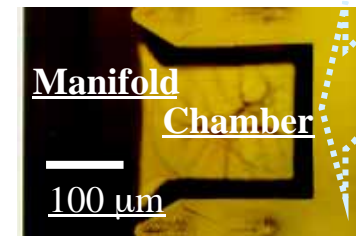
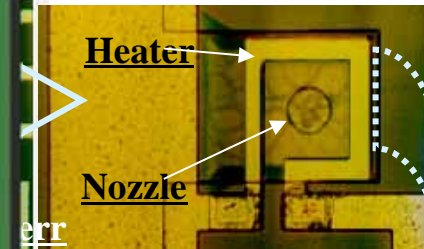
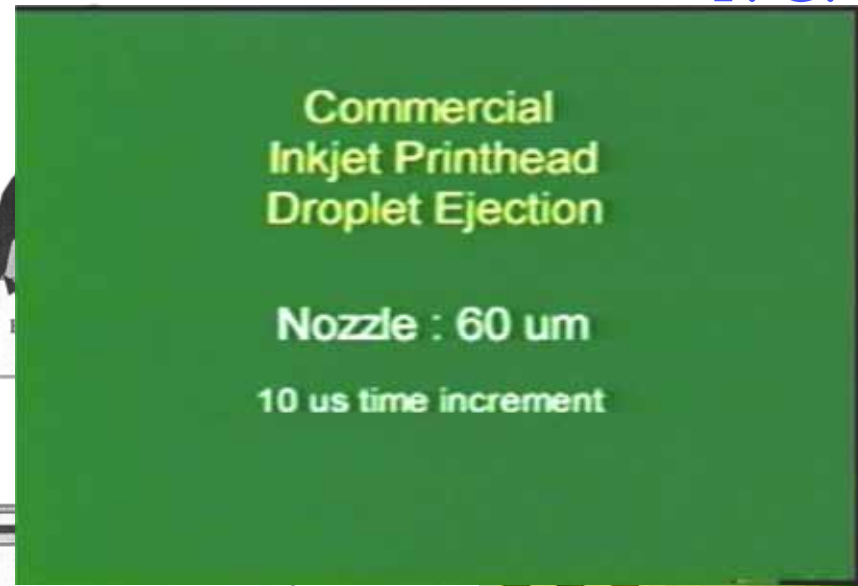
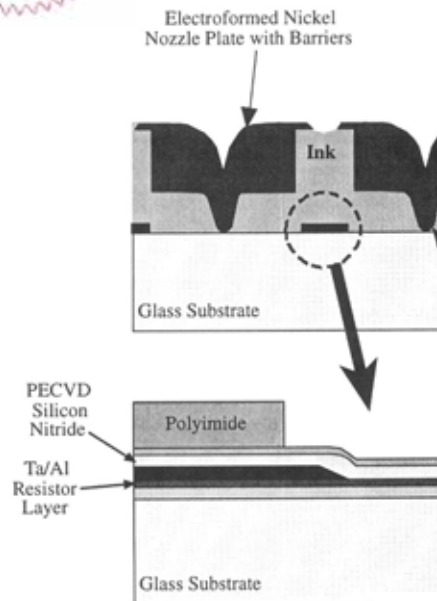




微液珠產生器

HP

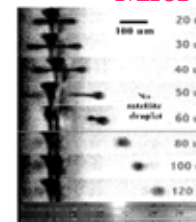
F. G. Tseng



Nozzle: 60 μm
Droplet: 50 μm
Frequency: 8 kHz



Microinjector



Nozzle: 40 μm
Droplet: 45 μm
Frequency: 18 kHz

Fastest one in market
Nozzle: 20 μm
Droplet: (5 pl)
Frequency: 12 kHz
Speed: 10 m/s

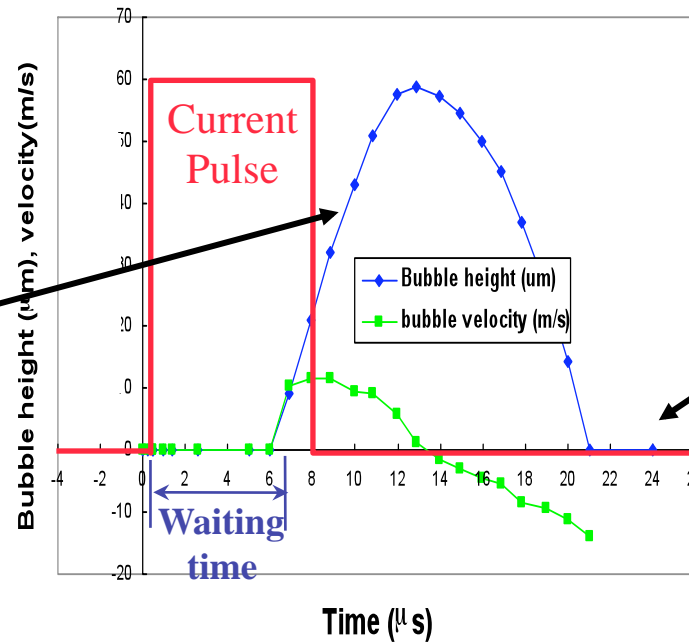
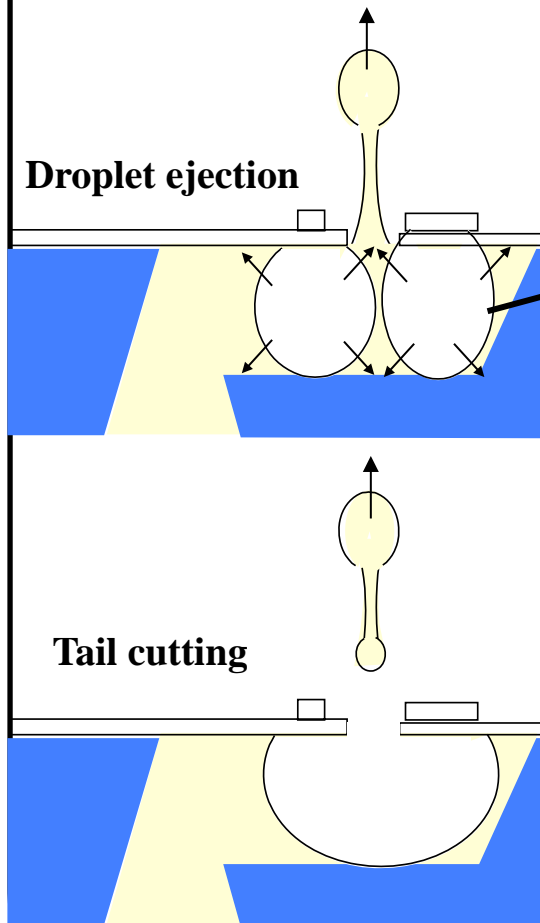
Fastest one
Nozzle: 10 μm
Droplet: 12 μm (0.9pl)
Frequency: 33 kHz
Speed: 10 m/s





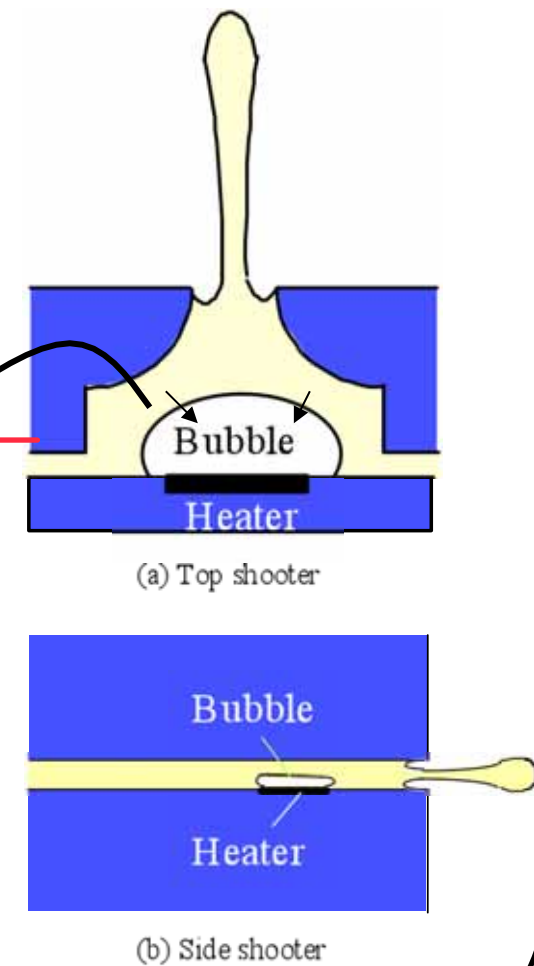
Droplet Tail Cutting

Microinjector



(Lee and Tirumala, IBM, 1988)

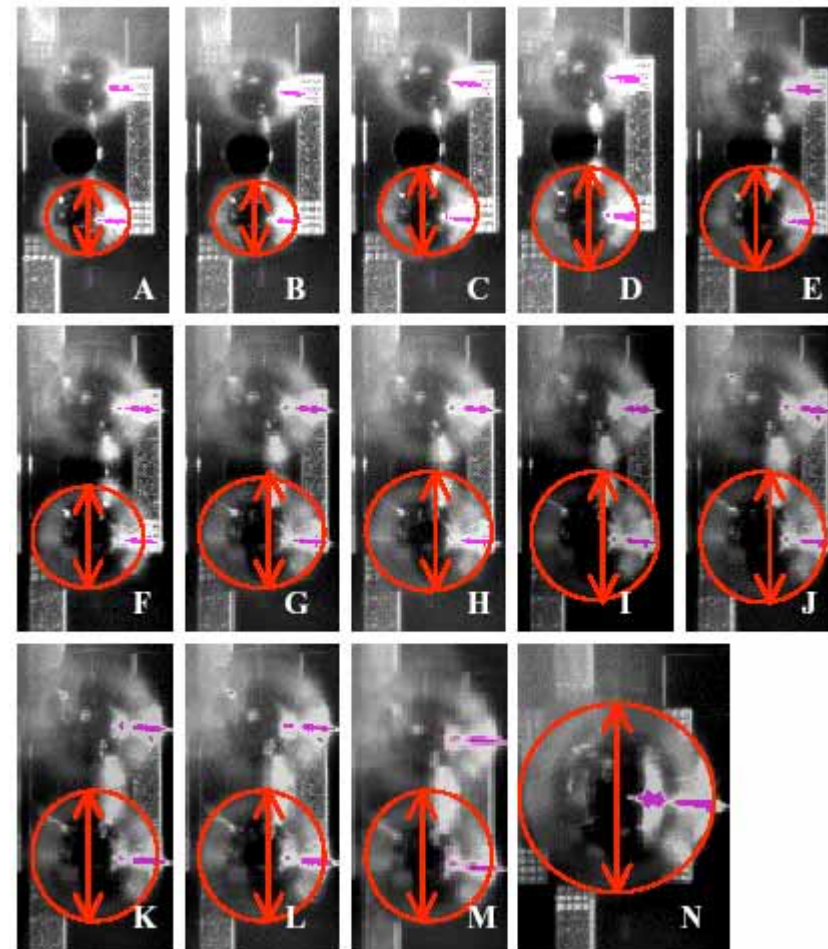
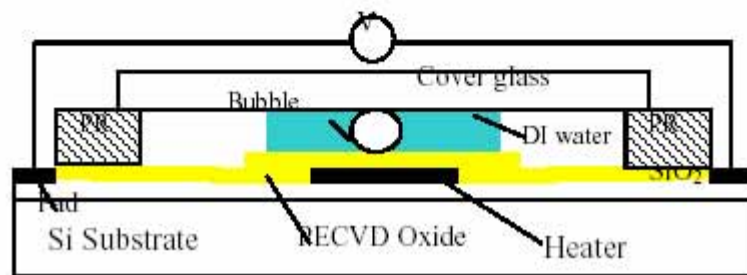
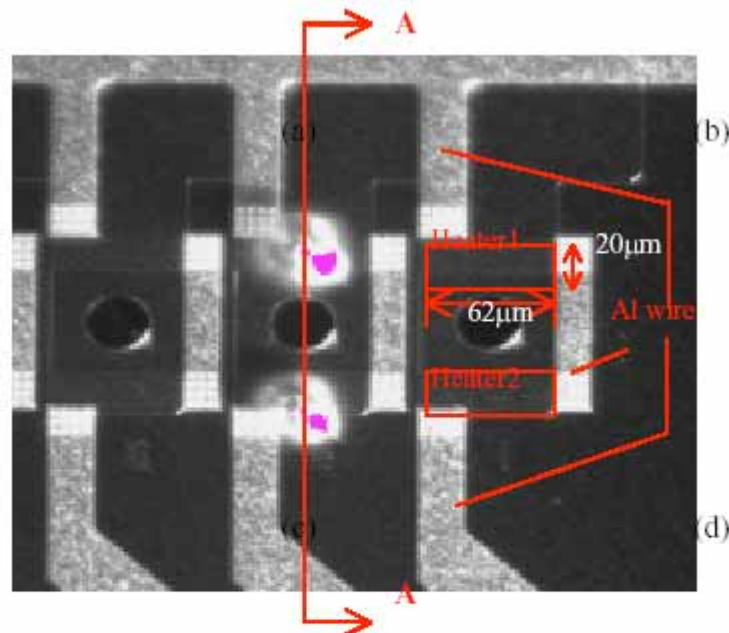
Commercial Inkjet





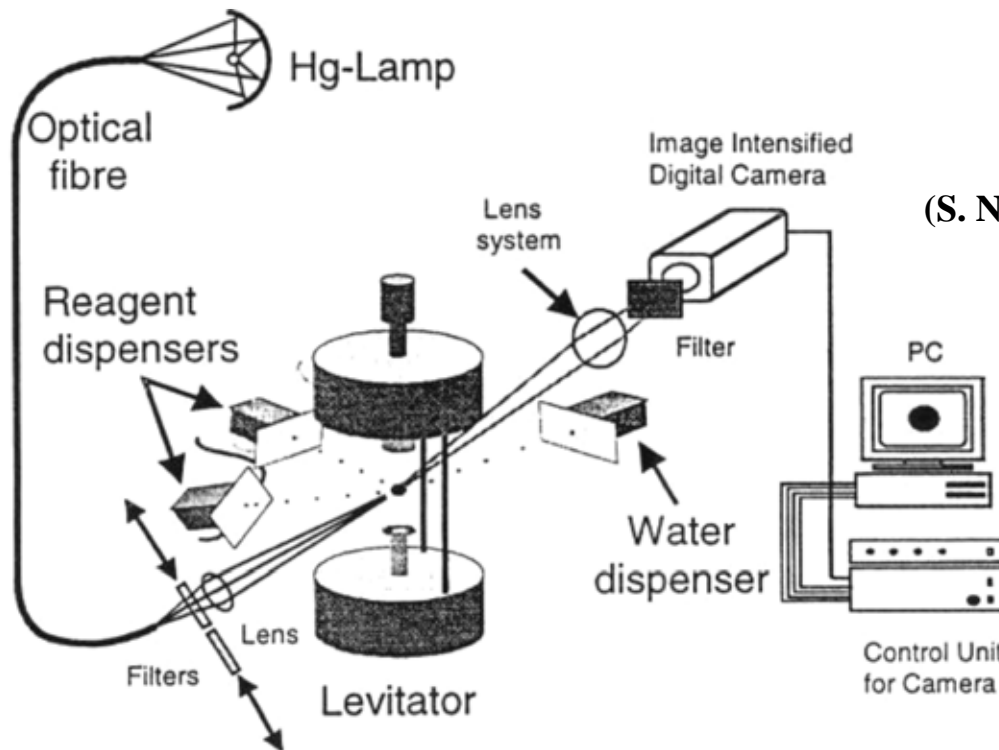
Bubble Merging for Tail Cutting

Bubble formation sequence (1 μ s interval)





液珠懸浮控制



(S. Nilsson, et. al., μ Tas'00)

1. Instrumental set-up for levitation cell experiments with fluorescence imaging detection, consisting of a Hg-lamp, an optical fibre, two alternating interference filters (405 and 435 nm), a cylindrical lens, an acoustic levitator, a lens system, and another interference filter (510 nm). A CCD camera is used to collect images of the levitated droplets, which are then analysed by a specially designed, in-house developed computer program for image analysis of the levitated droplets. Three continuous flow-through pico litre dispensers are used for additions to the levitated droplet, one for the addition of water and two for the addition of reagents (isoprenaline and insulin).

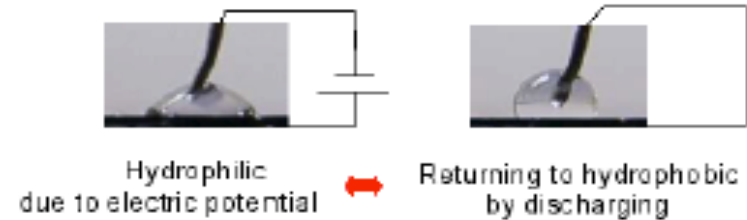


微液珠平面驅動方式

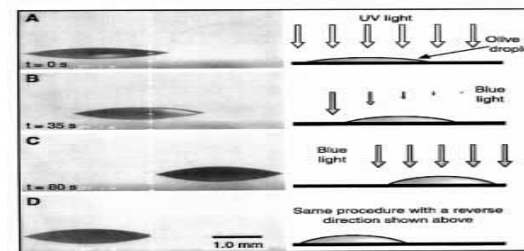
- 微液珠驅動方式:

1. 靜電及電潤濕 [2-4]
2. 光驅動法 [5]
4. 固態液體珠 [6]
5. 非對稱結構 [8]
6. 熱毛細力 [9]
7. 結合Marangoni效應, 熱毛細力, 凝結及成核效應 [7]
8. 表面奈米分子操縱

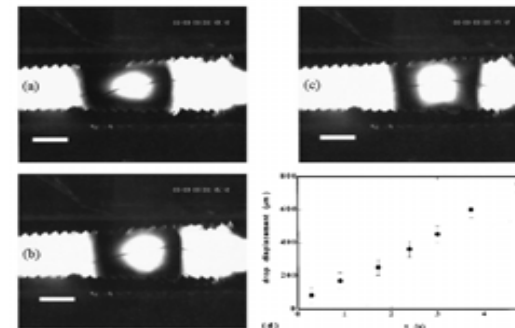
Most of them are employing surface tension gradient!!!



Lee, J, Sensors and Actuators 2002



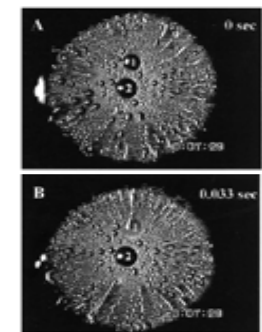
K. Ichimura, Science, 2002



O. Sandre, Physical Review E, 1999



P. Ausslous, Nature, 2001

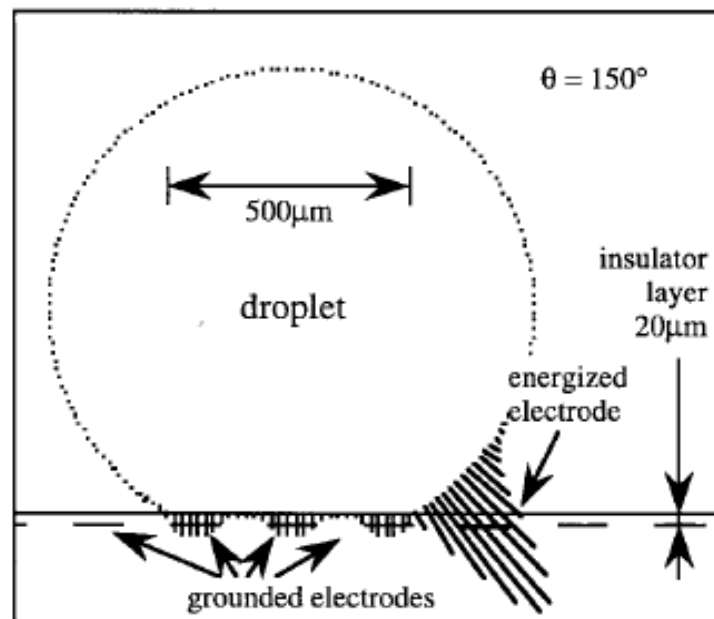


J. C. Chen, Science, 2001

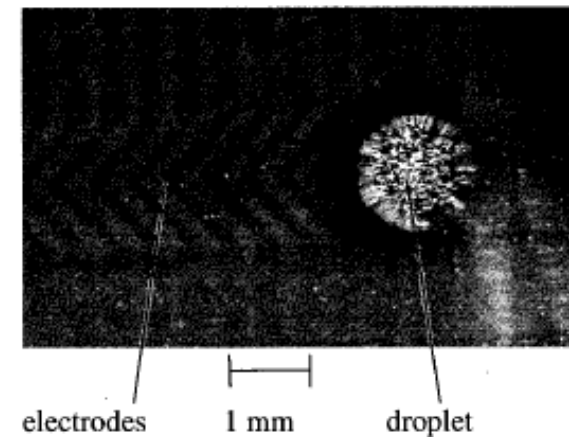
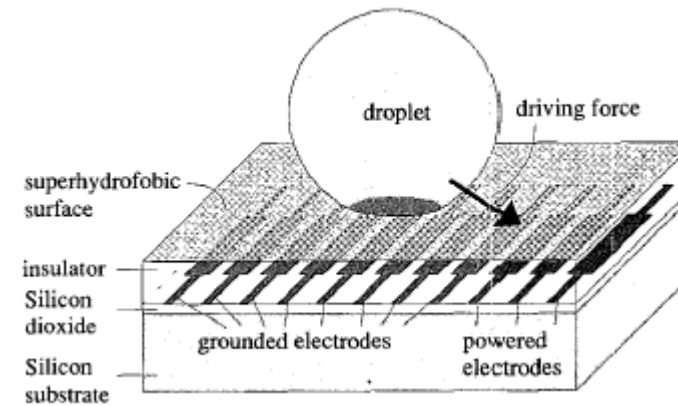


Electrostatic

- Very high voltage,
- electrolysis problem,
- charged bio-molecules may be attracted by electrical field



(Masao Washizu, *IEEE* 1998)



(Altti Torkkeli, *IEEE* 2001)



Electrowetting

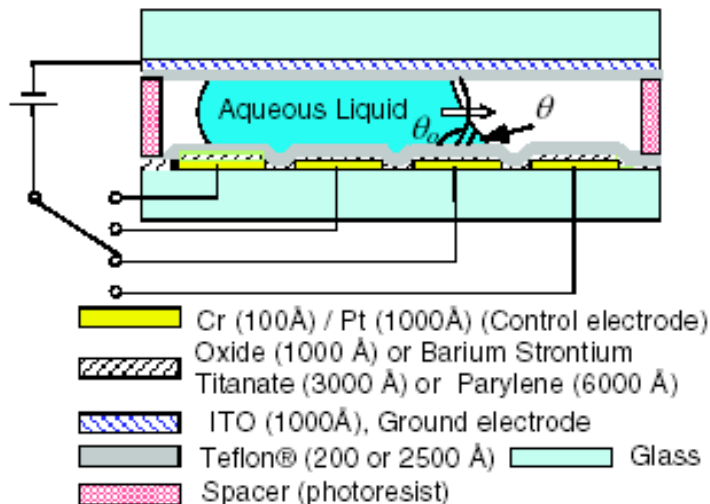
EWOD

(ElectroWetting on Dielectric)



Hydrophilic
due to electric potential

Returning to hydrophobic
by discharging



(Sung Kwon Cho, *IEEE* 2002)

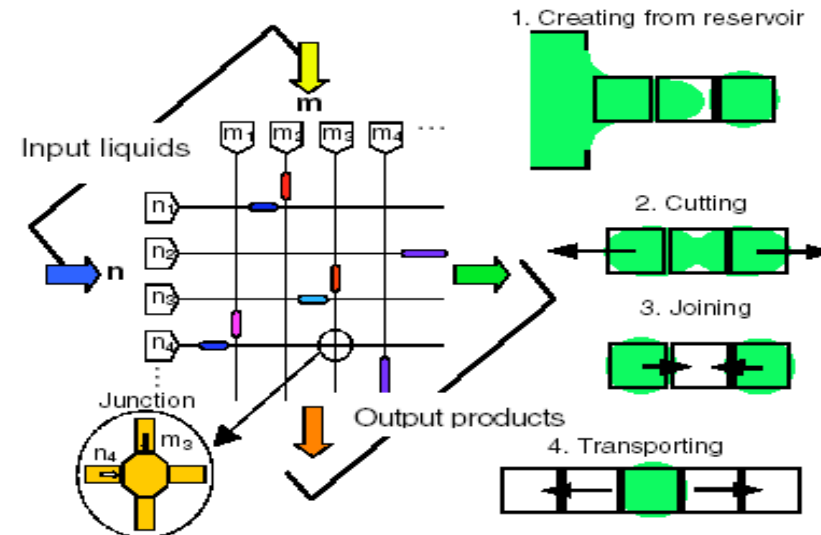


Fig. 1 Envisioned digital microfluidic circuit and the four fundamental droplet operations necessary

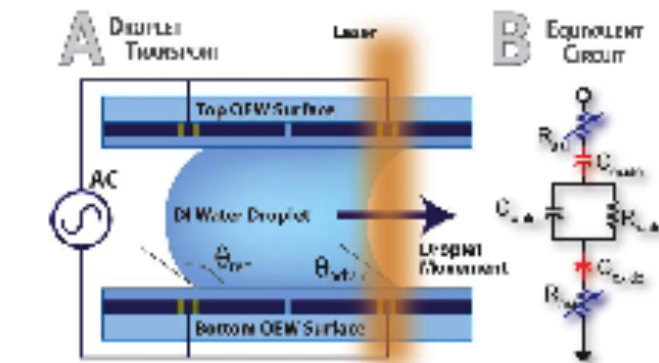


CJ Kim, UCLA

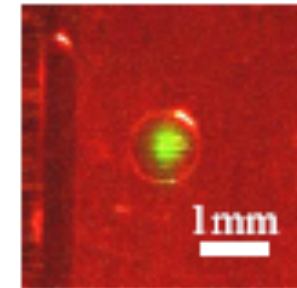
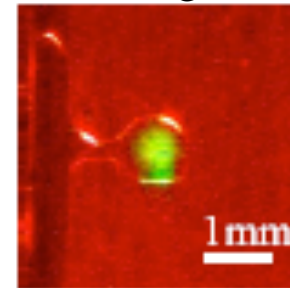


Electrowetting

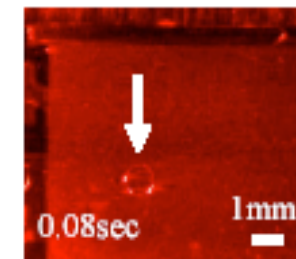
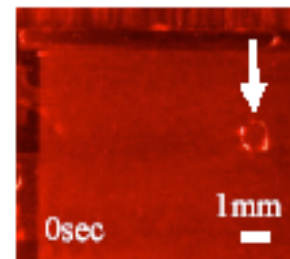
OWE (Opto-Electrowetting)



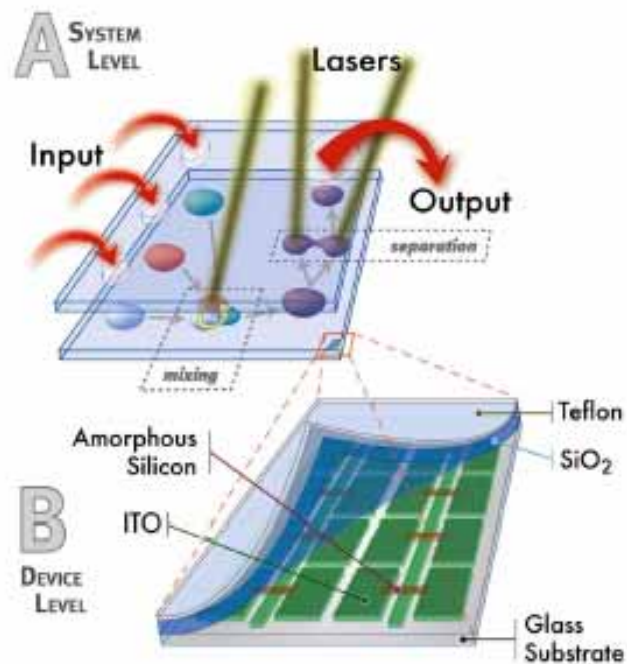
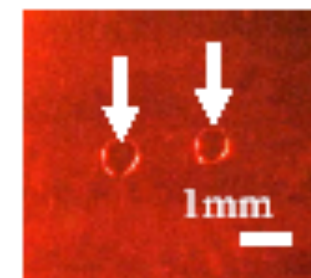
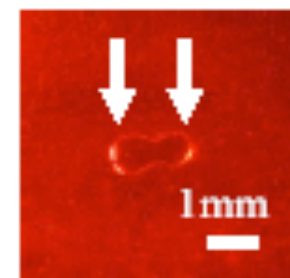
Creating



Moving



Separation



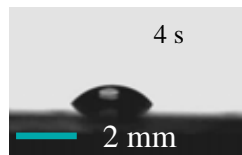
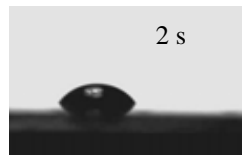
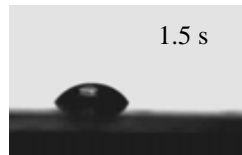
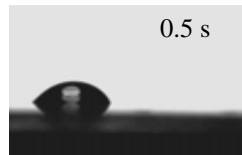
(Pei Yu Chiou, *IEEE* 2003)



Marangoni Effect

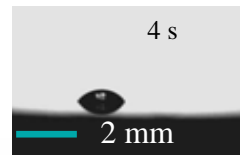
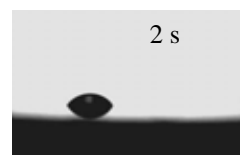
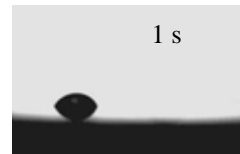
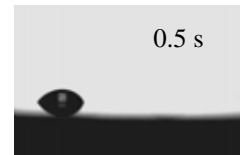
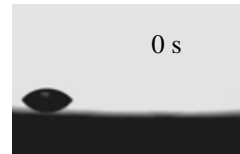
•Droplets Moving Behavior

1 μl

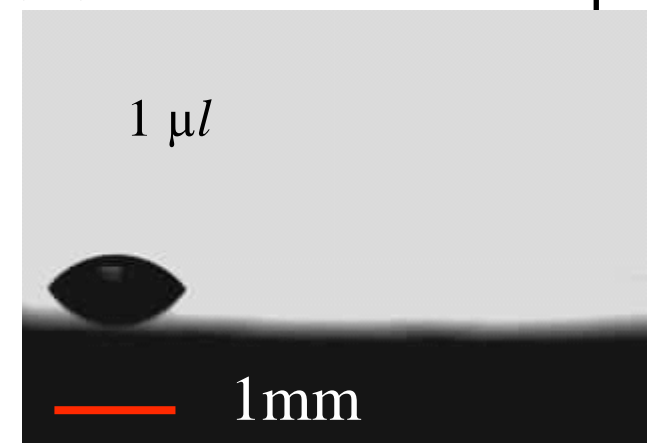
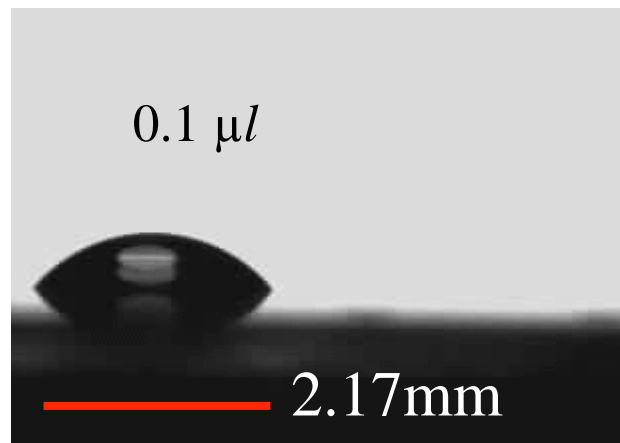
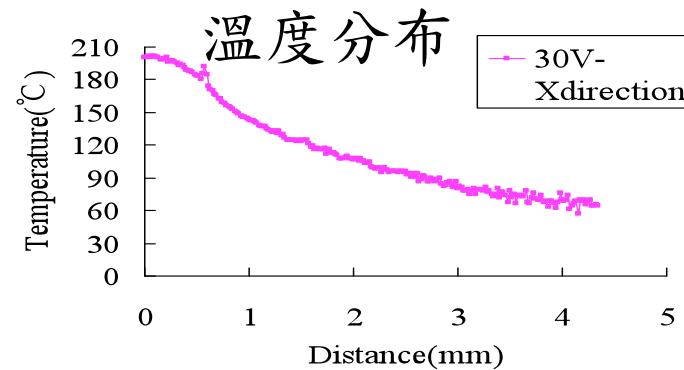
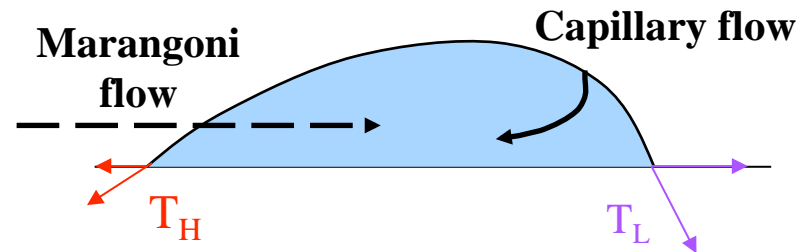


2 mm

0.1 μl



2 mm





Thermal Capillary Actuation

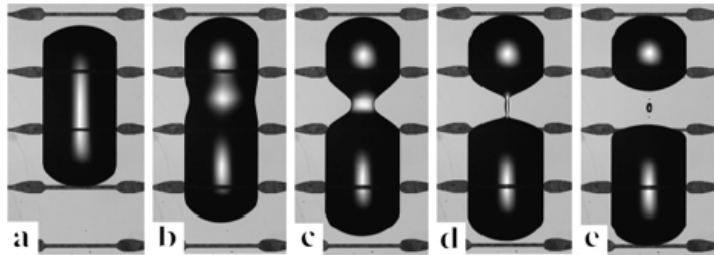


Figure 3. (a)-(e) Thermally induced splitting of a dodecane drop on a partially wetting stripe (droplet width = 1000 μm). Resistive heaters are defined by the light gray regions. The voltage applied to the 155 Ω resistor was 2.5 V. The images were recorded at $t = 0, 6.0, 7.5, 8.0$, and 8.5 s.

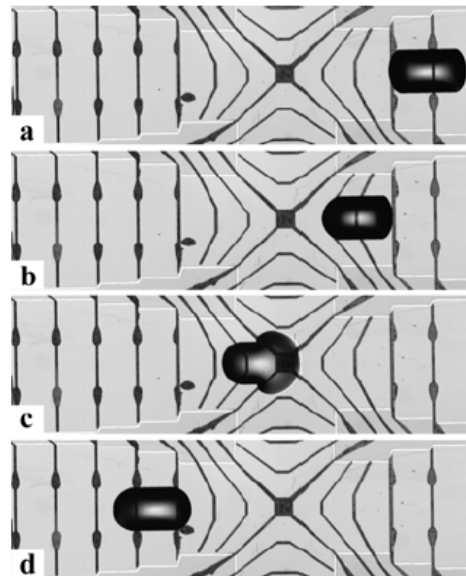


Figure 4. (a)-(d) Thermocapillary actuation of dodecane drop through intersection (droplet width = 1000 μm , time lapse = 104 s).

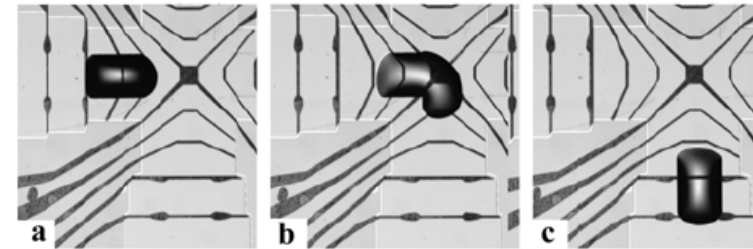
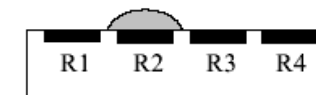
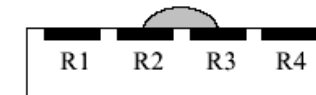


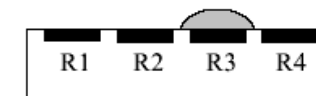
Figure 5. (a)-(c) Dodecane drop turning 90° corner. Power applied to each resistor ≤ 40 mW (Time lapse = 164 s).



a.) R1 and R3 on



b.) R1 and R4 on; R3 off



c.) Increase R2 voltage; R4 on; R1 off

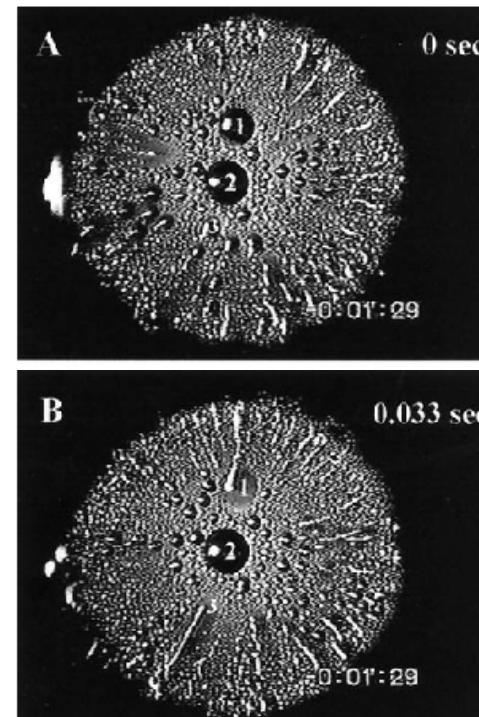
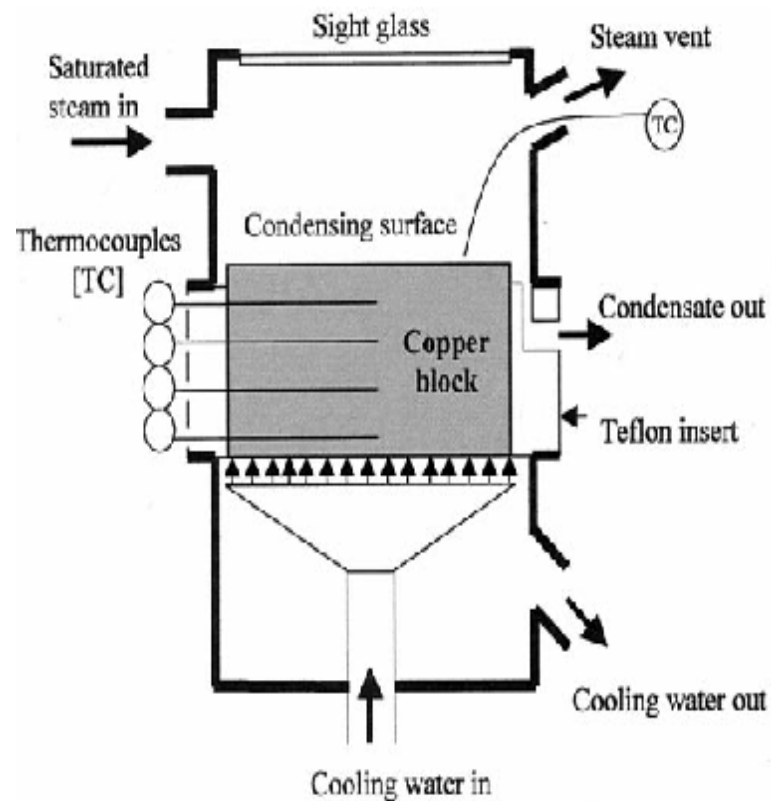
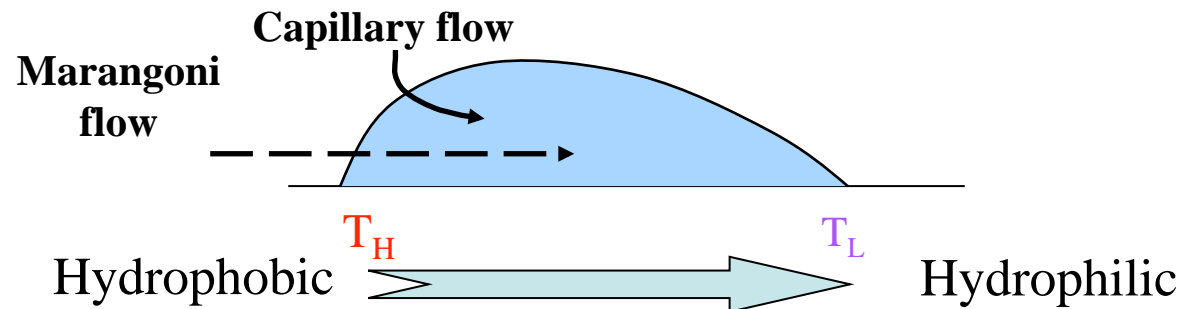
Figure 6. Cross-section of device showing sequential heating of resistors, R1, R2, R3, R4: a.) Voltage applied to R1 and R3: the drop is confined on top of R2. b.) Turn off R3 and apply voltage to R4: drop moves away from R1. c.) Apply voltage to R2 and turn off R1: drop is positioned above R3.

J. P. Valentino^a, A. A. Darhuber^b, and S. M. Troian, Transducers'03





Marangoni + capillary + coalesces Effect



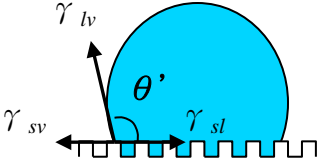
**Droplet movement
~10 cm/s, 10 times
faster**

(Susan Daniel, *Science* 2001)

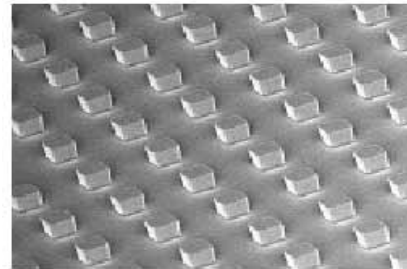


Surface Roughness

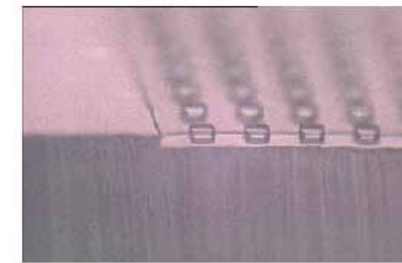
Winzel



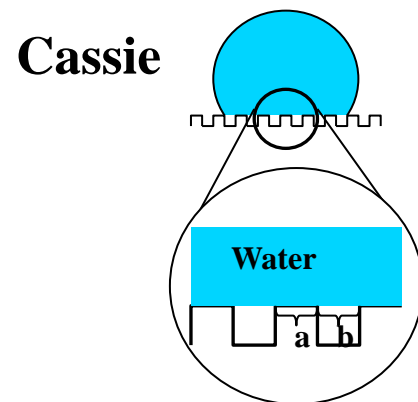
$$\cos \theta' = \frac{r(\gamma_{sv} - \gamma_{sl})}{\gamma_{lv}} = r \cos \theta$$



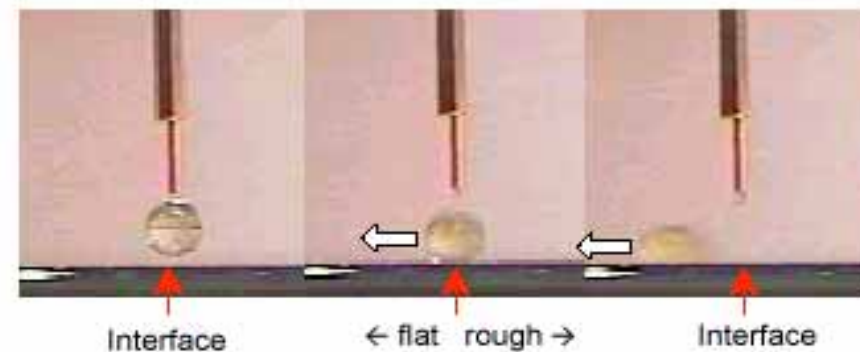
(a) PDMS pillars (SEM)



(b) Suspended PDMS membranes (optical microscopy)



$$\cos \theta' = f \cos \theta + f - 1$$



Wettability Switching by Surface Roughness Effect
(Bo He, *IEEE* 2003)



Temperature Responsive Surface

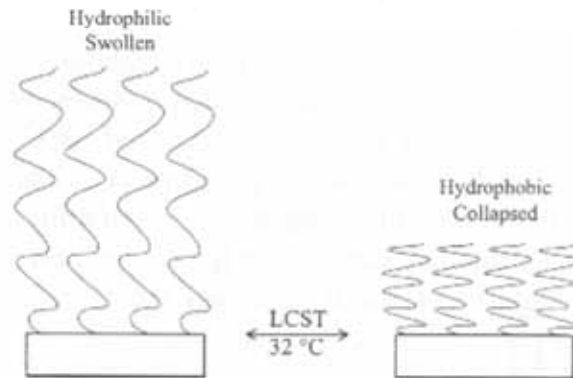


Figure 1. Depiction of temperature effects on pNIPAAm. Below the LCST pNIPAAm is hydrophilic and swollen. The reverse is true above the LCST.

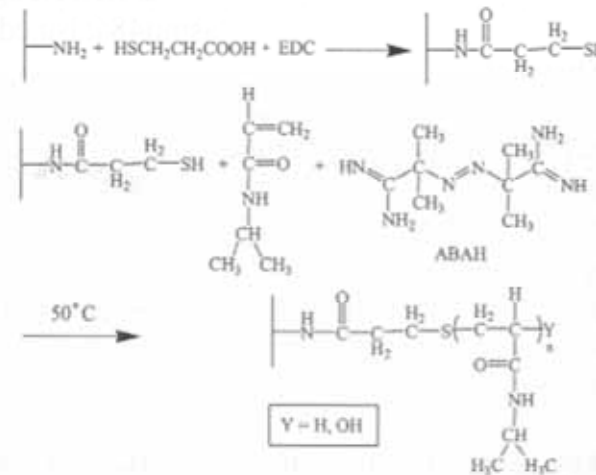
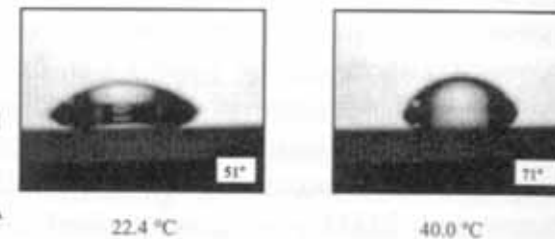
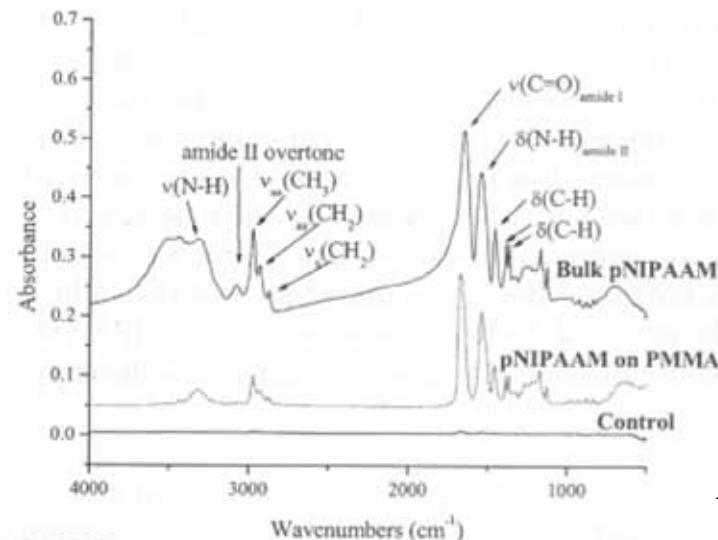


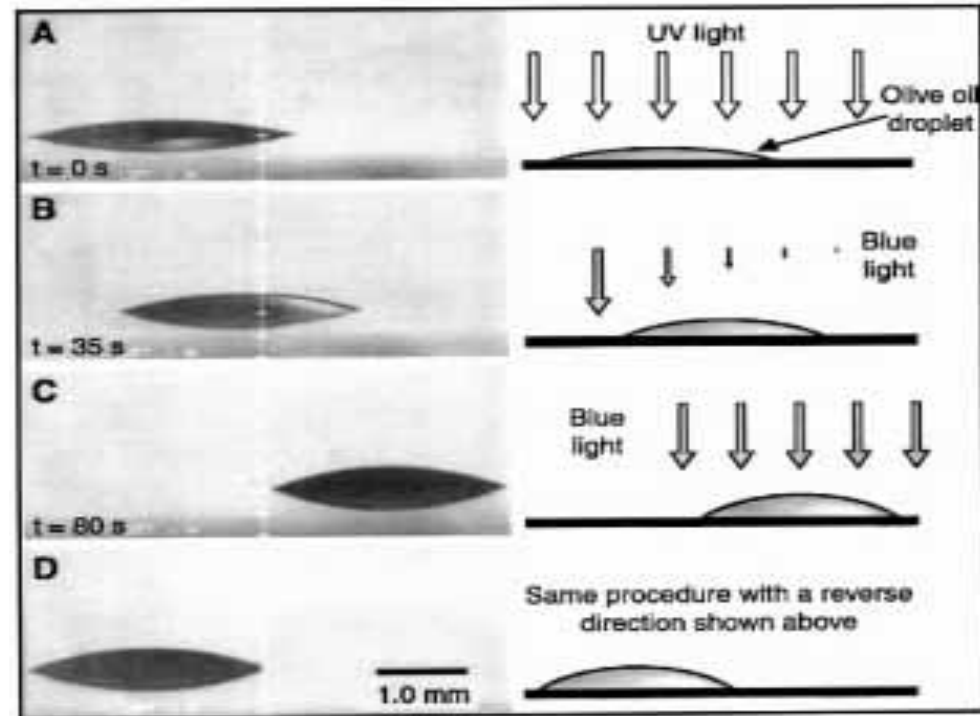
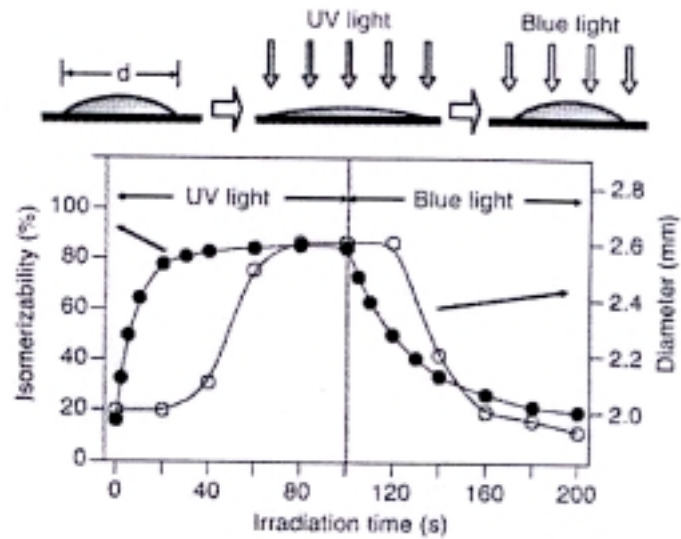
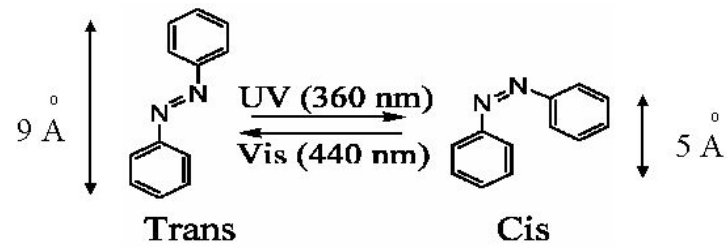
Figure 2. Reaction sequence leading to the free-radical polymerization of pNIPAAm from modified PMMA surfaces. All reactions were performed in aqueous medium.



A. F. Smith, R. L. McCarley, μ TAS 2002



Photonic & SAMs



(K. Ichimura, *Science* 2000)



Bending molecules by Electrical Potential

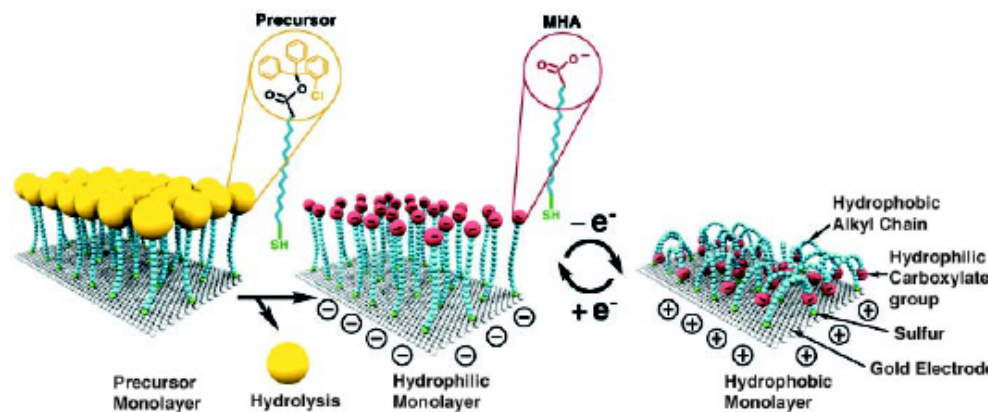
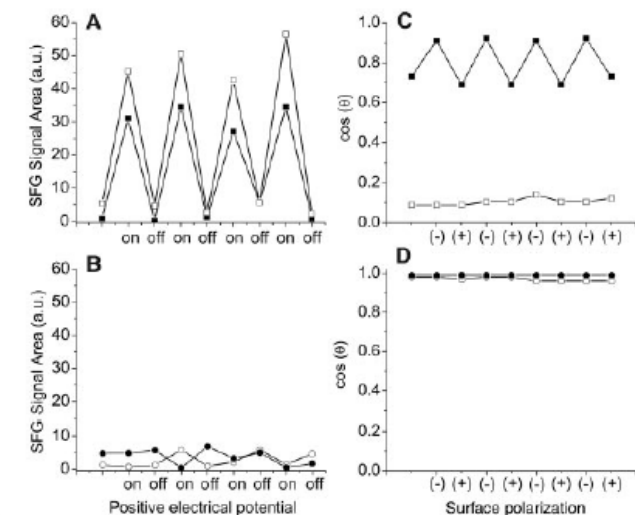


Fig. 1. Idealized representation of the transition between straight (hydrophilic) and bent (hydrophobic) molecular conformations (ions and solvent molecules are not shown). The precursor molecule MHA, characterized by a bulky end group and a thiol head group, was synthesized from MHA by introducing the (2-chlorophenyl)diphenylmethyl ester group.

Fig. 4. Microscopic and macroscopic responses of the low-density SAM to an electrical potential as monitored by SFG spectroscopy and contact angle measurements. Relative SFG intensities (peak areas) of the methylene modes at wavelengths of 2855 cm^{-1} (solid symbols) and 2925 cm^{-1} (open symbols) are shown for the low-density (A) and the dense (B) SAMs measured in d^3 -acetonitrile (0.1 M CT) when a potential of +25 mV w.r.t. SCE was repeatedly applied to the system. Cosine of the advancing (open symbols) and receding (solid symbols) contact angles for the low-density (C) and the dense (D) SAMs were determined while applying either +80 or -300 mV w.r.t. SCE to the underlying gold electrode. Four switch cycles were conducted, and contact angles were measured with an aqueous solution (0.1 M CT, pH = 11.5) at air using a goniometer (VCA-2500XE, Advanced Surface Technology) equipped with an electrometer (6517A, Keithley Instruments) and platinum and carbon fiber microelectrodes (Kation Scientific). Contact angles averaged at least 100 data points from nine samples with maximum errors of $\pm 3^\circ$. The SAMs were examined for chemical integrity and deprotonation by IR spectroscopy after an electrical potential was applied. The lines are drawn as a guide to the eye.

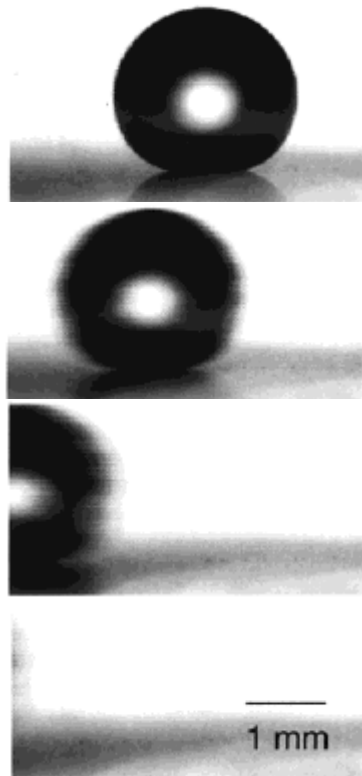


J. Lahann et al, Science 2003.



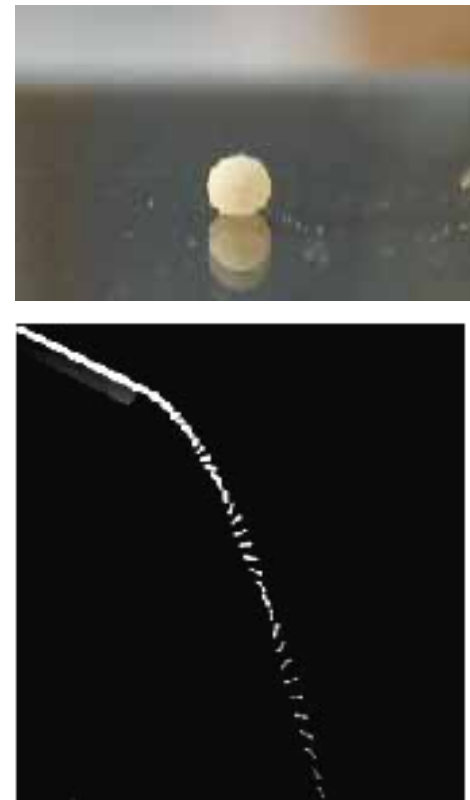
Superhydrophobic & Gravity

Superhydrophobic Surface (SAMs)



Water Droplet Weight **7mg** with tilt angle of surface **1°** (Masashi Miwa, *Langmuir* 2000)

Liquid Marble (Powder coating)



Hydrophobic powder (20 μ m) coating (Pascale Aussillous, *Nature* 2001)



Comparasion

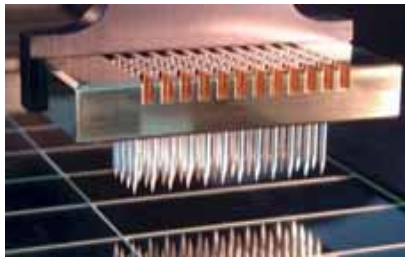
Principle	Max. Velocity (mm/s)	Droplet Size (μ l)	Power
Electrstatic (Altti Torkkeli, <i>IEEE</i> 2001)	10	2 ~ 50	Yes(124V _{AC})
Electrowetting (S. K. Cho, <i>IEEE</i> 2002)	250	1	Yes(100V _{AC})
Optic (K. Ichimura, <i>Science</i> 2000)	0.035	2	Yes
Temperature Gradient (Susan Daneil, <i>Science</i> 2001)	~ 20	0.001 ~ 1	Yes
Roughness (Bo He, <i>IEEE</i> 2003)	?	7	No
Gravity (P. Aussillous, <i>Nature</i> 2001)	?	1 ~ 10	No



Conventional array machine system

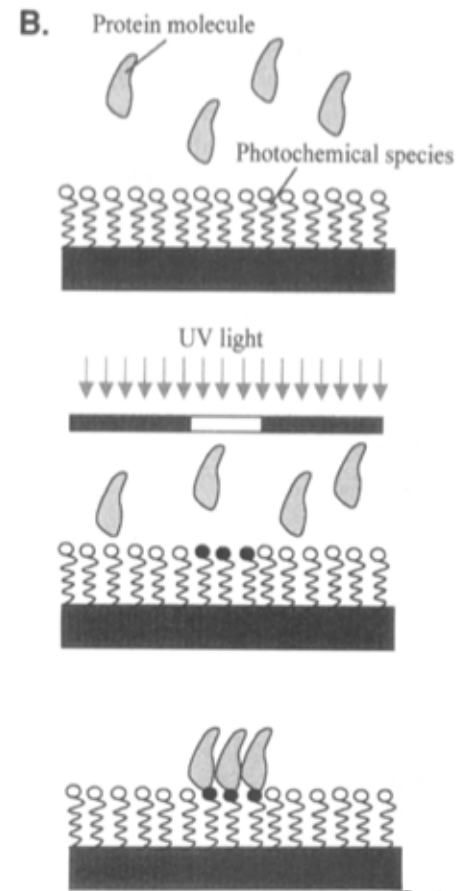
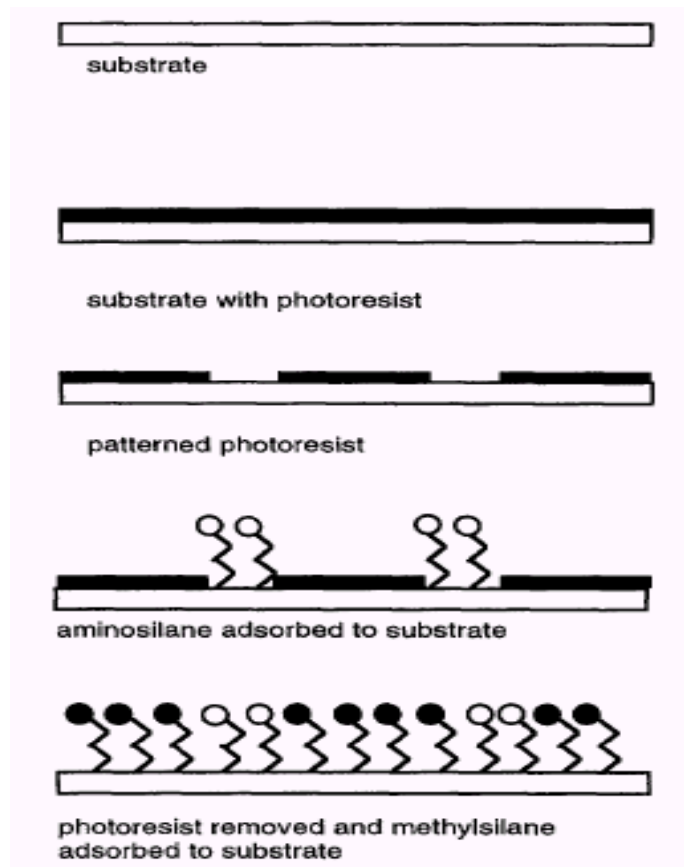
機械手臂點針法

- Robotic machine and steel pin
- **Serial process:** long running time
- **Need wash:** (cross contamination)
- **Expansive:** position control system
- **Sample dry out:** not good for protein





光學微影法



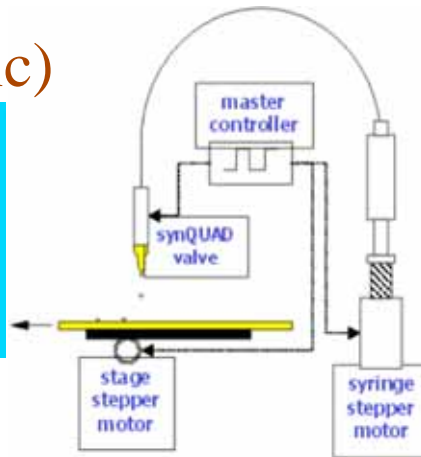
Blawas, *Biomaterials*, 1998

缺點：化學藥品可能傷害檢體、不適合多種檢體



微噴墨法

壓電式
(Piezoelectric)



Spot size: 80~50 μ m
(SPIE Microfluidics and BioMEMS 2001)

缺點

- 噴嘴及管路重複使用需清洗
- 致動器須控制良好以使產生的液珠體積均勻且避免衛星液珠

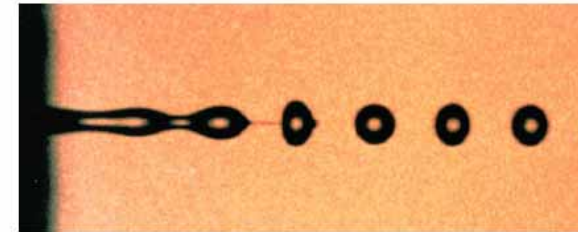
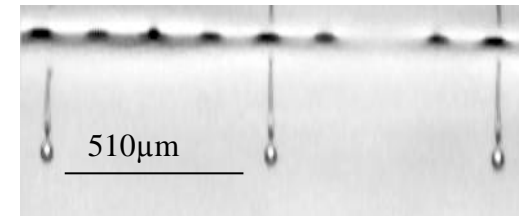


Figure 1: A 50 μ m jet of water breaking up due to Rayleigh instability into 100 μ m droplets at 20kHz.



Nozzle: 50 μ m

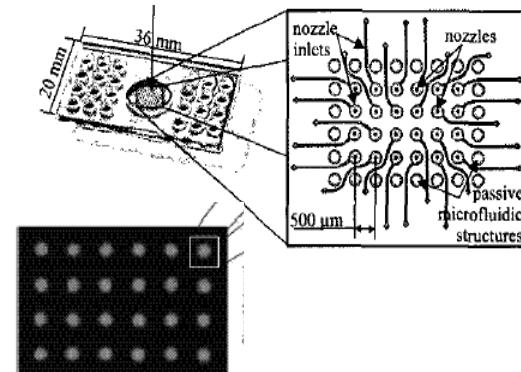
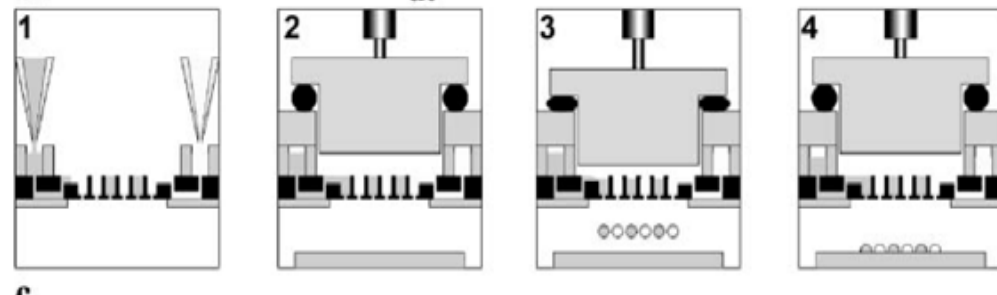
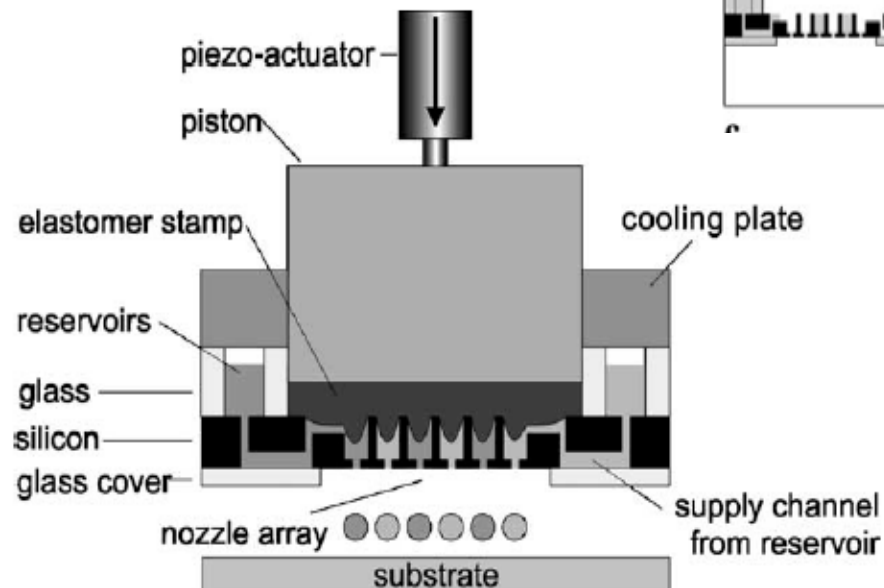
Pizeo stroke: 3~9 μ m

Droplet volume: 200~1400pl



氣動式微噴墨法

氣動式
(Piezoactuator)



Spot size: 400~50μm

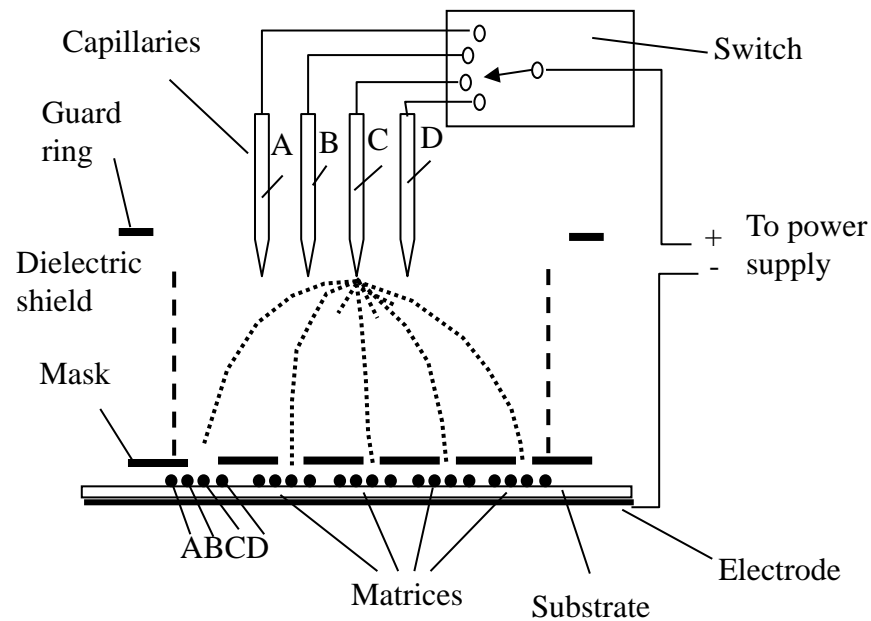
氣壓需要控制良好

間距大

(Gustmann, Germany Transducer, 2003)



電噴灑法



(Electrospray Mozorov 1999)

以電噴灑法沉積蛋白質及DNA的主要問題在於蛋白質及DNA在電噴灑沉積後，並在接續的帶電電噴灑生成物撞擊下，是否仍能保存本身的活性。電噴灑法需要使用極高的電壓，以噴灑蛋白質為例，需要高達3-4kV的電壓，安全上的考量不可不慎。再者，以電噴灑法形成的點形狀並不均勻，需要再配合其他的設計才能解決，增加製程上的麻煩。



雷射法加熱法 Biological laser printing

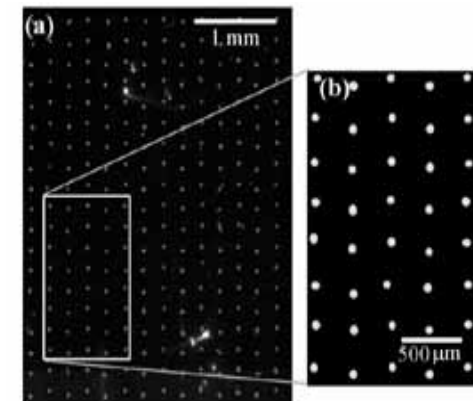
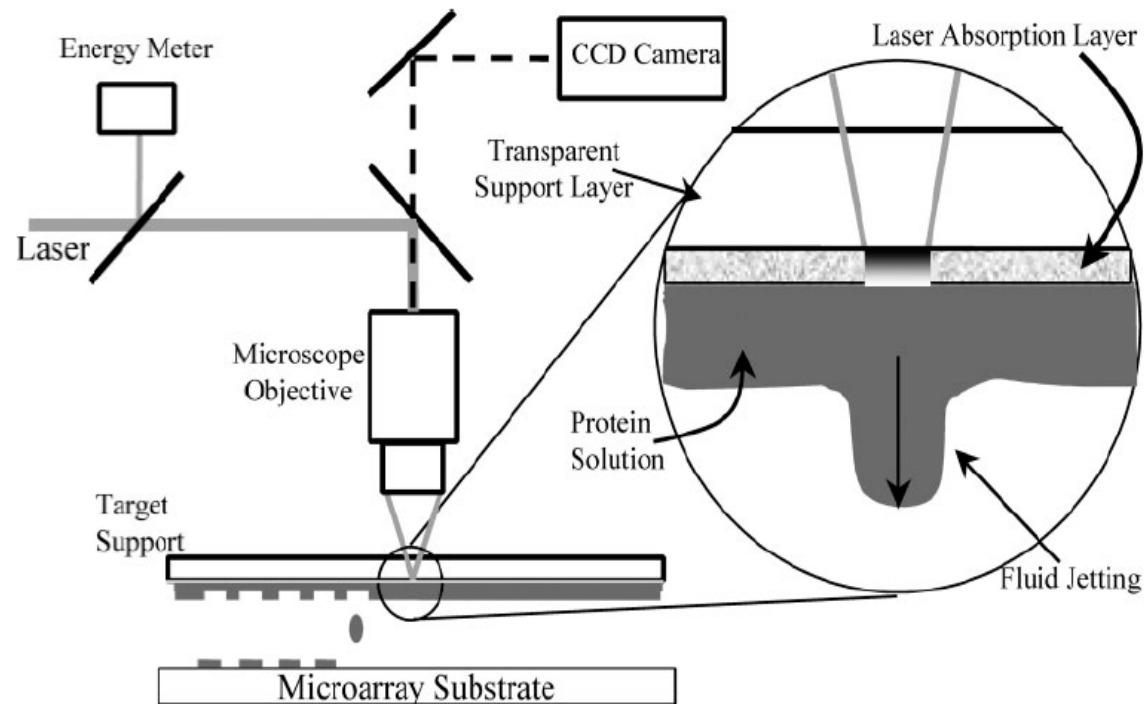


Figure 5. (a) A 2000-spot BSA microarray after immunoassay with anti-BSA (imaged with fluorescent detection; 266 spots shown). Standard deviation is 10% of the average spot size of 60 μm . (b) Higher magnification of one portion of the microarray.

(J.A. Barron Proteomics2005)

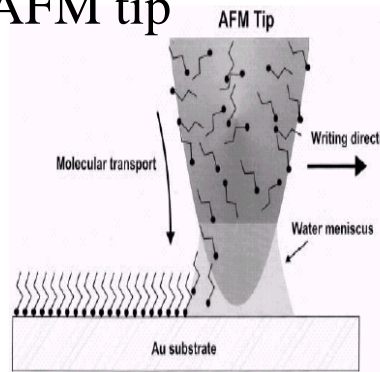
- Microscope objective to focus the laser beam
- Quartz substrate and metal or metal oxide absorption layer

需考量能量對檢體所造成的影響

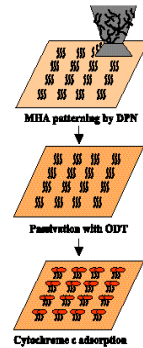


AFM沾水筆微影法

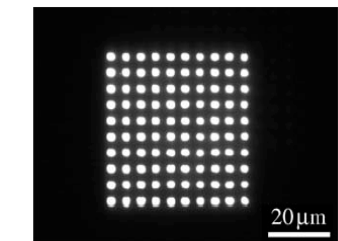
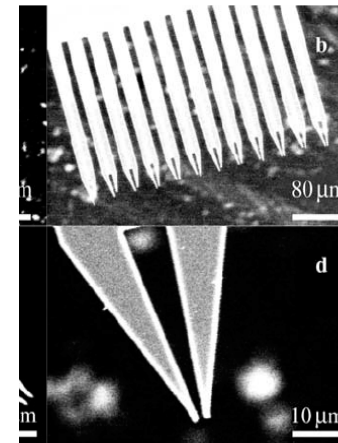
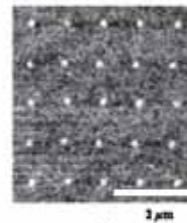
AFM tip



(Piner, Science 1999)



(J. W. Choi, 2004)

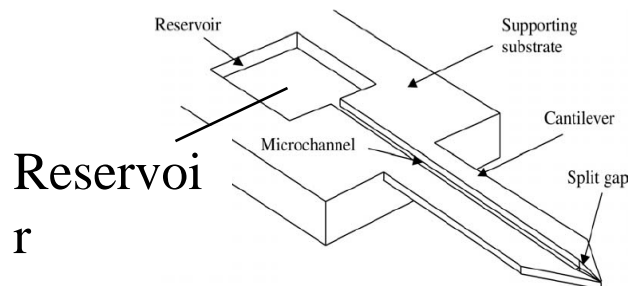


Spot size:
2~3 μm

Space :5 μm

缺點

- ❑ 需AFM移動軸筒做精密移動控制及施力下針控制以行成陣列
- ❑ 機台成本高且打印3000點需1小時
- ❑ 蛋白質點讀取分析不易

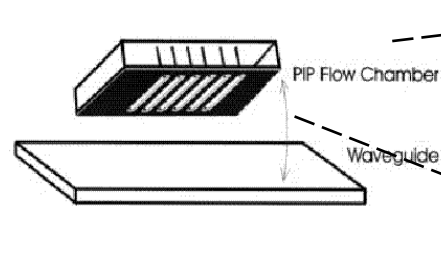


(Henderson, Biomedical Microdevice 2004)

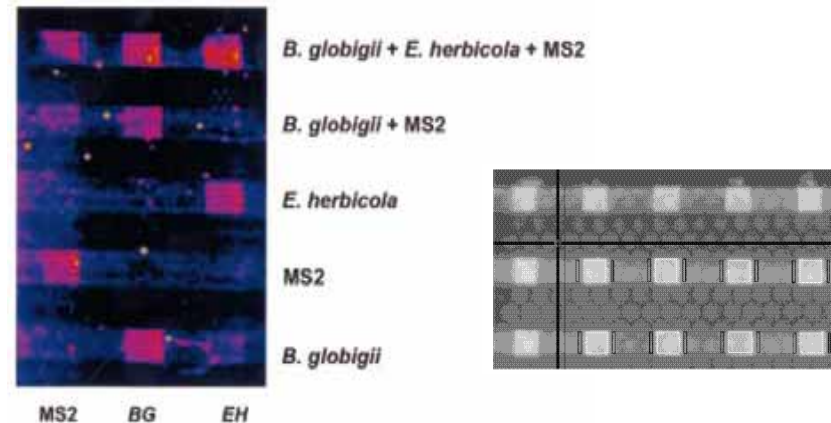
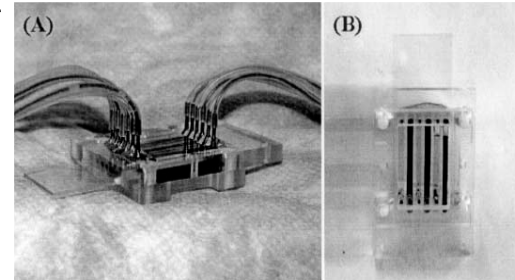
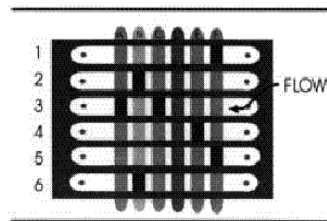
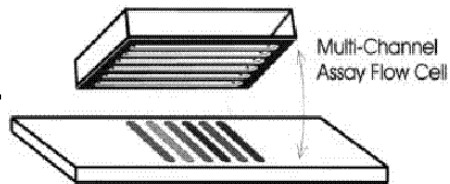


用PDMS微流道作蛋白質陣列

(a) 微流道通檢體在玻片上



(b) 微流道晶片轉90度, 通檢體在玻片上

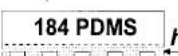
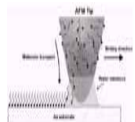
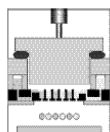
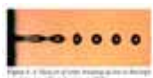
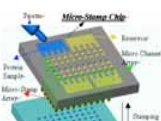


Size 尺寸間距大 (400~1500 μ m) 怕交互污染

(Ligler, Biosensor & Bioelectronics 02)



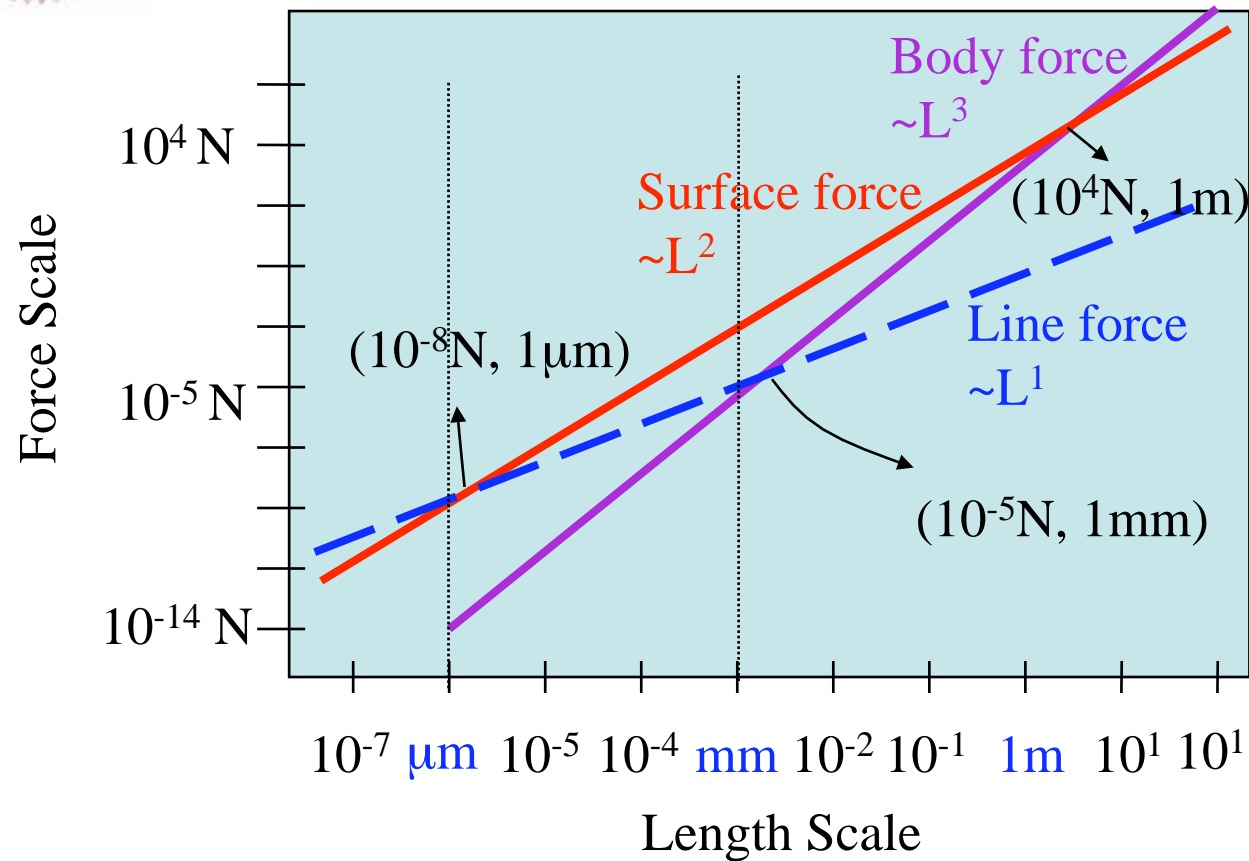
各微陣列技術比較



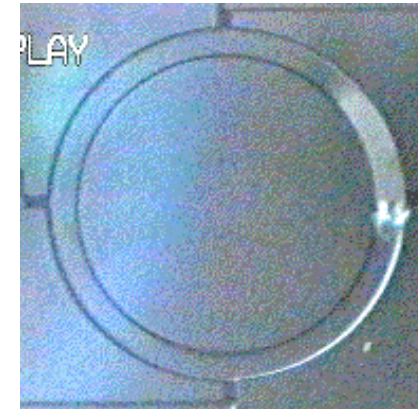
	液珠尺寸(um)	時間	一次可上種類	點體積(pl)	成本	拋棄式
微壓印法 (Lin) (Bernard)	50-100 5	快 200點/次	>100 1	400	低	Yes
點針法 (P.O.Brown 2001)	100~65	慢	48	500	高	No
噴墨法(壓電式)	150~50	快 100~4kHz	10	120	中	No
噴墨法(氣壓式) (C.P. Steiner et 2003)	400~50	中	24(9 6)	125~ 1700	中	Yes
沾水筆法 AFM	0.1 2	慢 3000點/1hr	1 12	(0.01)	高	Yes
奈米壓印法	1~0.25	快	1	(0.05)	低	Yes



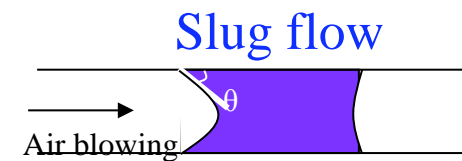
Force in Scale



Mercury motor



J. Lee, and C.-J. Kim,
J of MEMS, June 2000

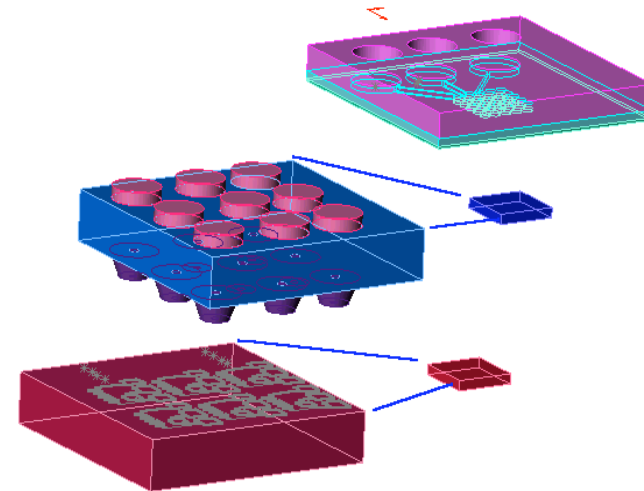


Surface tension force (line force) is dominate in nano scale and important in micro scale!!



❑ 3-in-1 Protein Chip

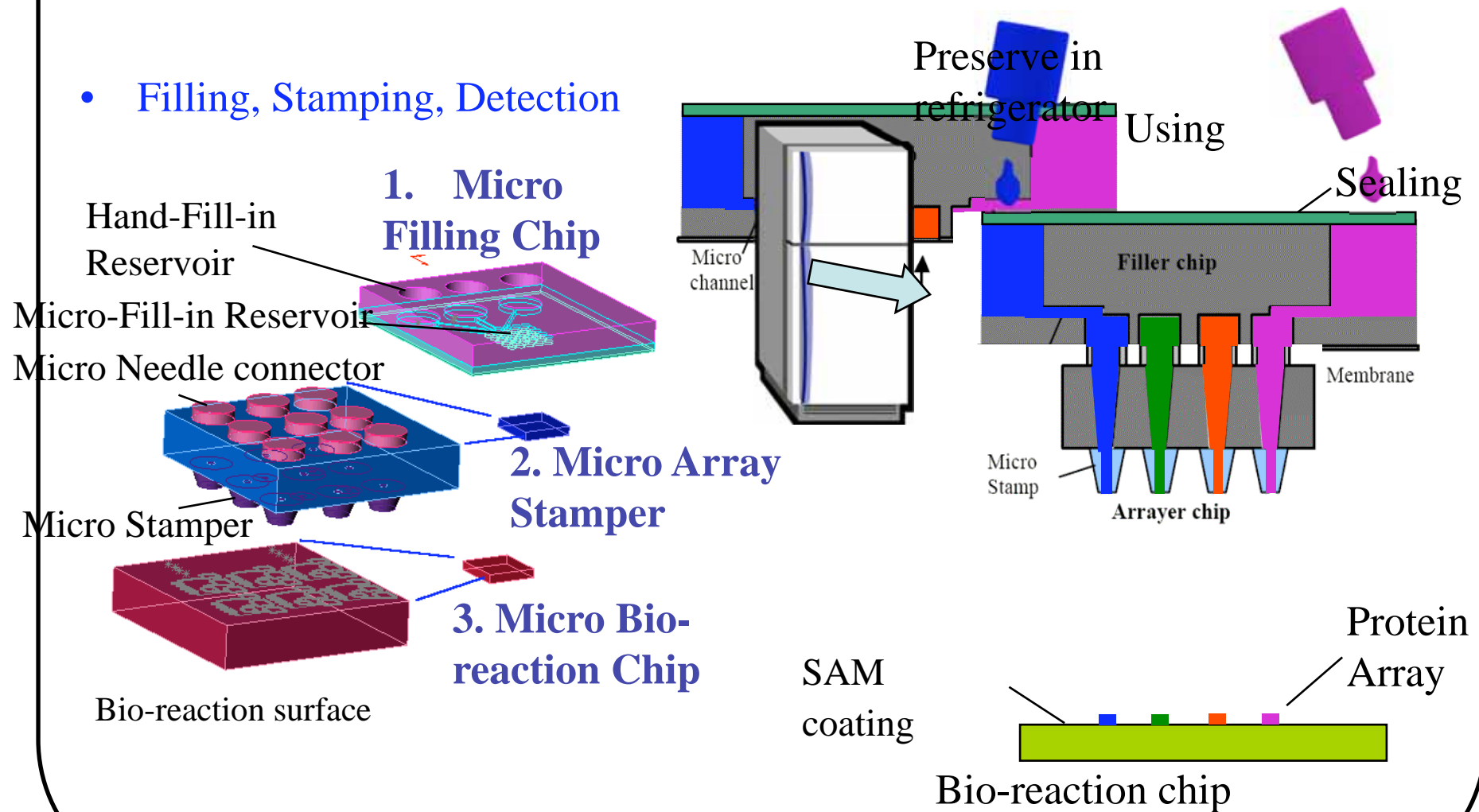
- Micro filling chip
- Micro stamper chip
- Micro bio-reaction chip





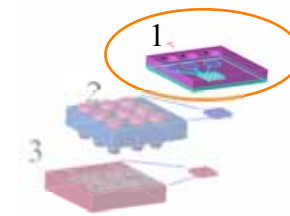
Chip System Integration

- Filling, Stamping, Detection

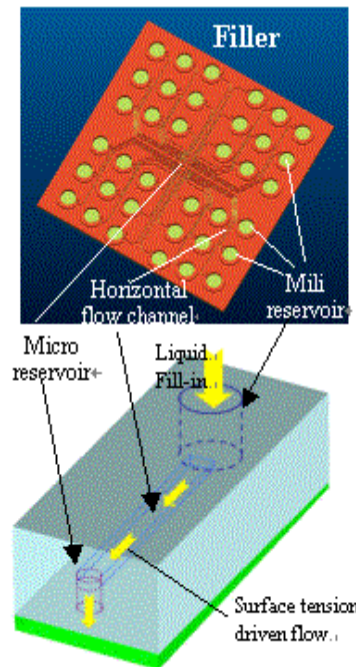




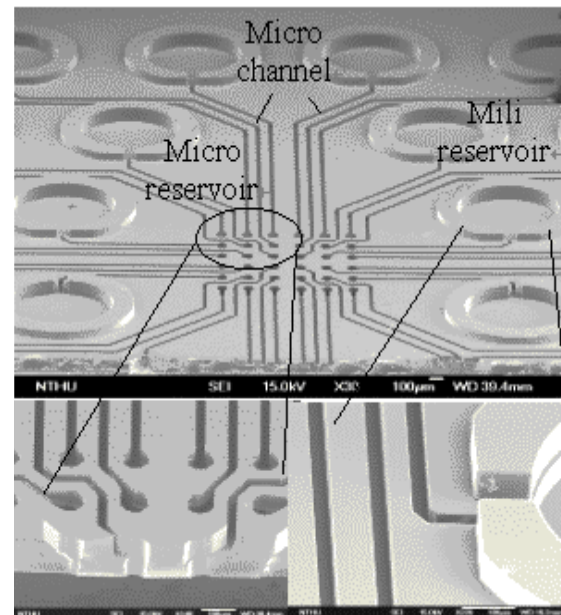
1. Micro Filling Chip



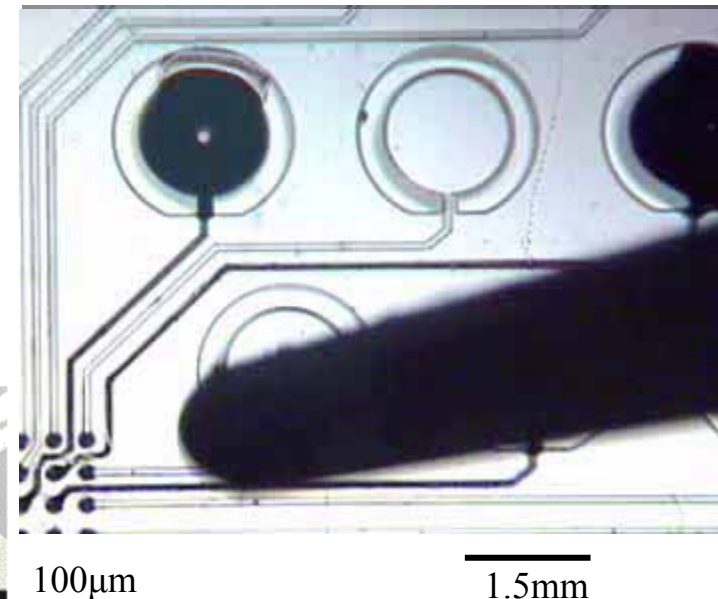
- Hand fill in
- Micro flow channel to micro filling reservoir
- PDMS membrane sealed. Conserved in refrigerator



a. μ flow channel connect the Hand fill-in reservoir and μ -reservoir



b. Micro flow channel cross section

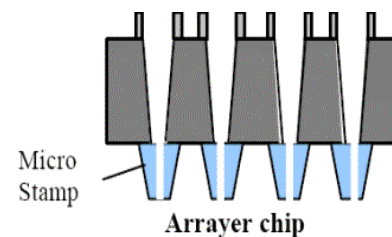
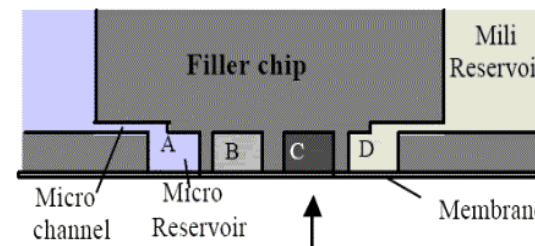
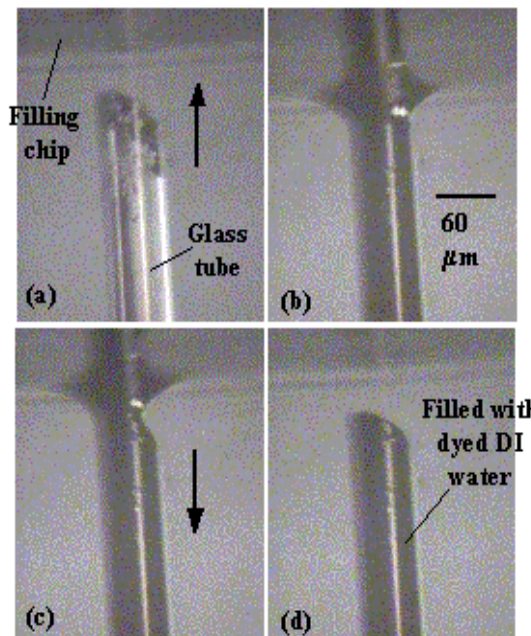
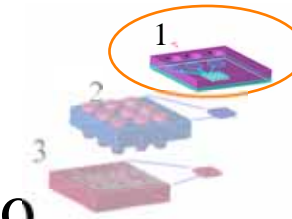


c. Filling testing. From hand-fill reservoir to micro reservoir

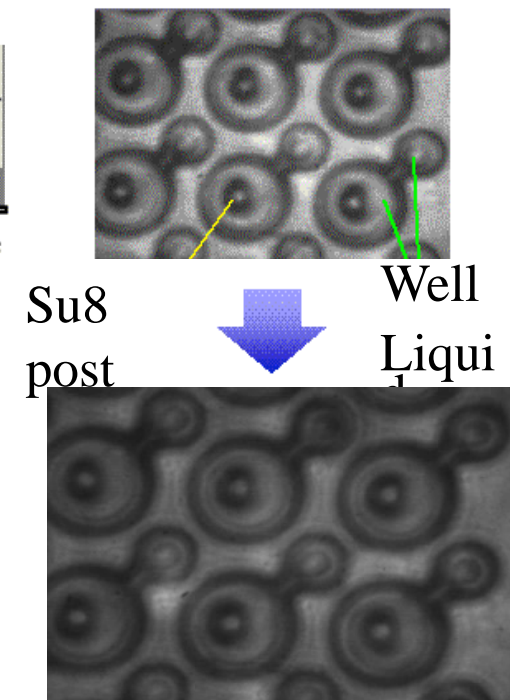


1. Micro Filling Chip

- Sample fluid **filled parallel** from micro reservoir into the micro stamper.
- Filling the micro stamper **by the capillary force**.



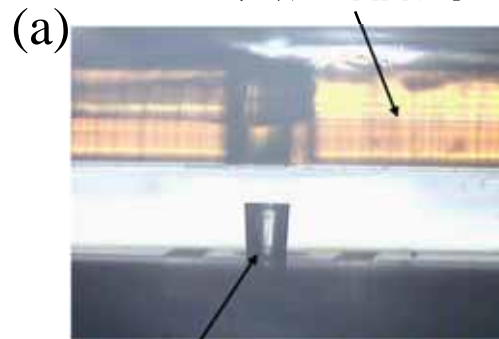
Filling Process



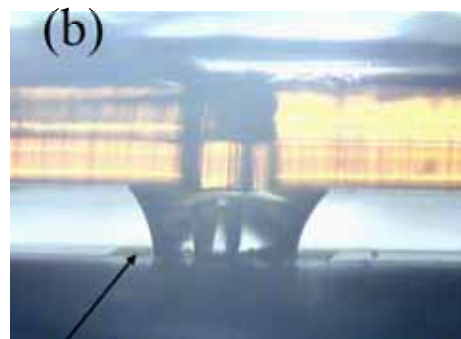


Teflon疏水區隔防止填充時側向擴散

填充晶片



導棒

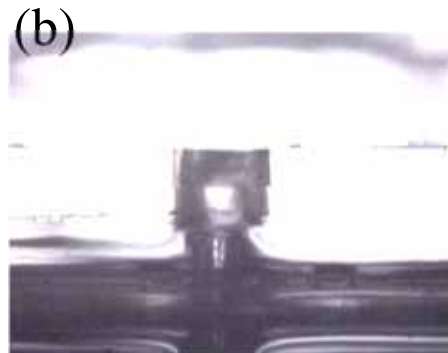


Teflon 疏水區隔微流道



液珠

有
Teflon作
疏水區隔



(c)



100um

無
Teflon作
疏水區隔

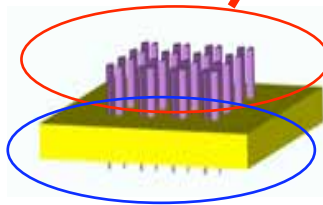
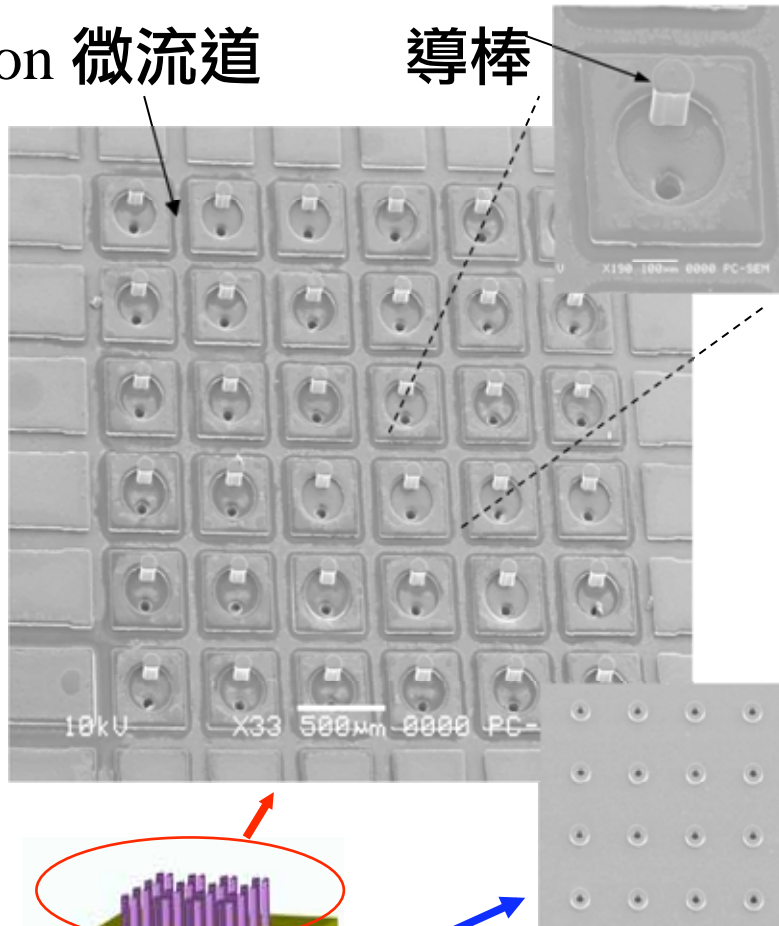


微陣列壓印晶片

Teflon 微流道

導棒

A



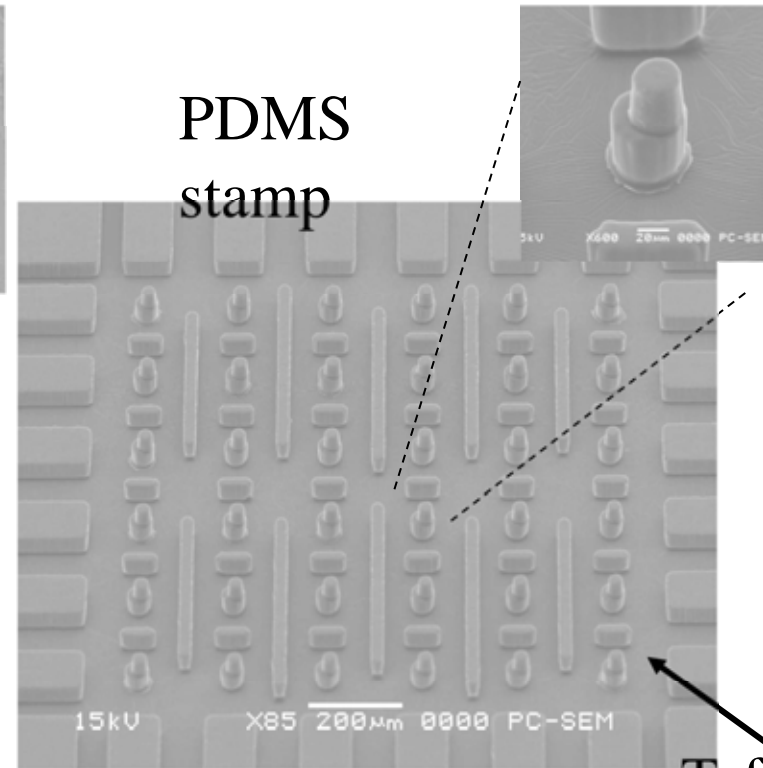
Type A Connector-filling micro
stamper



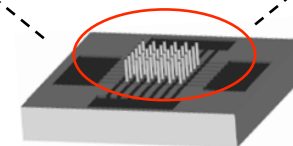
µ-Nano Bio & fluidic Systems Lab

PDMS
stamp

B



Teflon
微流道

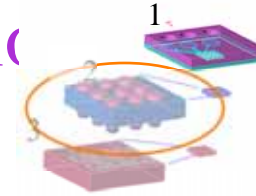


Type B PDMS stamp-
filling

Prof. Fan-Gang Tseng

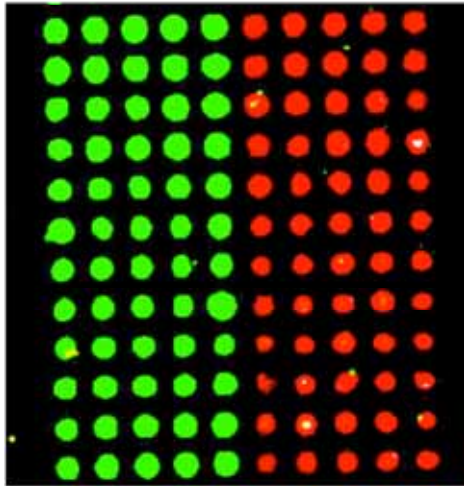


2. Stamp different types solutio simultaneously



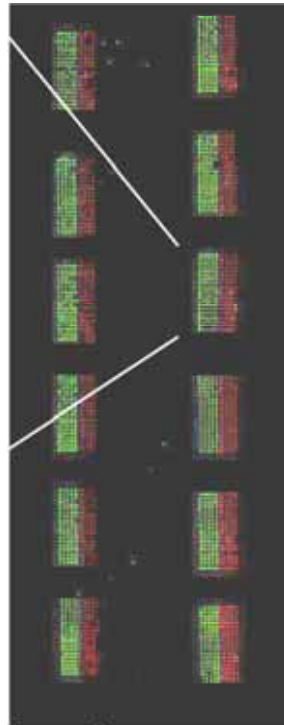
Stamp two types solution

Cy3 anti-rabbit IgG, Cy5 anti-mouse IgG



120 points array

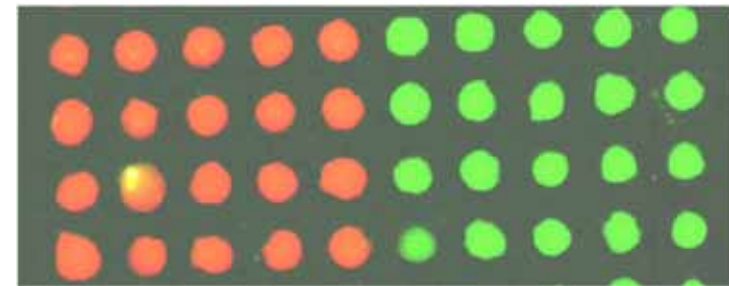
Cy3 10^{-3} ; Cy5 10^{-1}



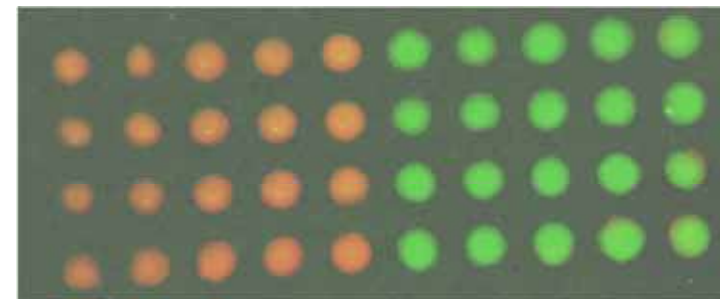
Continuous
printing 12 times

Stamp 4 types solution

Concentration: Cy5 10^{-1} ; Cy3 10^{-3}



200μm



Cy5 10^{-2} ; Cy3 10^{-4}

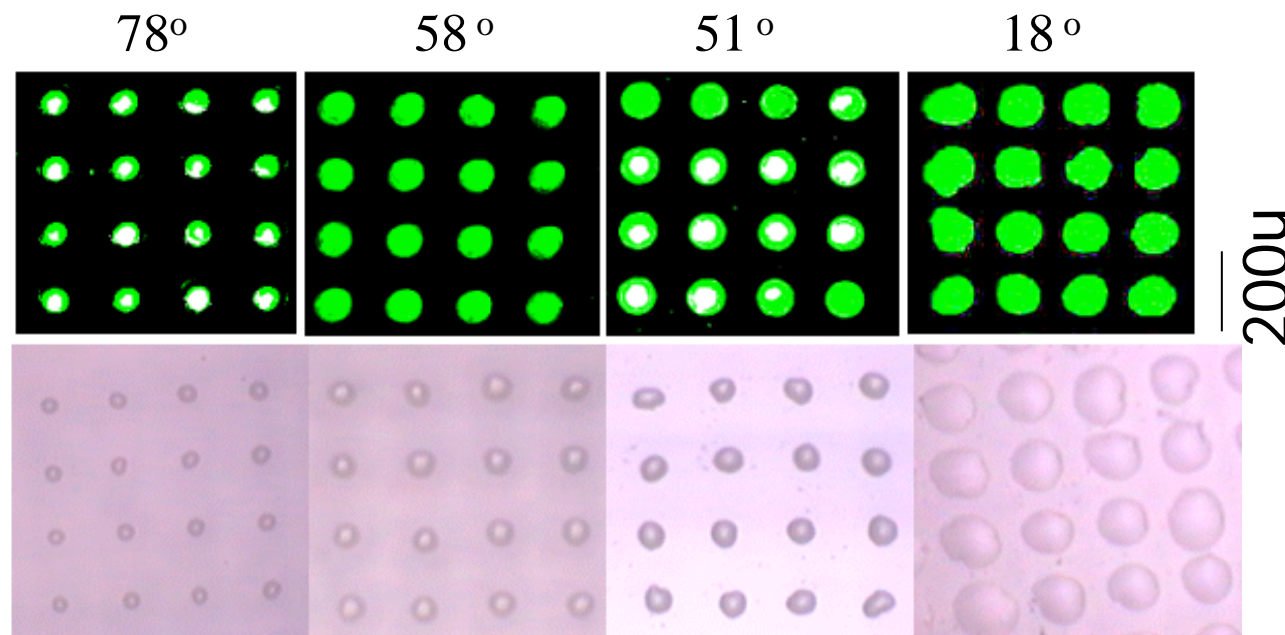
PBS solution with 30% glycerol

C Lin, F. Tseng, and C. Chieng, S&A B, 2004.



Protein Stamp result on substrates with different wettability

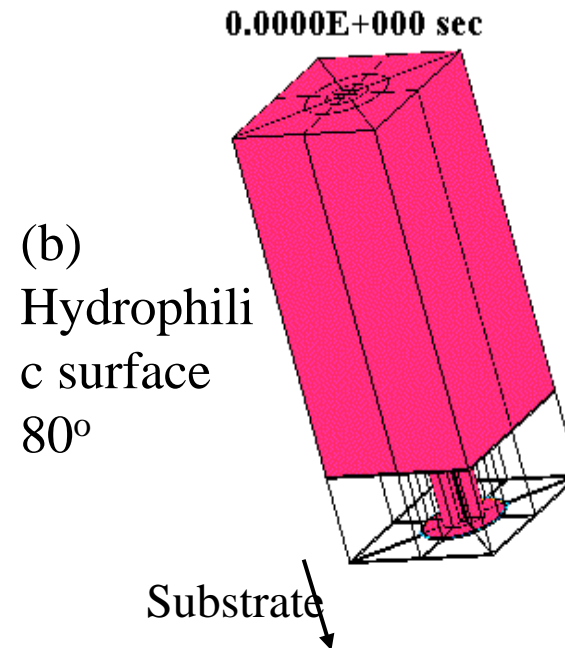
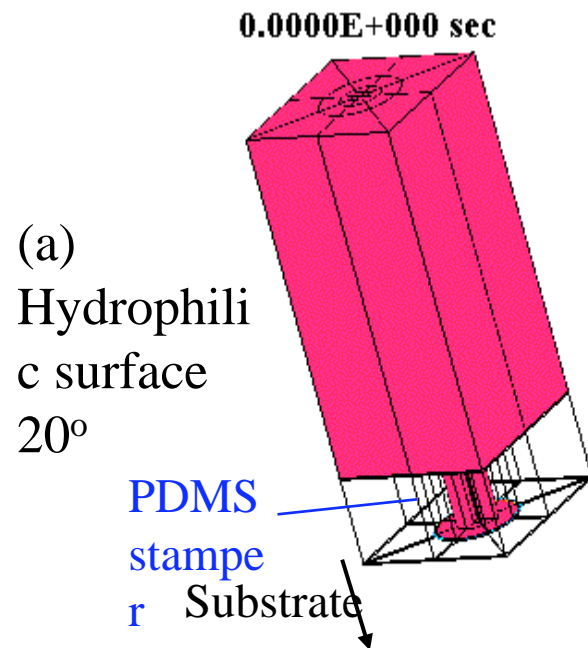
- The drop size increases with the wettability of the chip surface. Observed from fluorescent scanner and optical microscope.



Su8 photo resist APTS+DSC APTS+BS³ Glass

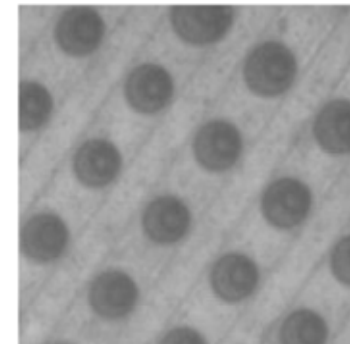


Simulation of drop formation process



- Substrate wettability effect the drop size

Experiment



Flow channel filled with sample fluid

Drop formation



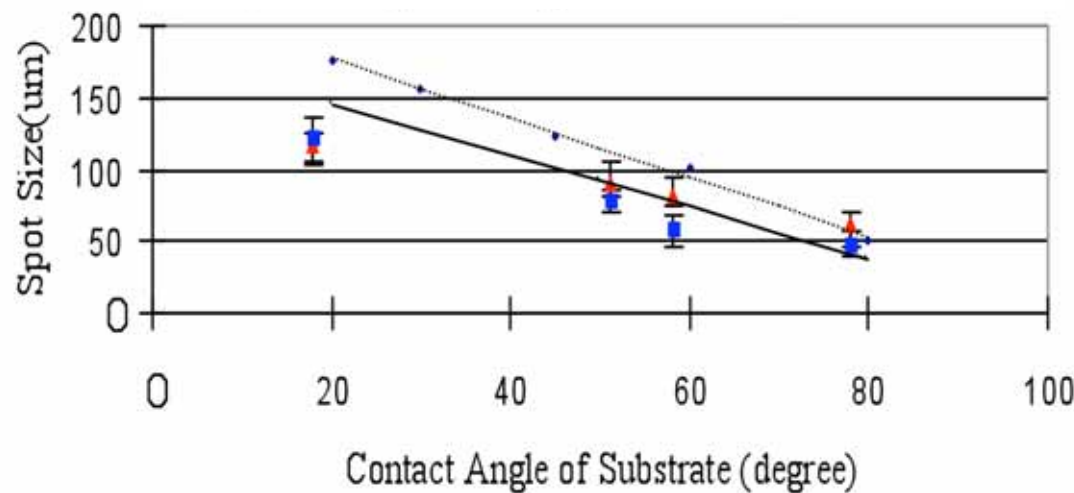
PDMS stamper



Substrate



Comparison of Computed and Measured Spotsizes on various SubstrateSurfaces



Simulation

--- solution

viscosity (1.02cp)

— solution

viscosity (3.20cp)

Experiment

▲ fluorescent
observation spot

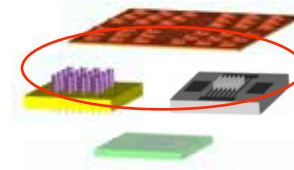
■ optical
microscope observed
spot PBS
+30% glycerol
solution(viscosity
3.20)

On different wettability of surface, the spot size of soft printing decrease with the decreasing of the surface wettability.

C. Ho, F. Tseng, and C. Chieng, J MM, 2005.

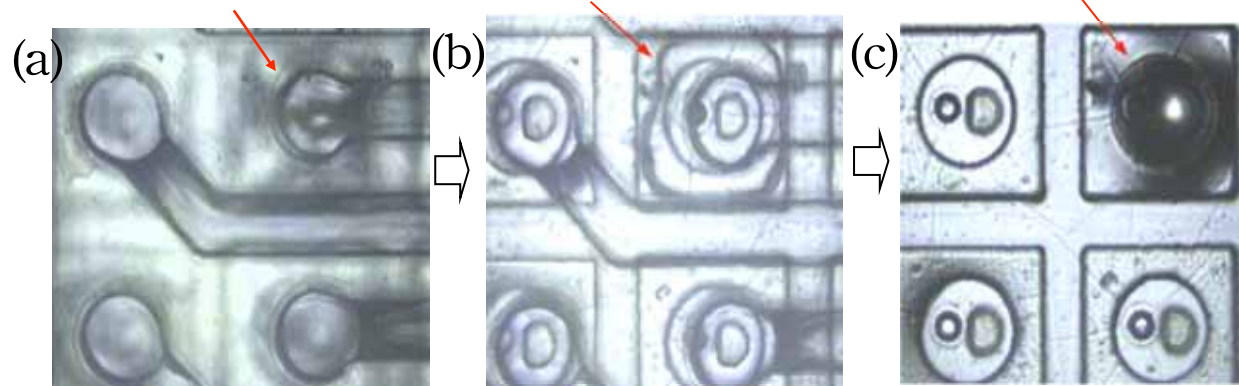


晶片結合填充過程

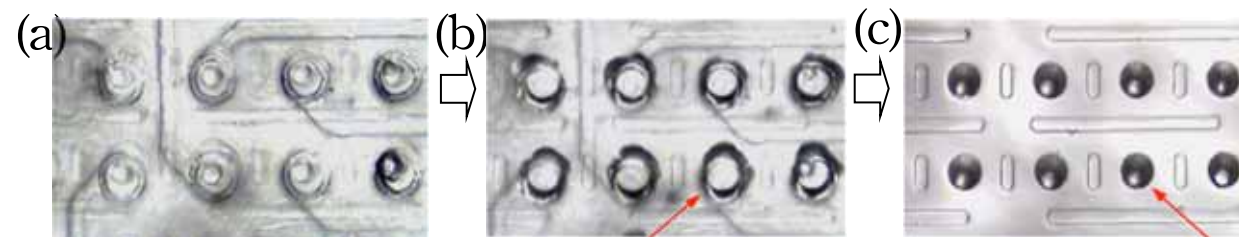


填充晶片之填充孔液面被限制住無擴散液體留在導棒上

Type A



Type B



fluid boundary

fluid left on the PDMS stamper

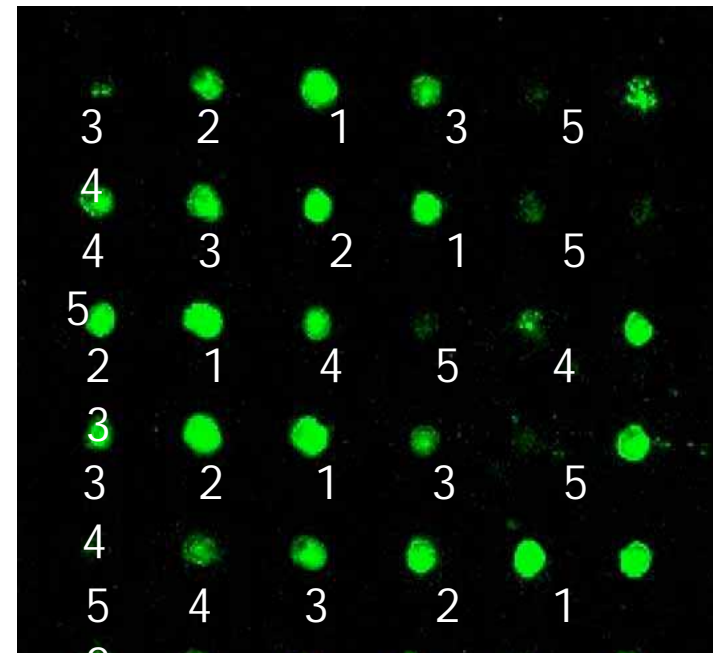
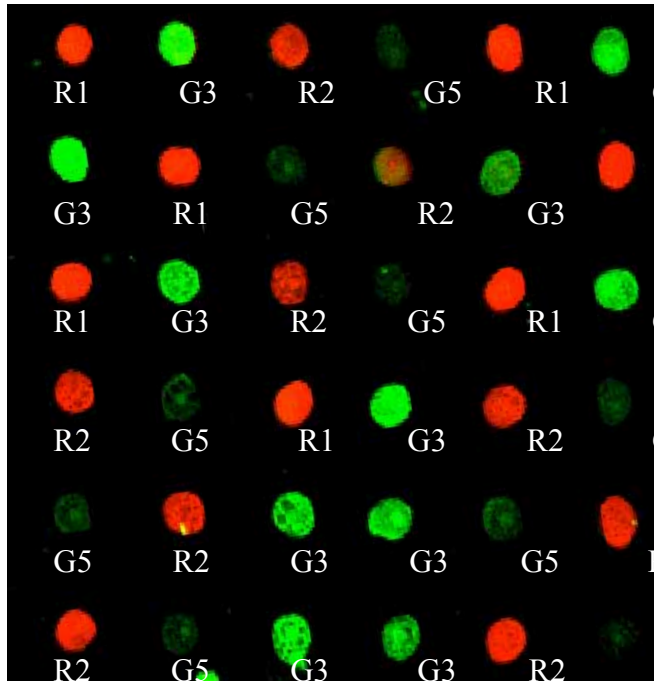
填充晶片與
壓印晶片結
合填充時

液體被週遭
Teflon 所限制住，
無擴散

填完後 移開填充晶
片，液珠留在壓印
晶片上



PDMS同時平行一次蓋印多種之結果



200μm

R1: anti-mouse IgG cy5 0.6mg/mL,

R2: anti-mouse IgG cy5 0.1 mg/mL,

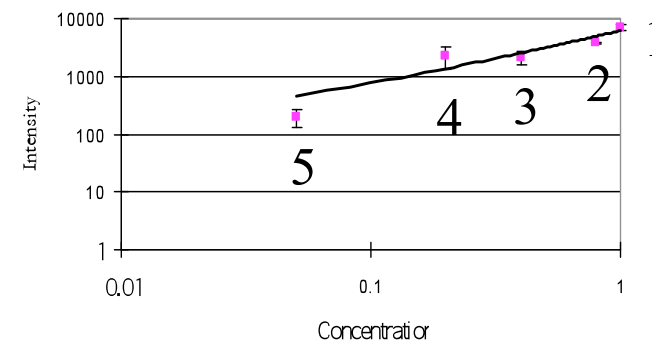
G1: anti-rabbit IgG cy3 1.0mg/mL

G2: anti-rabbit IgG cy3 0.8mg/mL,

G3: anti-rabbit IgG cy3 0.4mg/mL,

G4: anti-rabbit IgG cy3 0.2mg/mL,

G5: anti-rabbit IgG cy3 0.05mg/mL,



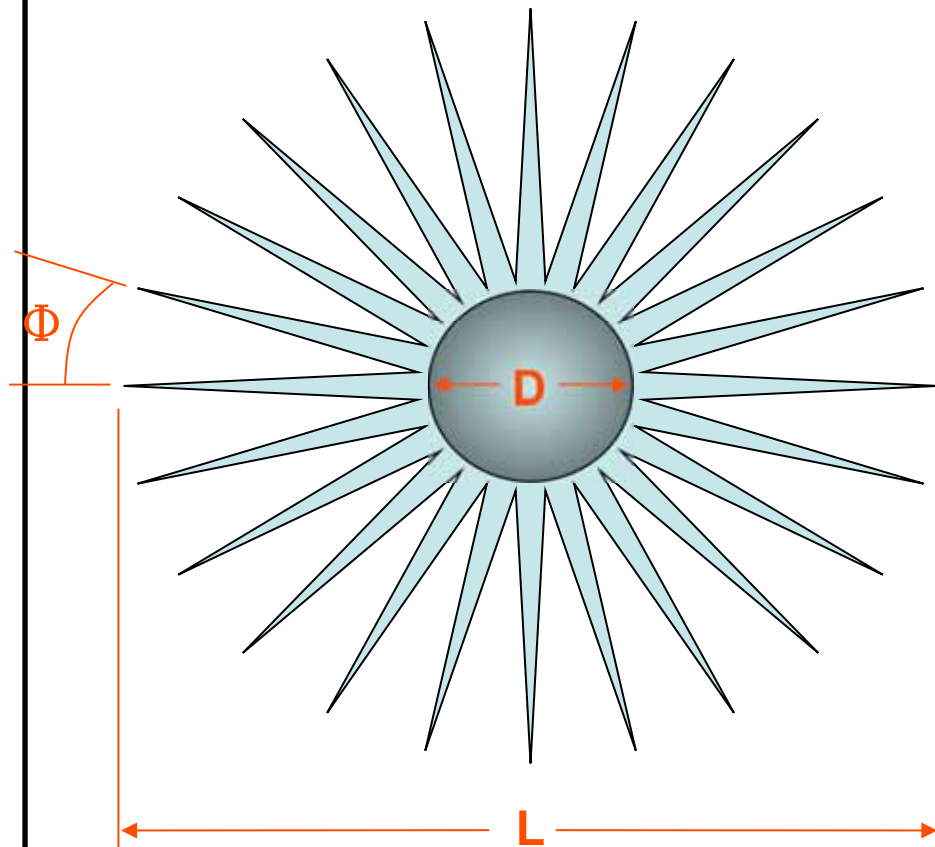


E. 三微奈米結構梯度引發之 快速液珠自推動系統

曾繁根



Multiple Dispensing on the Same Spot



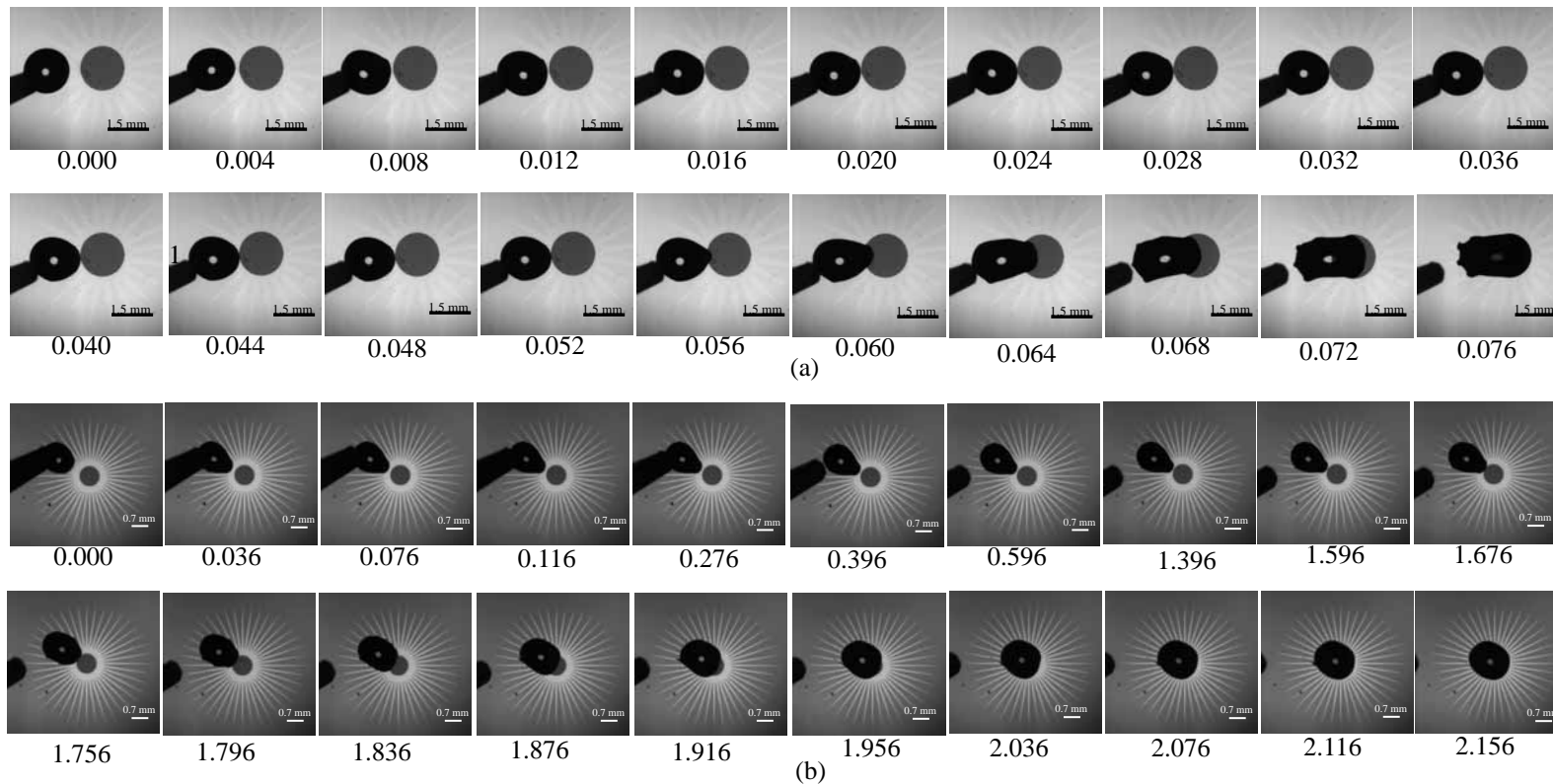
hydrophobic
 In between
 hydrophilic

Parameter Type	L (mm)	D (mm)	Φ (°)
Dual SAMs	6.0	1.5	18
Single SAM	5.0	0.7	9

Design of Double SAMs and Single SAM Systems



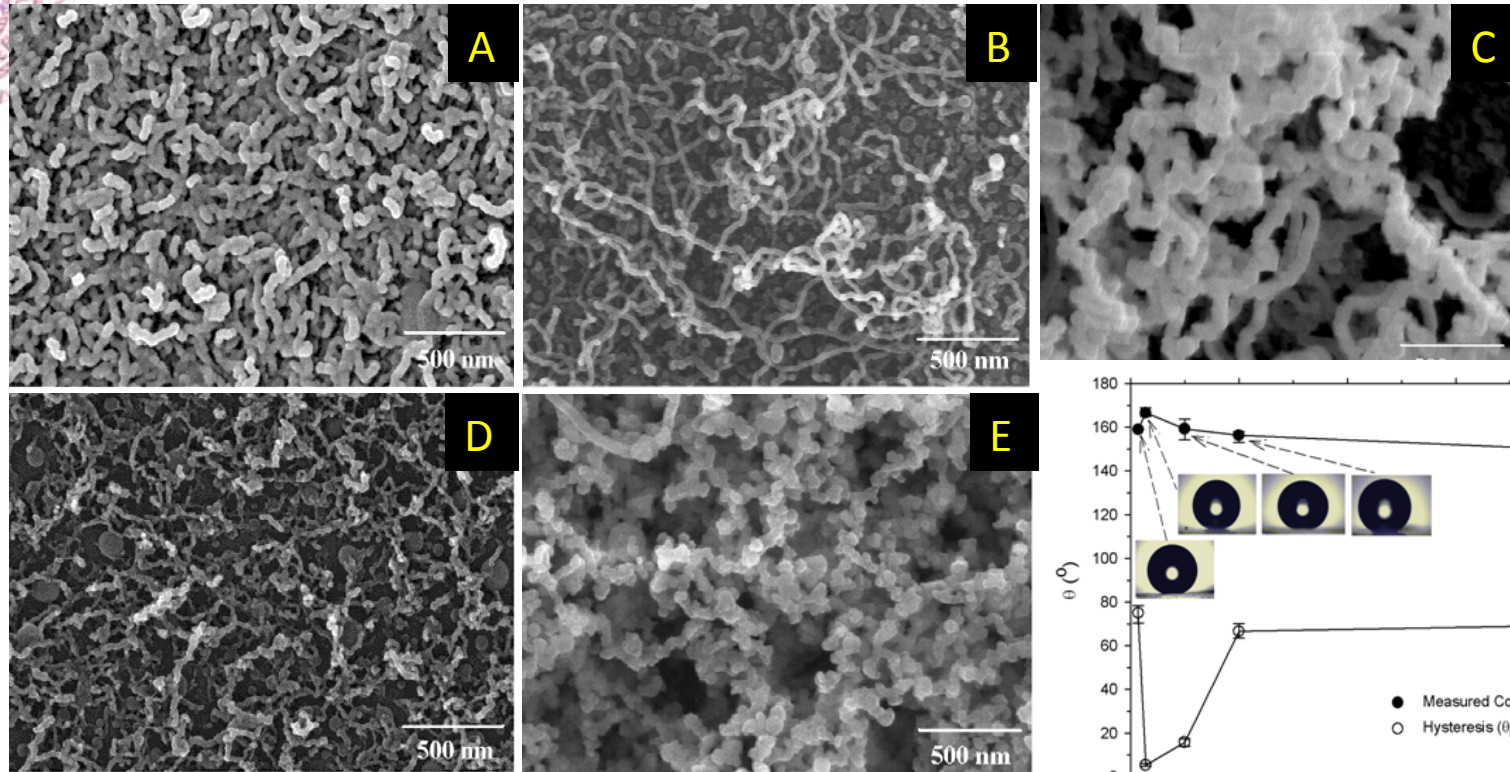
Self-Directed Movements of Droplets on Radially Patterned Surfaces Based on Self-Assembled Monolayers (Cont'd)



The motions of (a) 1.1 μ L DI water droplet on the **dual SAMs** and (b) 0.4 μ L DI water droplet on the **single SAM** systems taken using high speed CCD camera with a speed of 250 frames/sec (units in sec).



3D Nano-Textures of Methyltrichlorosilane (MTS)

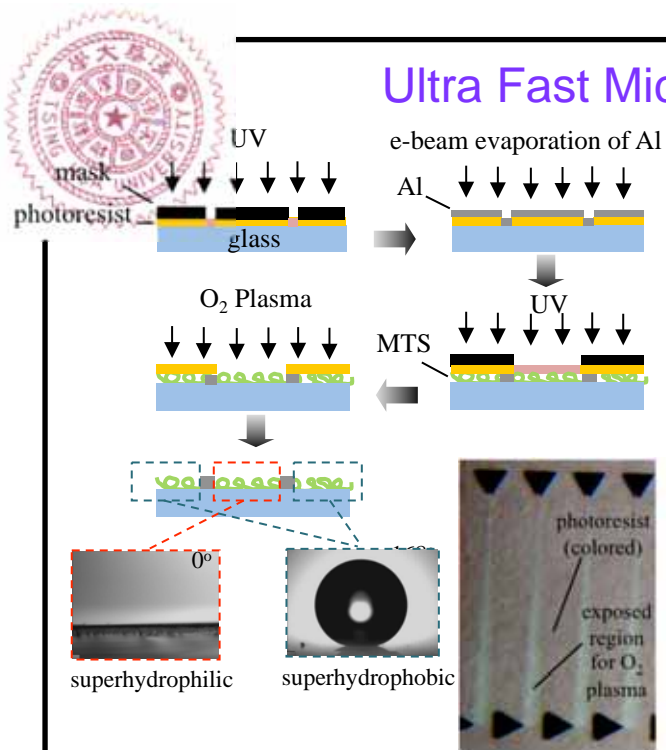


superhydrophobic

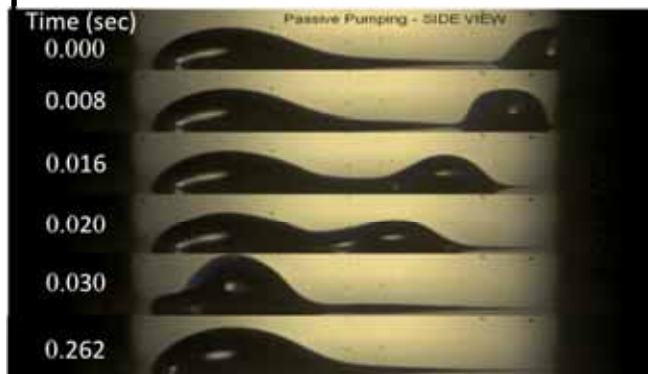
SEM images, static contact angles and hysteresis of methyltrichlorosilane (MTS) fibers generated under various concentrations at 2 h and 60%RH: A) 0.007 M; B) 0.014 M; C) 0.05 M; D) 0.1 M; E) 0.5 M.

Three-dimensional nano-architectures with varying shape, morphology and size were fabricated by the phase separation of methyltrichlorosilane (CH_3SiCl_3) on commercially available glass substrates.

Ultra Fast Micro- and Nano-Liter Droplet Manipulations



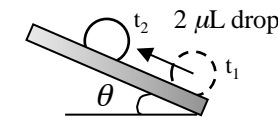
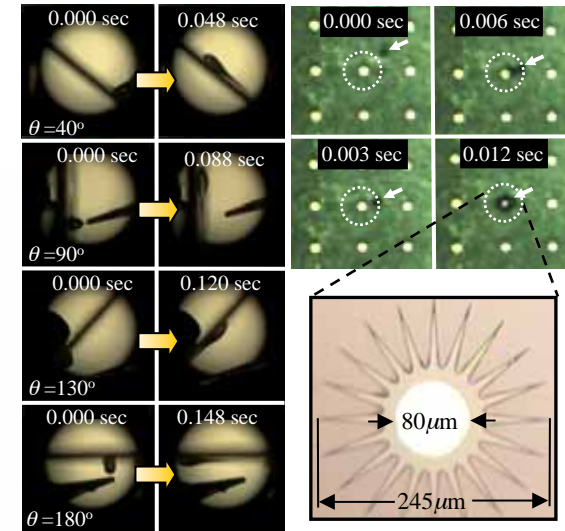
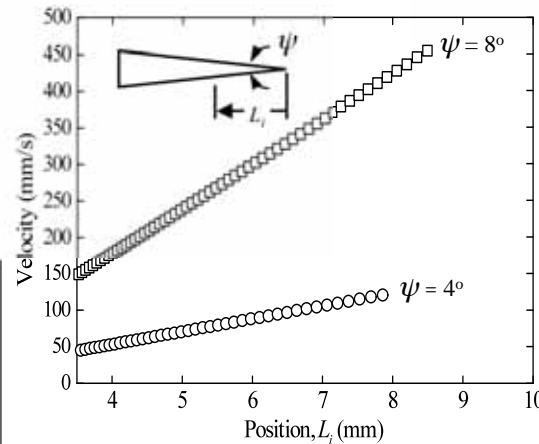
Fabrication Method



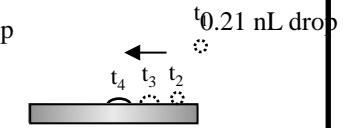
Passive pumping of a 2 μL water droplet;
 $\psi = 8^\circ$ and $L=12\text{ mm}$



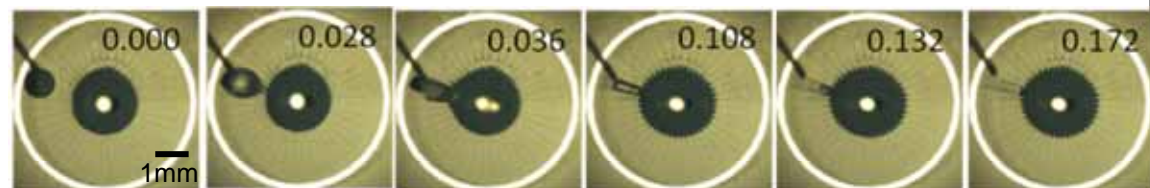
2 μL water droplet,
 $\psi = 4^\circ$, and $L=12\text{ mm}$



2 μL surface-
ascending water
droplet; $\psi = 8^\circ$ and
 $L=12\text{ mm}$



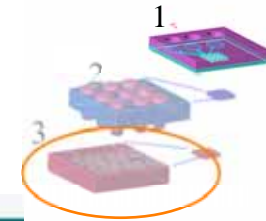
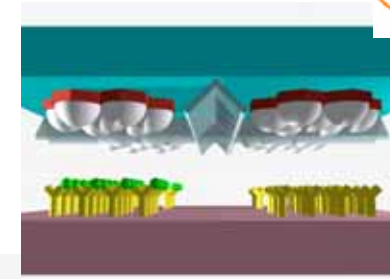
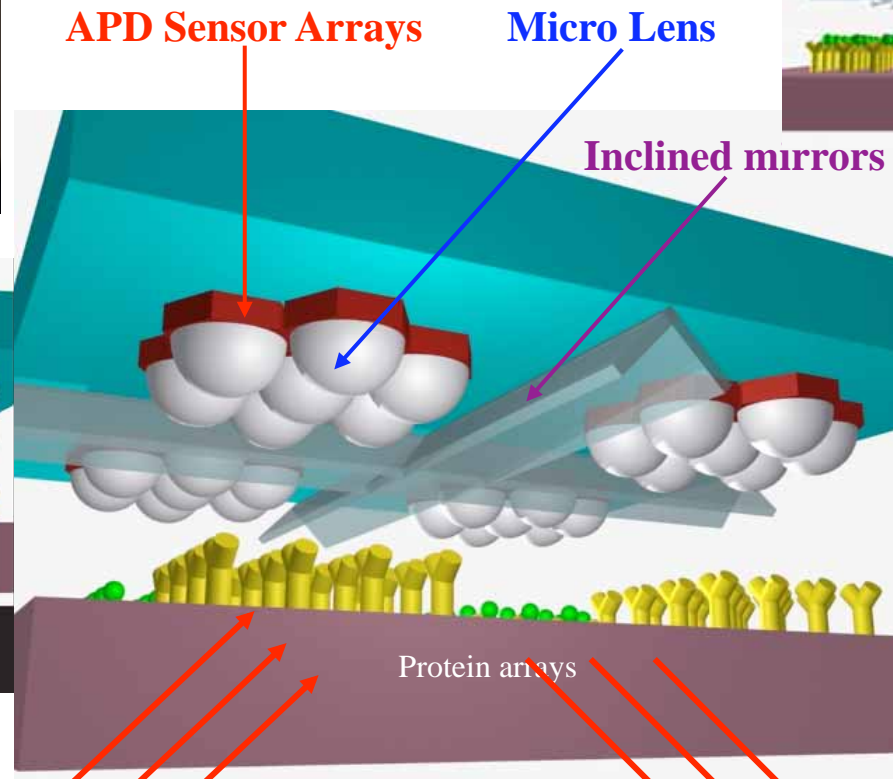
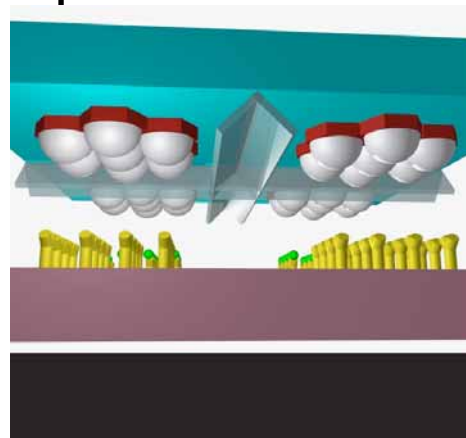
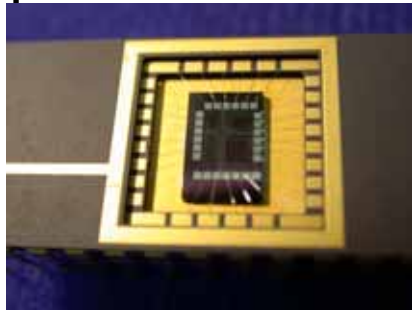
0.21 nL water droplet
movement



Droplet coalesce for mixing of a 2 μL water droplet (numbers is time in sec)

5. Bio-detection Chip

Micro Bio-Optics

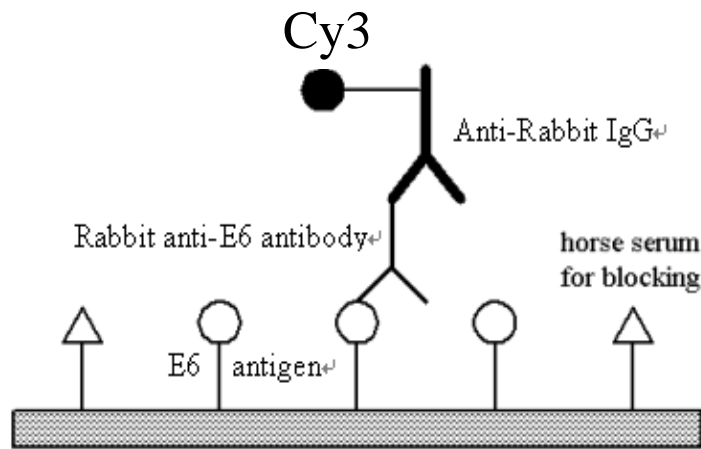


Characteristic:

1. In parallel detection
2. Fast
3. Near distance
4. Evanescent wave excitation, low background



ELISA of tumor marker test result



- Hurp: liver cancer antigen
- E6 Papillomavirus antigen

ELISA (Enzyme linked immunosorbent assay) bio-reaction detection.

Hurp
250ng/ul

E6
38ng/ul

Hurp 125ng/
ul

E6 76ng/
ul

Hurp
1ng/ul

Hurp
60ng/
ul

Hurp
30ng/ul

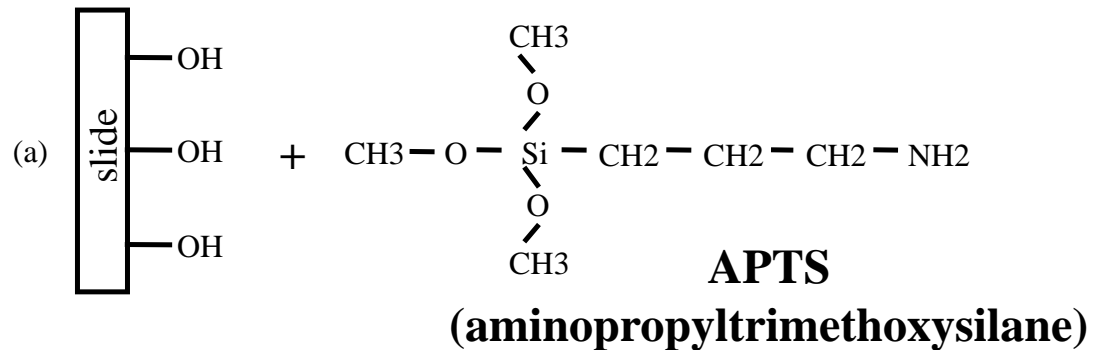
Hurp
100ng/ul



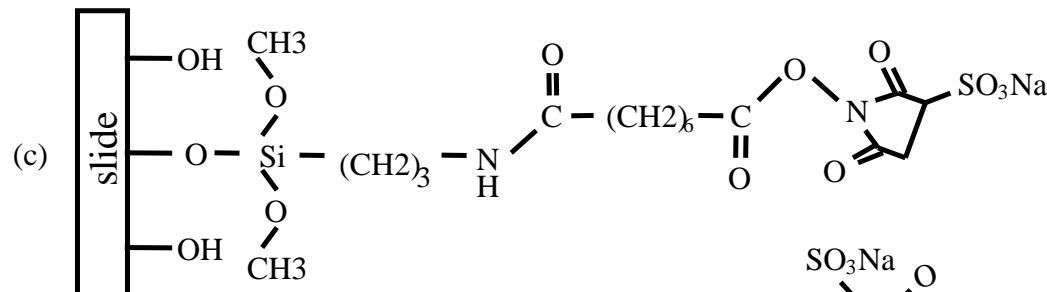
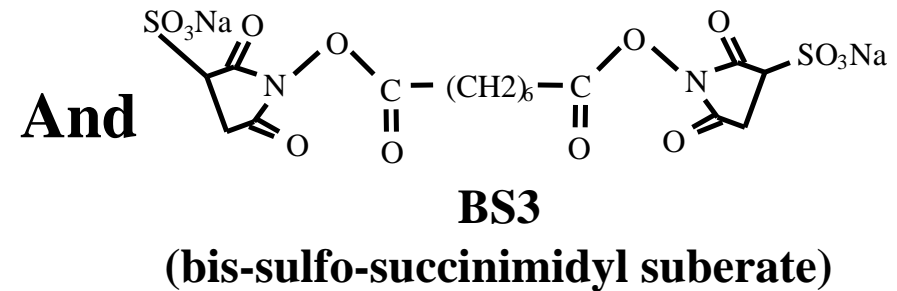
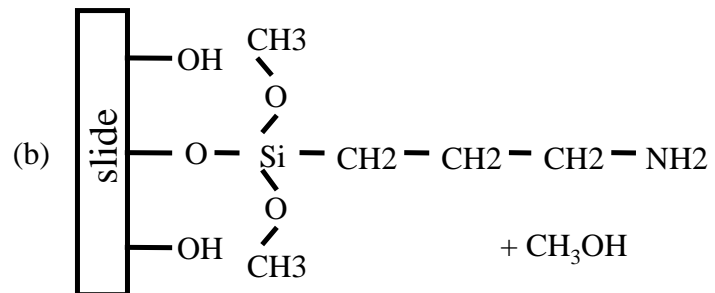
Protein Binding Efficiency Improvement by Mixed SAMs



Single SAMs for Protein binding

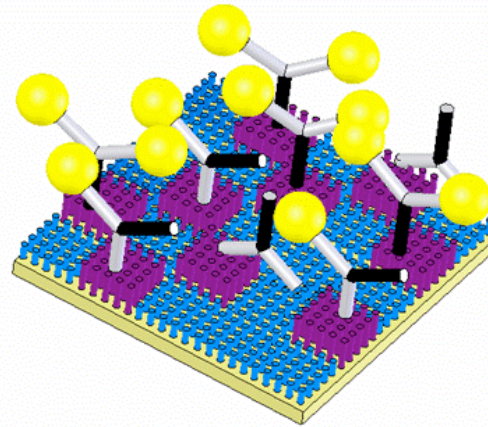
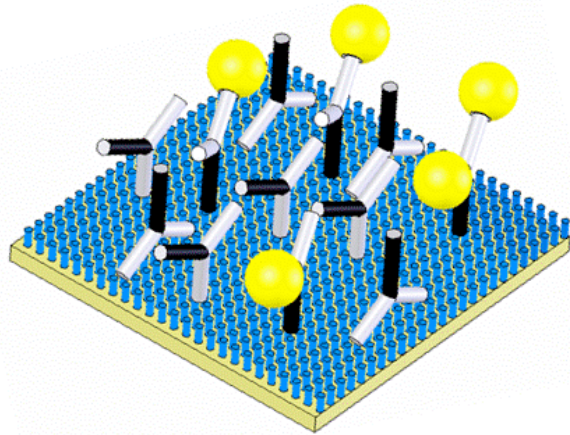


Methoxyl group
reacted with
hydroxyl group

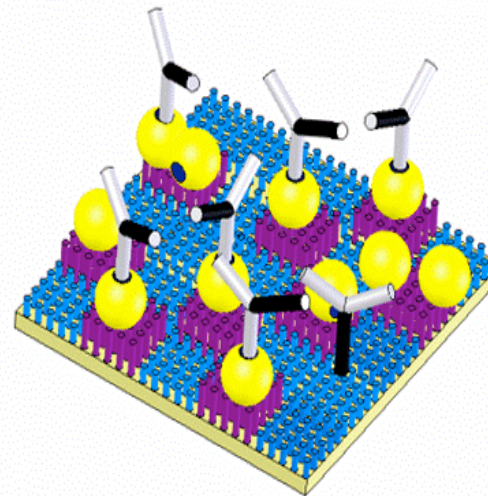
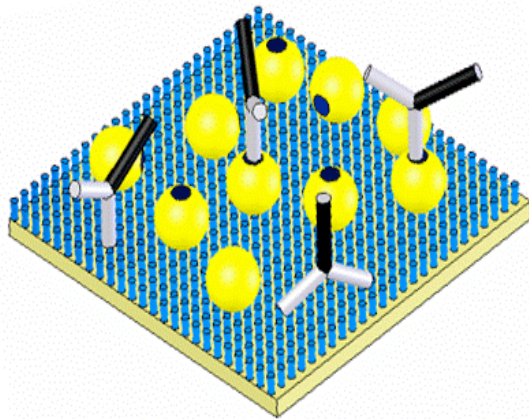




Antibody recognition/binding efficiency on protein chip



The schematic diagram of the principle for the improvement of recognition efficiency of antibody to antigen by mixed SAMs surface.

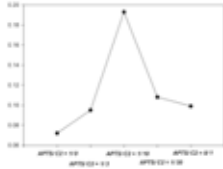


The schematic diagram of the principle for the improvement of binding efficiency of antibody to antigen by mixed SAMs surface



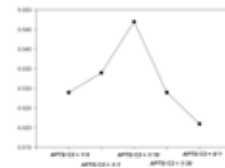
Antibody recognition/binding efficiency measurement by SPR and Fluorescence for different Mixed SAMs

The Recognize Efficiency Of Antibody to Antigen



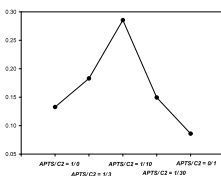
SPR
2.68

The Binding Efficiency Of Antibody to Antigen



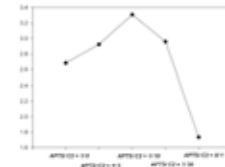
SPR
1.62

The Recognize Efficiency Of Antibody to Antigen

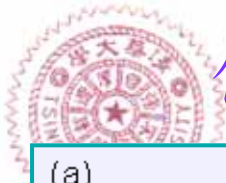


Fluorescence
2.15

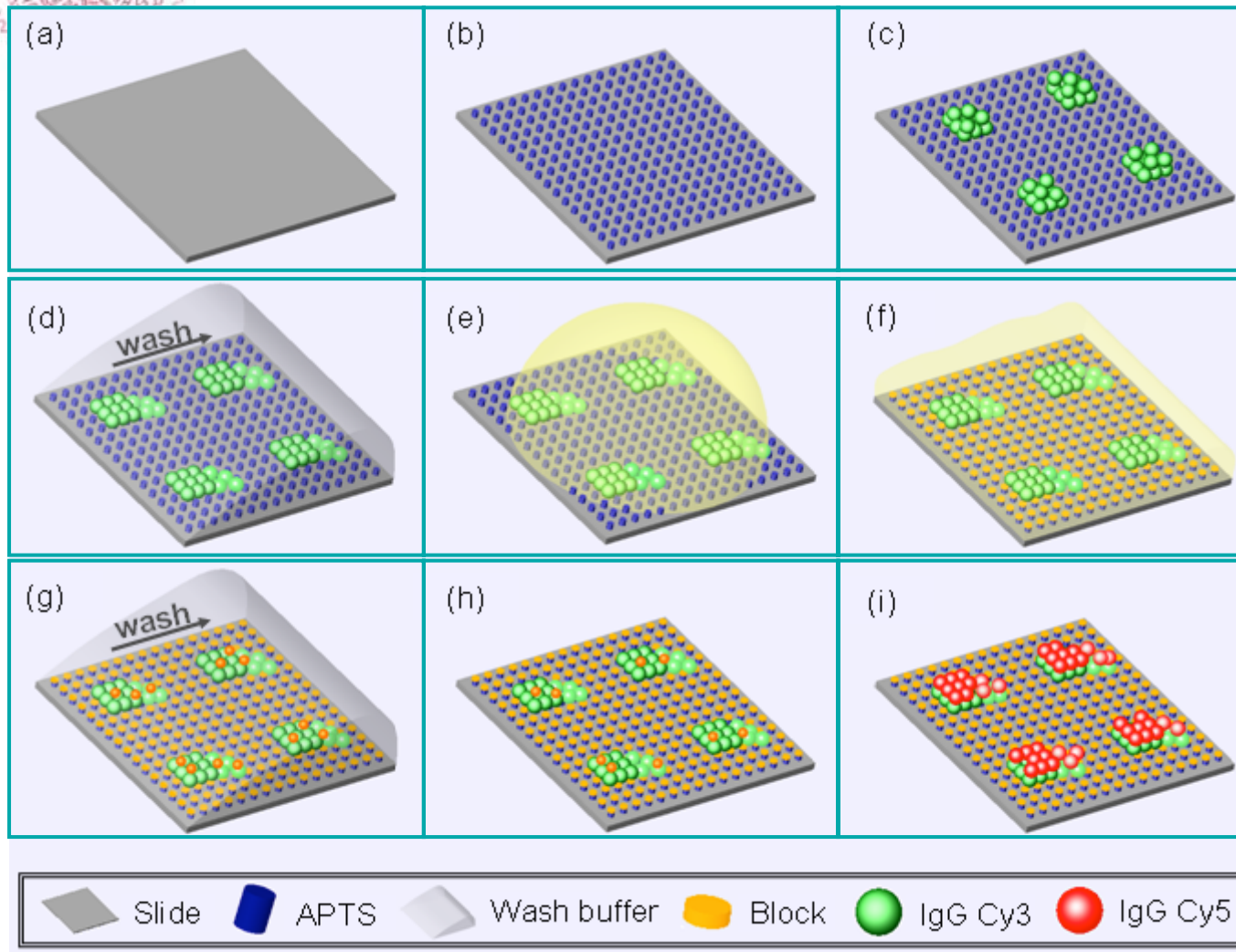
The Binding Efficiency Of Antibody to Antigen



Fluorescence
1.233



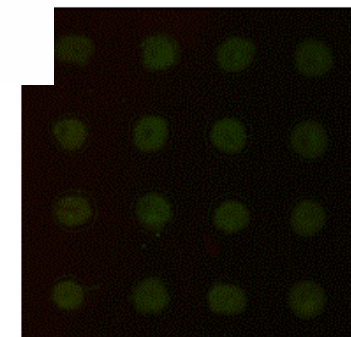
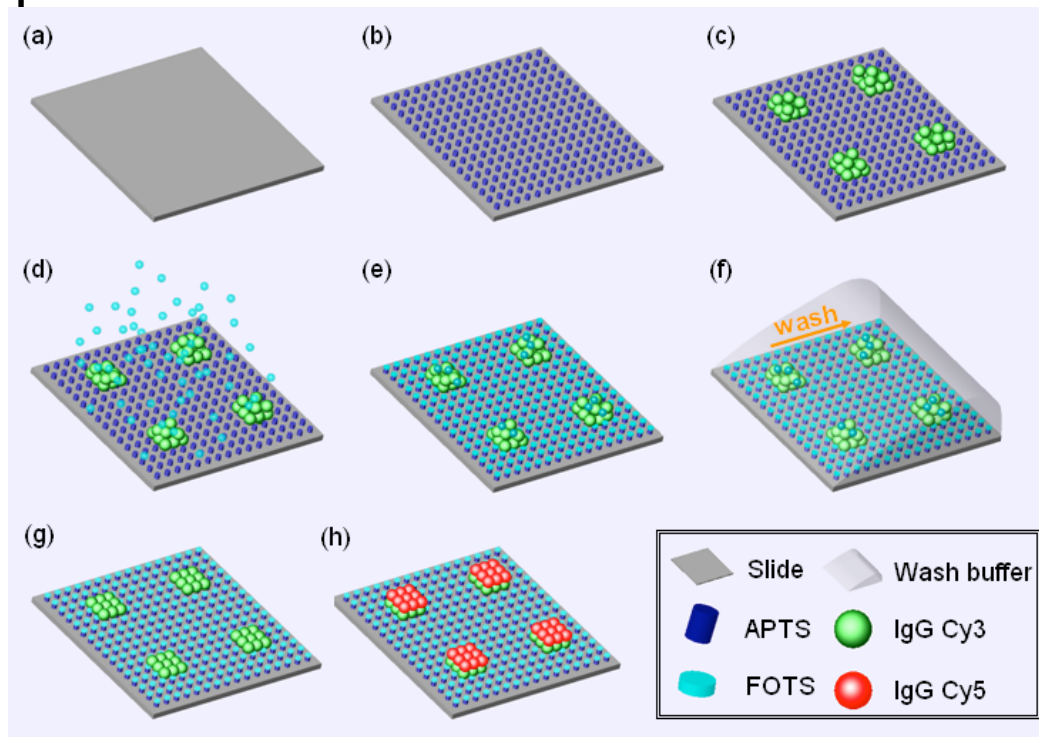
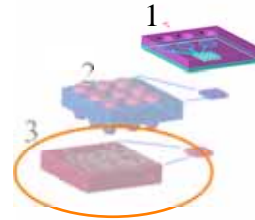
傳統採用生物血清於晶片上之鍵結阻絕實驗流程



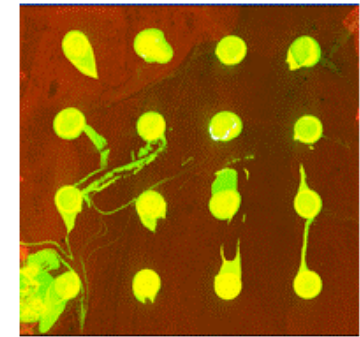
IgG Cy3 (第一級抗體) : Rabbit anti-mouse IgG Cy3

IgG Cy5 (第一級抗體) : Goat anti-rabbit IgG Cy5

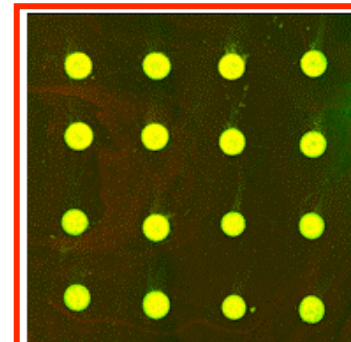
Vapor phase bio-blocking



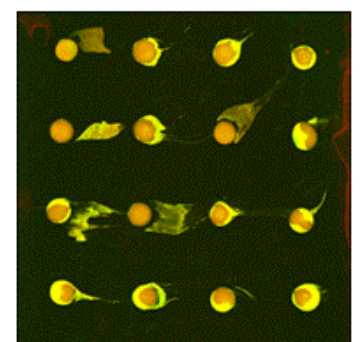
SiO₂_no block



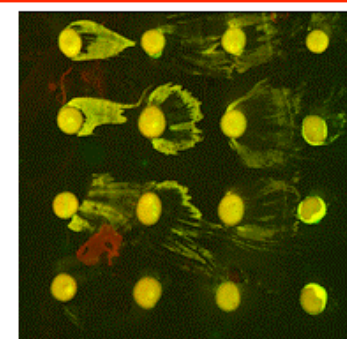
APTS_no block



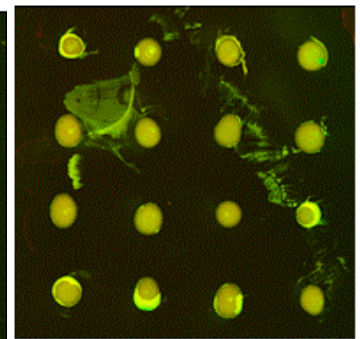
FOTS



BSA



MILK



HS

Binding time improved from hours to 5 minutes, efficiency improved by 2-4 folds!!!, no tailing issue!



奈米國家型科技計畫學術卓越創新研究計畫

Atto-Liter侷限空間激發及表面張力/電動力高度分子集中之單一分子奈米陣列酵素動力分析

The Kinetics/Dynamics of Single Enzyme Molecule Array
Excited in aL-Confined Volume Reacted
with Surface Tension/Electrokinetic Concentrated Substrates

計畫主持人: 曾繁根 教授, 國立清華大學/工科系, 奈米工程與微系統所
中央研究院/應用科學中心
奈微米生醫系統, 奈微米流體物理(總計劃及子計畫一)

計畫共同主持人: 潘榮隆 院長/講座教授, 國立清華大學/生命科學院
單一分子奈米陣列之酵素動力學研究(子計畫二)

計劃共同主持人: 魏培坤 副研究員, 中央研究院/應用科學中心
近場侷限空間螢光激發及單分子遠場觀測(子計畫三)

06.5.2009



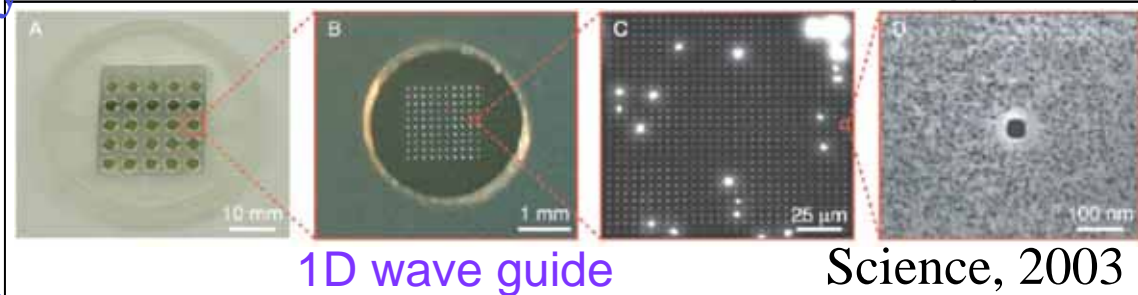
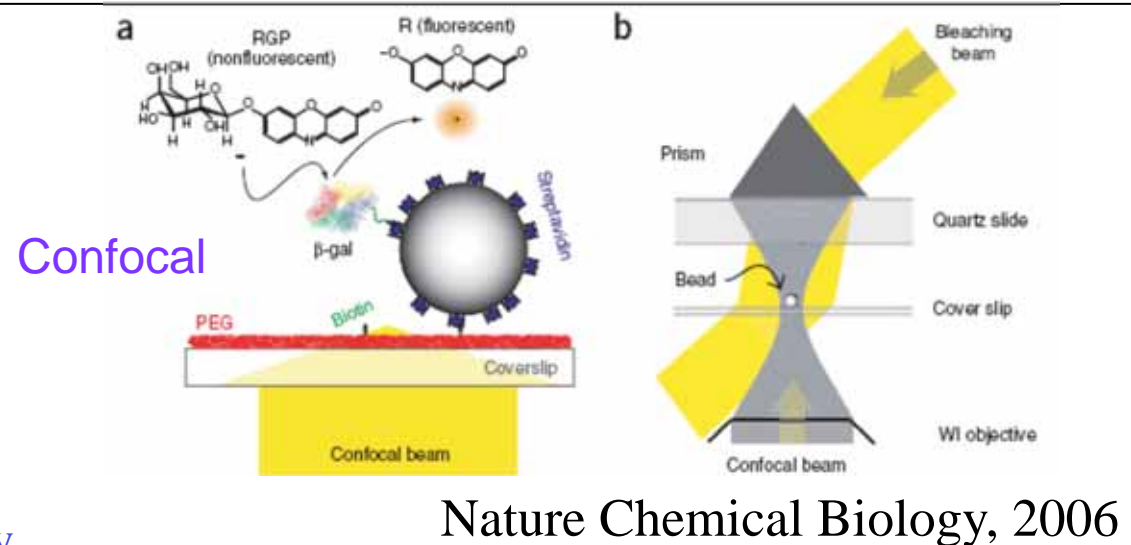
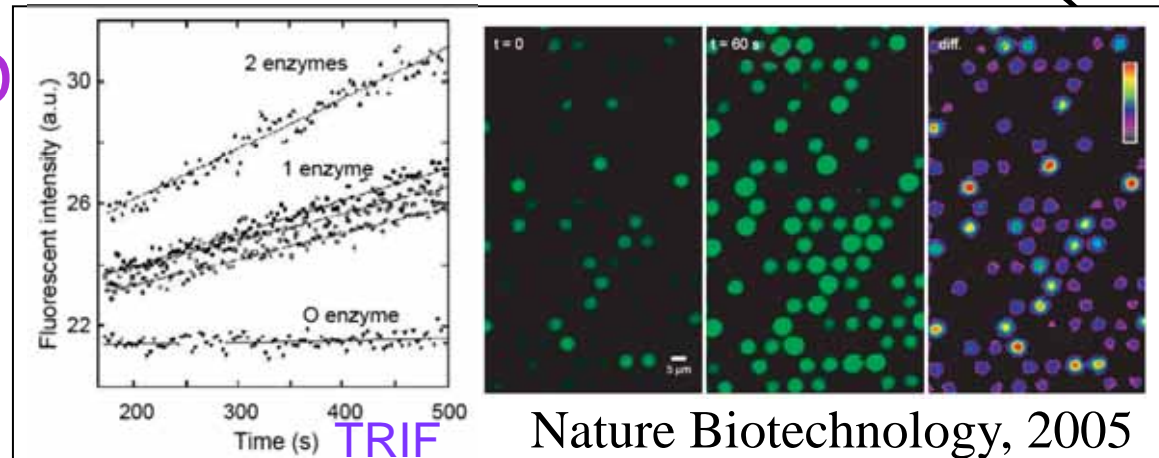
Importance and Limitation of SMD

Advantages:

1. Single molecule events possible
2. Low background noise
3. Low-middle concentration
4. High parallelism

Disadvantages:

1. Ambiguity of single molecule immobilization/reaction
2. Random distribution
3. Low possibility of single molecule event-huge effort to obtain statistically meaningful data
4. long observation time -not easy for dynamic observation
5. Numbers of proteins on a cite (chamber, bead)
6. Low dynamic range





Motivation and Objectives

How to obtain **non-ambiguous** single molecule events in **high dynamic range**, **very low background level** and **high efficiency**?

Keys to answer the above questions:

1. **True** and **controllable** single molecule immobilization at the binding site
2. **Large array** - High parallelism
3. **Fluidic concentration** - Increase reaction possibility
4. **Nano-localized** signal excitation



1.重要研究成果

- A. 利用分子級掀離技術製作特殊奈米金球陣列結構以增強螢光激發訊號 (曾繁根 魏培坤)
- B. 配合單一奈米金修飾之掃描探針顯微術及其單分子檢測之應用 (曾繁根 潘榮隆)
- C. 奈米金屬結構之侷域性表面電漿共振應用於次波長之光捕捉 (曾繁根 魏培坤)
- D. 奈米金球增強訊號之連續式光纖免疫感測器(曾繁根 楊重熙)
- E. 三微奈米結構梯度引發之快速液珠自推動系統 (曾繁根)
- F. 利用奈米碳管與奈米流體蛋白質濃縮技術 (曾繁根 潘榮隆)



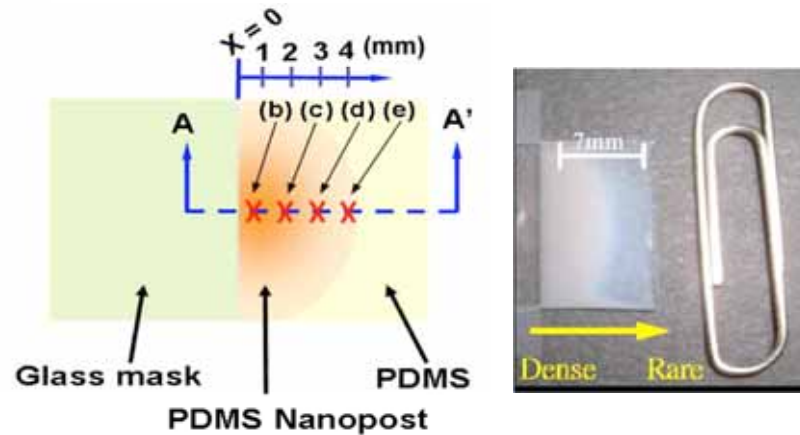
A. 利用分子級掀離技術製作特殊奈米 金球陣列結構以增強螢光激發訊號

曾繁根

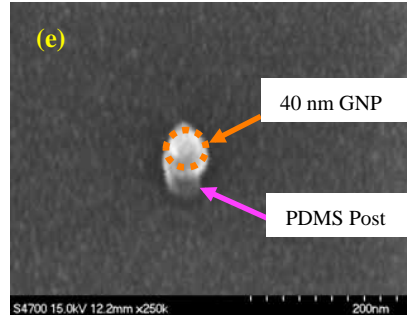
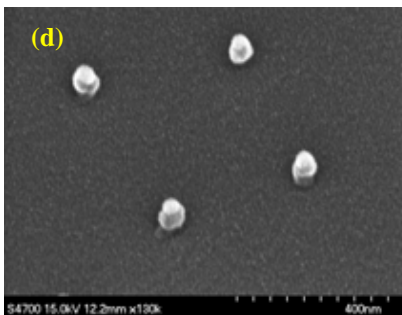
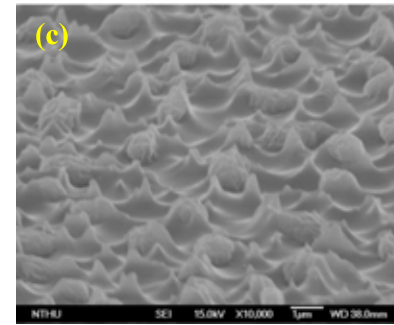
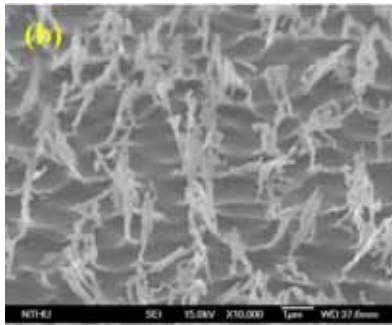
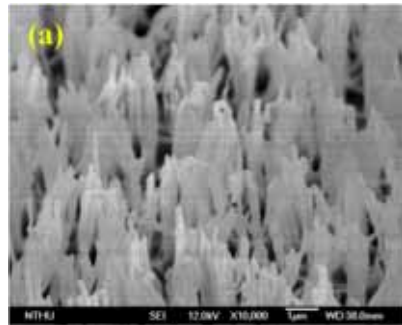


Preliminary Results

1. Self generated Nano PDMS structures (Tseng)

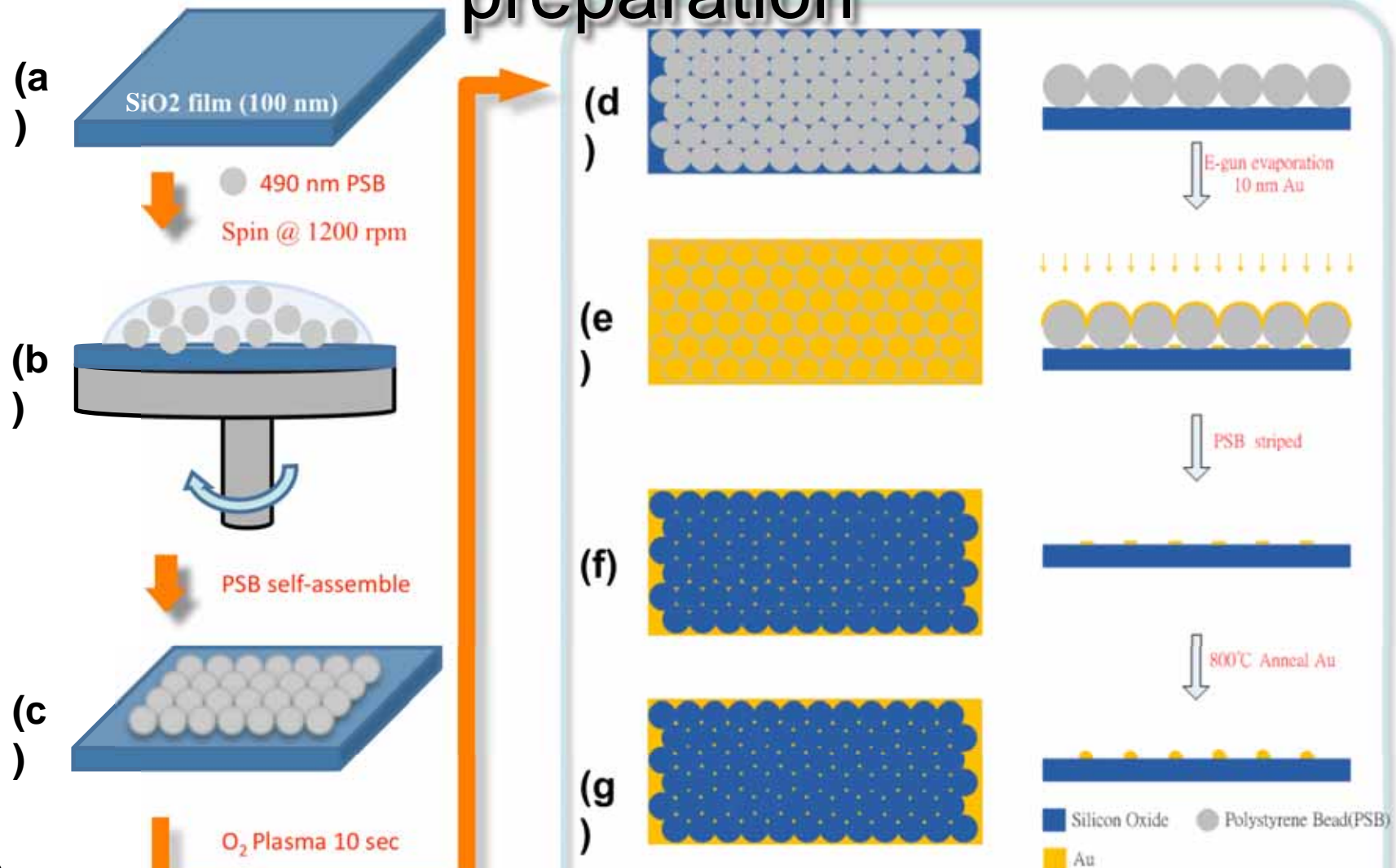


RIE etched PDMS surface with SiO_2 as a mask on the side. The density of the nano-posts decreases as the distance away from the glass mask region.



(a) SiO_2 mask/ $\text{CF}_4:\text{O}_2 = 5:3$; (b) SiO_2 mask/ $\text{CF}_4:\text{O}_2 = 5:6$; (c) Cu mask/ $\text{CF}_4:\text{O}_2 = 5:3$. (d) nano PDMS post array formed by gold nanoparticle as etching mask. (e) close-up of the nano post structure

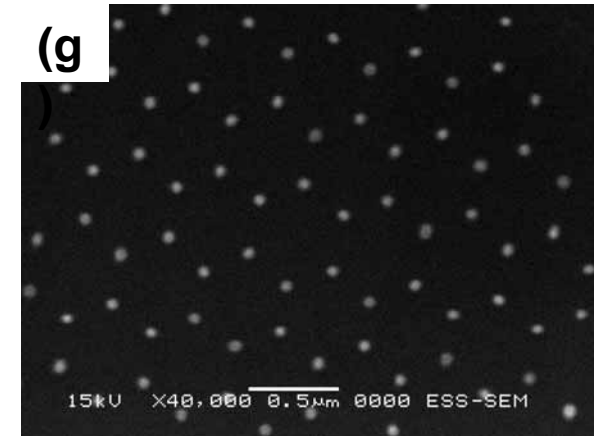
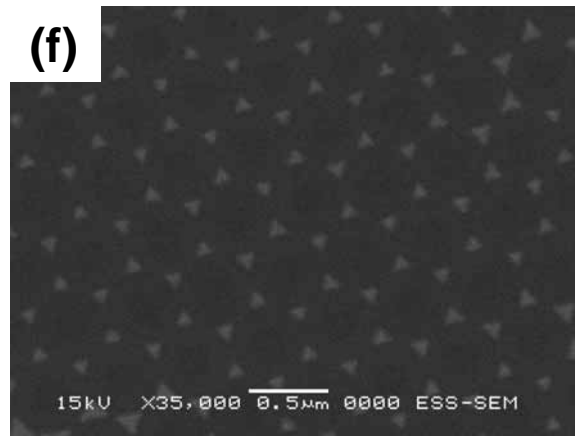
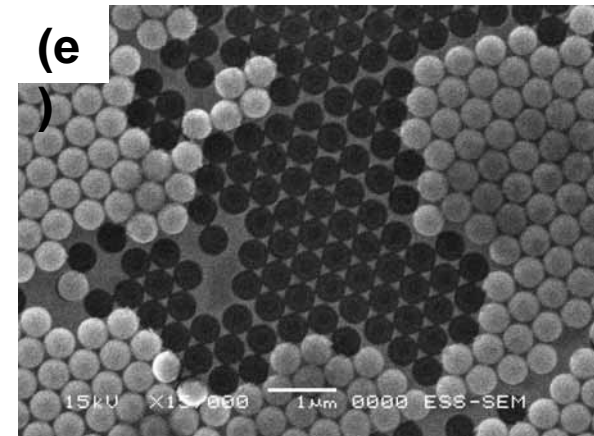
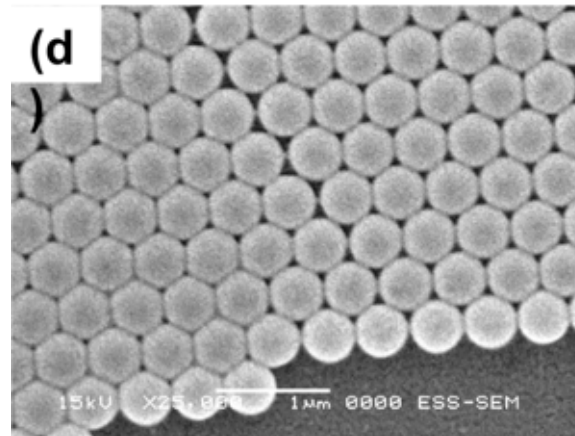
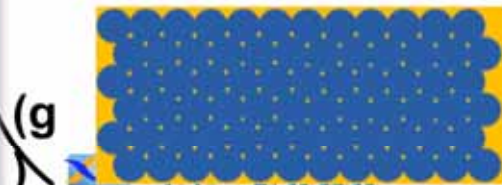
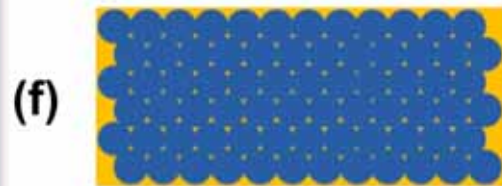
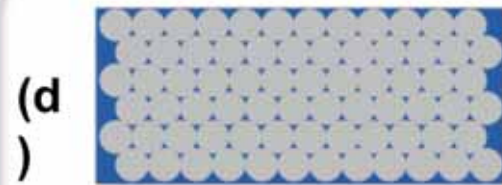
Topic #1 Ordered Au mask preparation





Topic #1 Ordered Au mask preparation

ESS/MEMS Institute



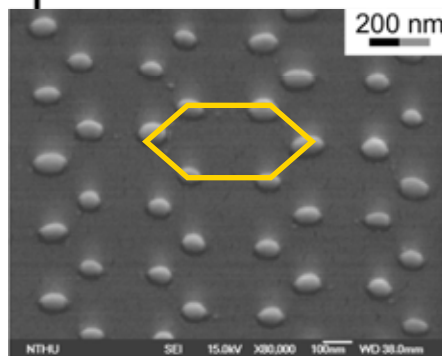
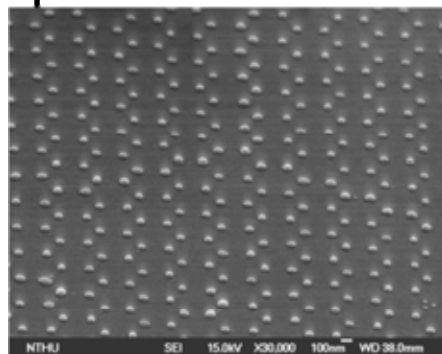
100 nm \pm 10nm

62.5 nm \pm 2.5nm

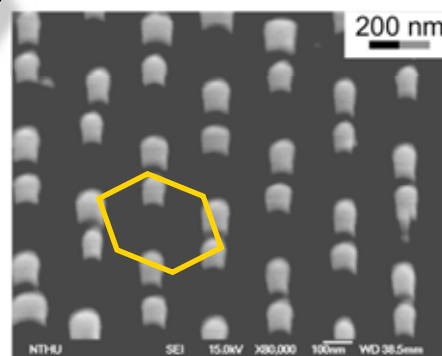
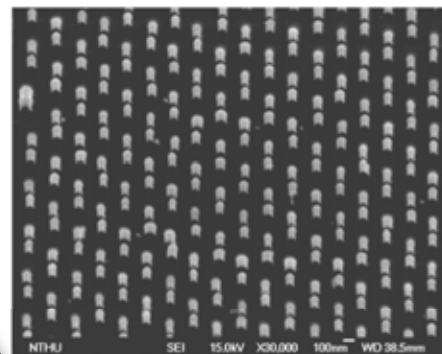


Nanocones formation

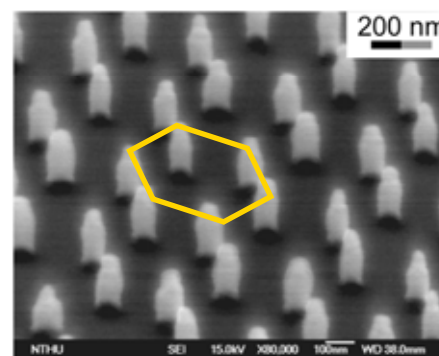
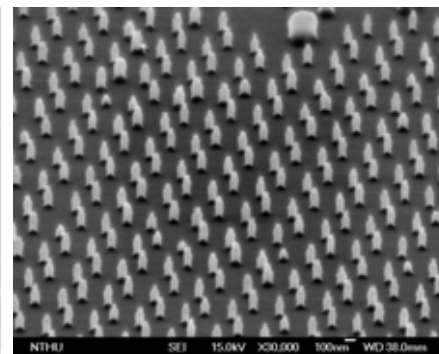
Au mask



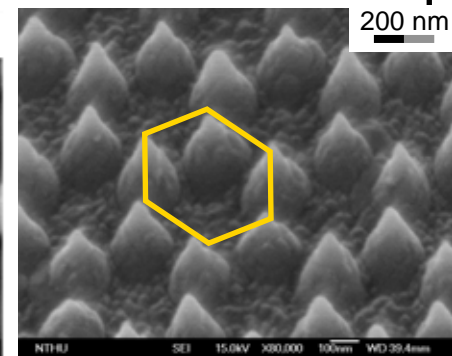
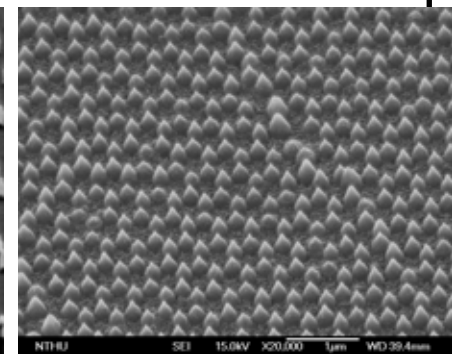
ϕ : 65 ~95 nm



H: 110 nm
 ϕ : 78 nm



H: 190 nm
 ϕ : 50 \rightarrow 150 nm

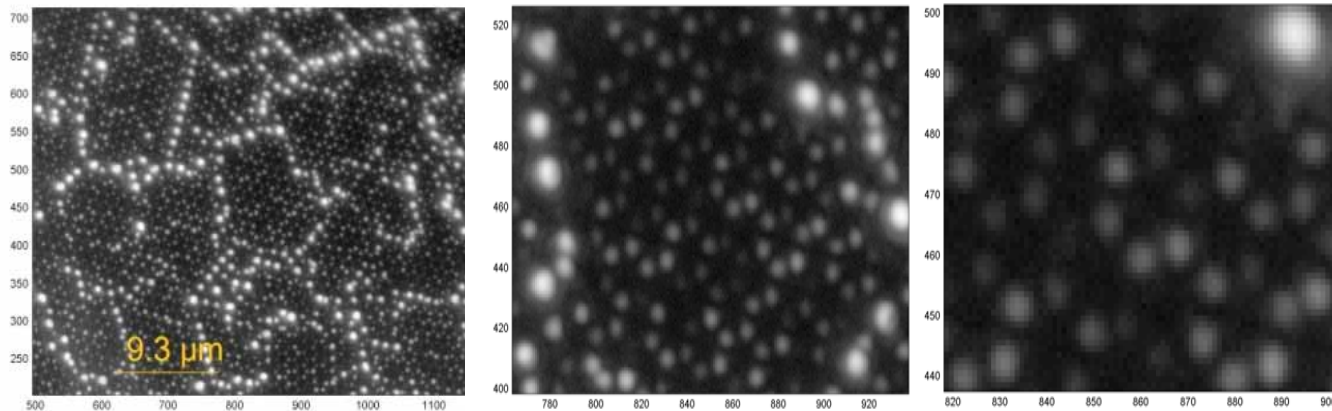


H: 200 nm
 ϕ : 25 \rightarrow 225 nm

FG Tseng, in preparation for submission



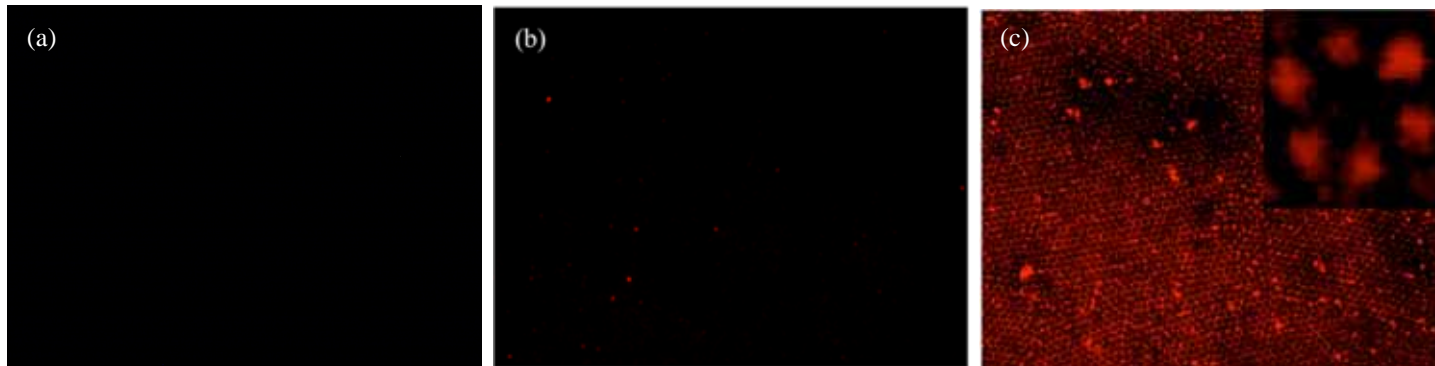
奈米金球陣列影像分析



A. 暗場影像分析:

汞燈550 nm(奈米金球在此波段有最強散射光)波段入射，局域性放大的影像:

- a. 規則排列的六角形奈米金球
- b. 奈米金球的大小不一，較大的顆粒有較亮的影像
- c. 奈米金球分佈在70 nm到80 nm有最大分佈



B. 螢光影像 (a) 尚未接合螢光標定蛋白之奈米金球陣列；(b) 浸泡在螢光標定白溶液中之奈米金球陣列，此處奈米金球上未修飾16-MHA，因此並無觀測到螢光標定蛋白出現在奈米金球陣列表面；(c) 螢光標定蛋白接合於奈米金球陣列表面之觀



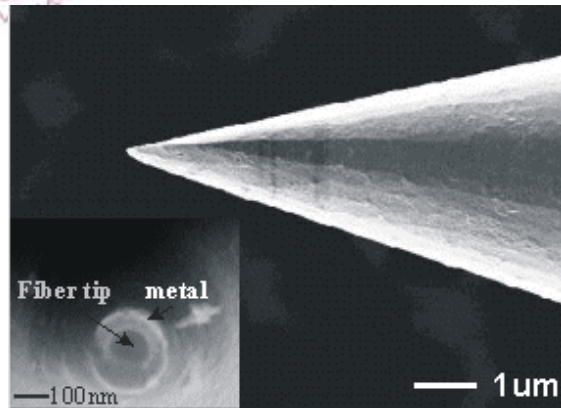
C. 奈米金屬結構之侷域性表面電漿共振應用於次波長之光捕捉

曾繁根 魏培坤



2. Near field Detection (Prof. Wei)

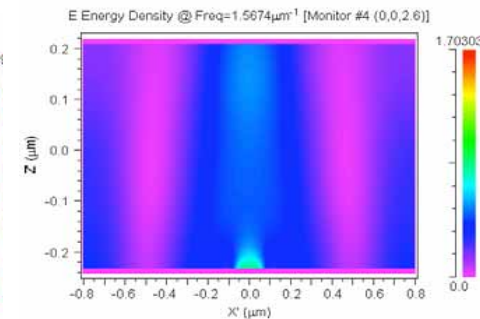
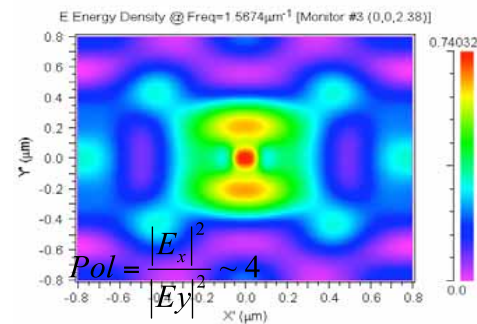
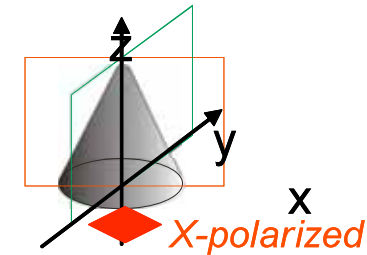
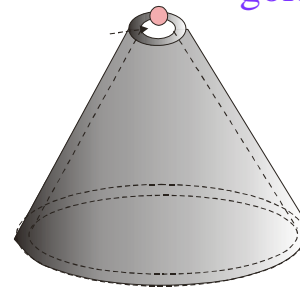
Enhance near-field properties:
gold nanoparticle on a nanocone



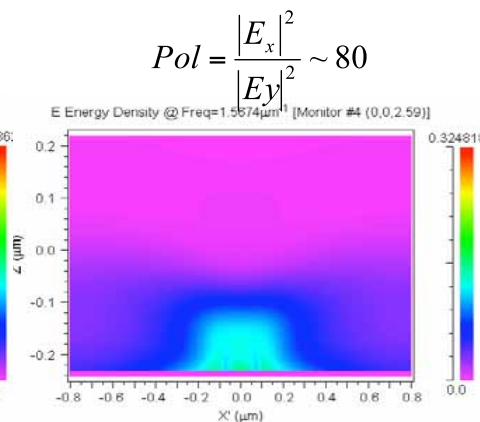
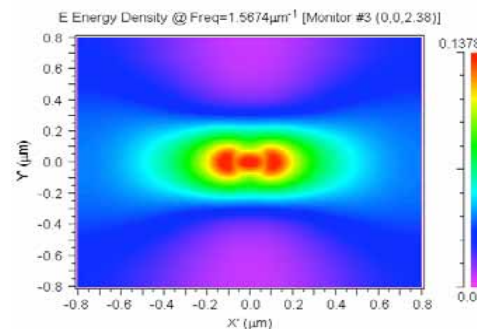
(a) The SEM image at the probe tip.



(b) Optical image of a tapered fiber probe.



with NP on cone tip



FDTD simulations of nanocone and nanocone-nanoparticle structure

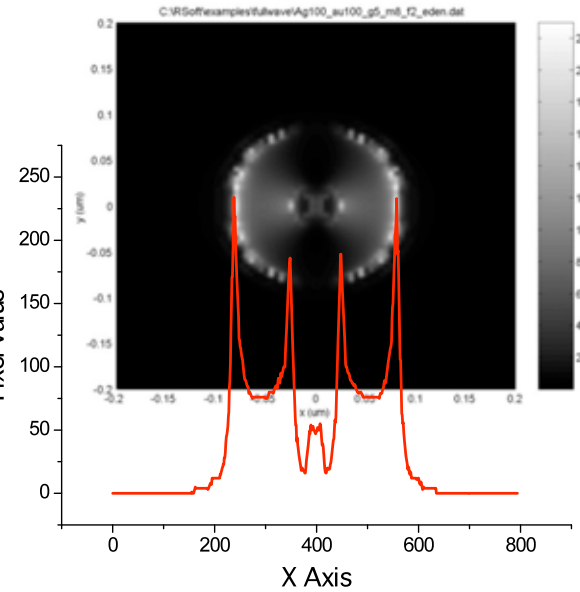
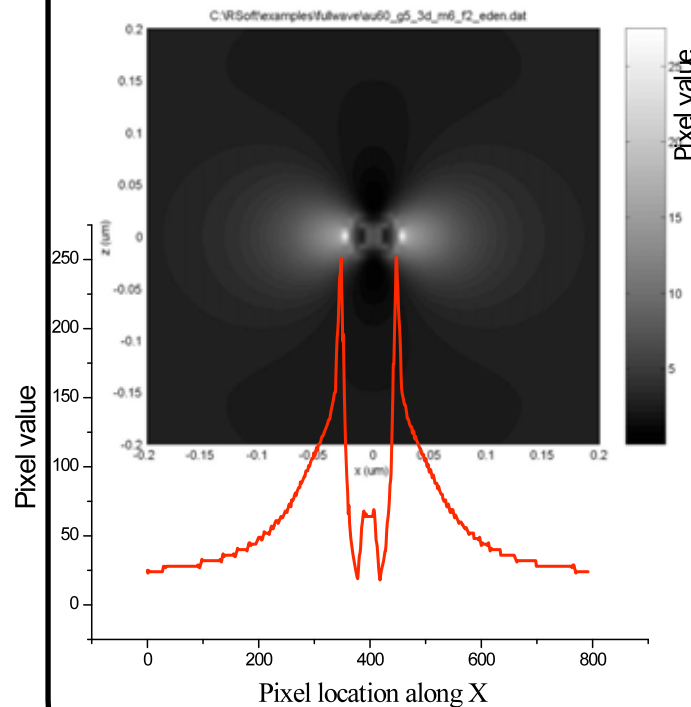


Electrical Field Simulation of GNPs Trap in Ag Nano Hole

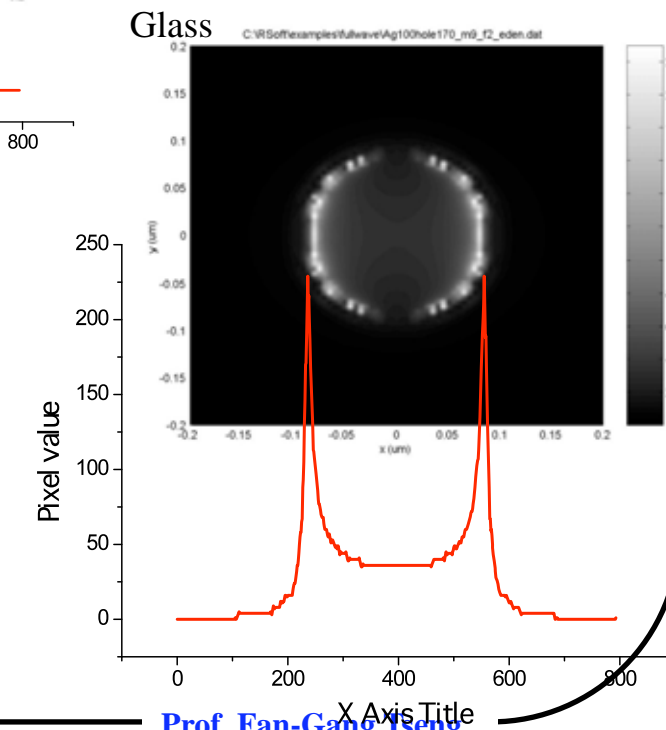
Silver hold with gold nanoparticle



Single gold nanoparticle



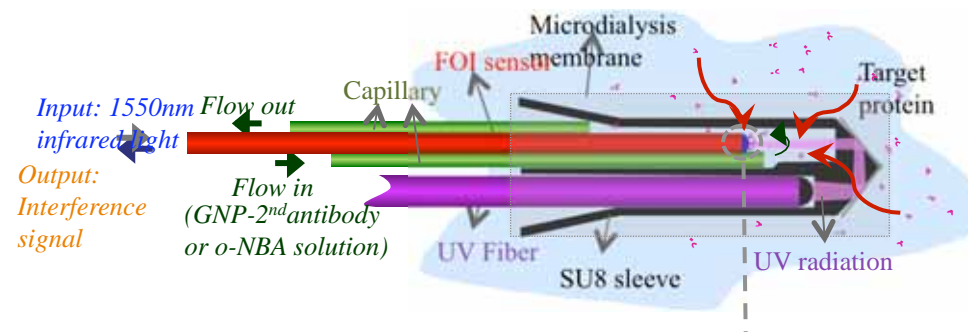
Silver hole





D.奈米金球增強訊號之 連續式光纖免疫感測器

曾繁根 楊重熙



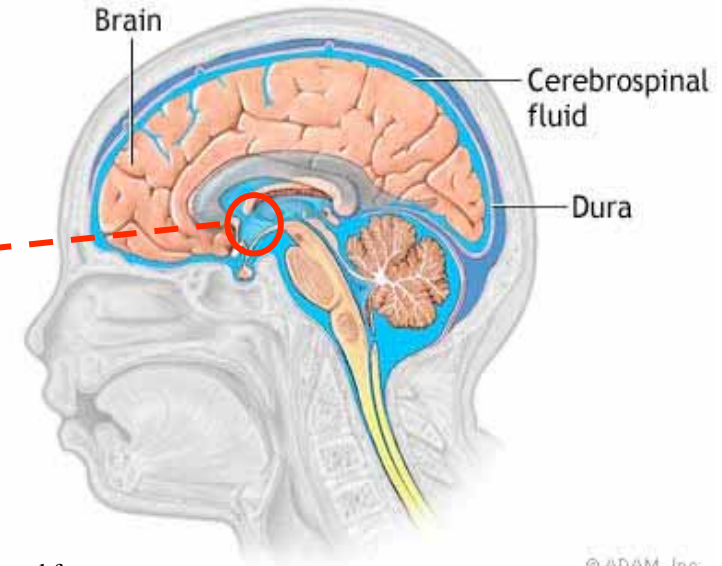


Introduction

Continuous Protein In-Vivo In-Situ Detection

- Proteins in cerebrospinal fluid can facilitate cell signaling or coordinate biological functions, such as *cytokines*, *chemokines*, and *neurotransmitters*, etc..

Hypothalamus
(Inflammation can stimulate the increase of $\text{TNF-}\alpha$)



Originated from:
<http://health.nytimes.com/health/guides/disease/csf-leak/overview.html>

© ADAM, Inc.

- Challenges for dynamic detection of these proteins:

(1) Low concentrations
(10pg/ml~100ng/ml)

⇒ High sensitivity

(2) Concentration variation
(several tens minutes)

⇒ Real time response

(3) In-situ, in-vivo detection
(in 10~100mm³ constrained space)

⇒ Needle type

Biosensor

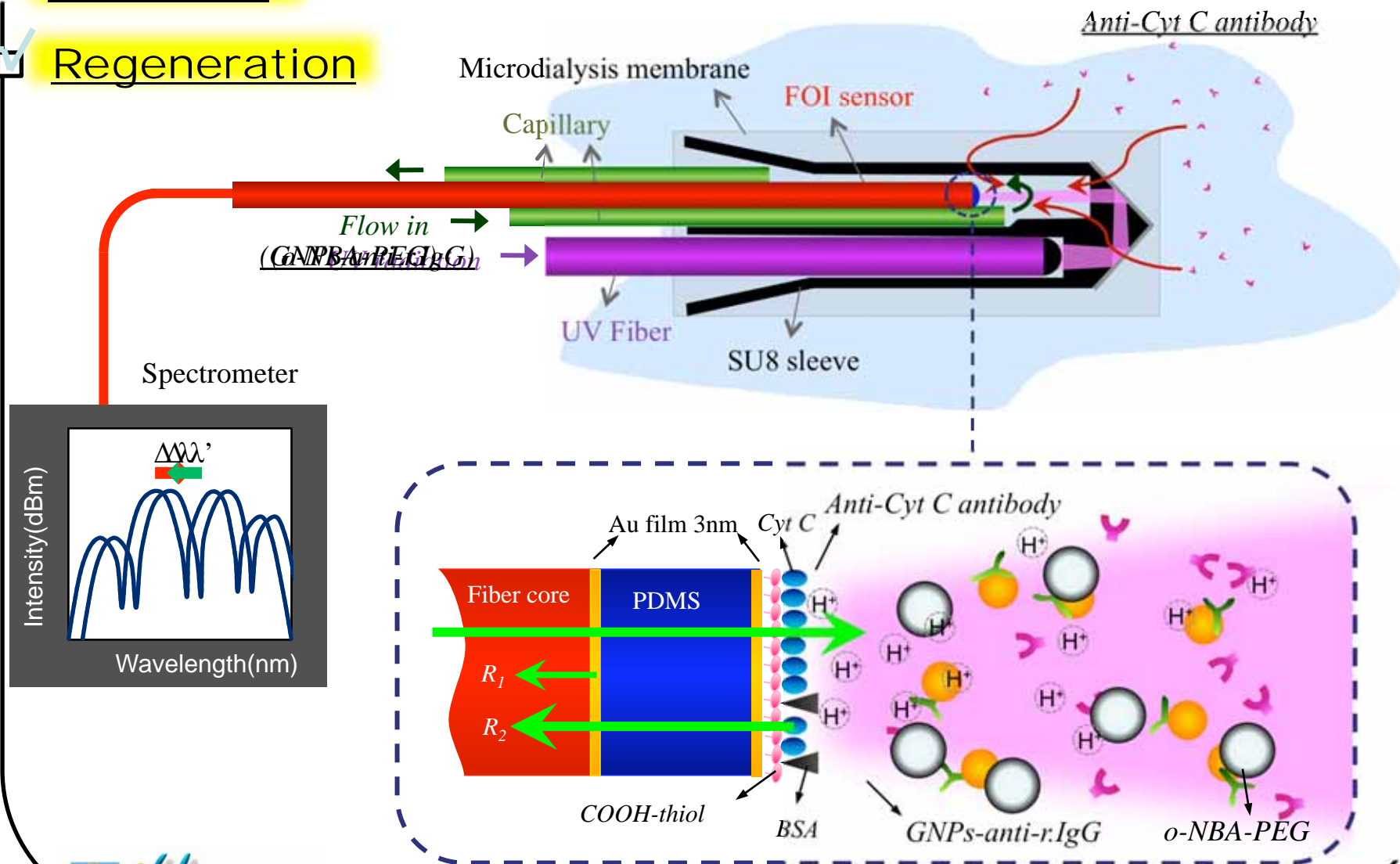


Design and Operation

Perfusion-based Micro Opto-Fluidic System (PMOFS)

☑ Detection

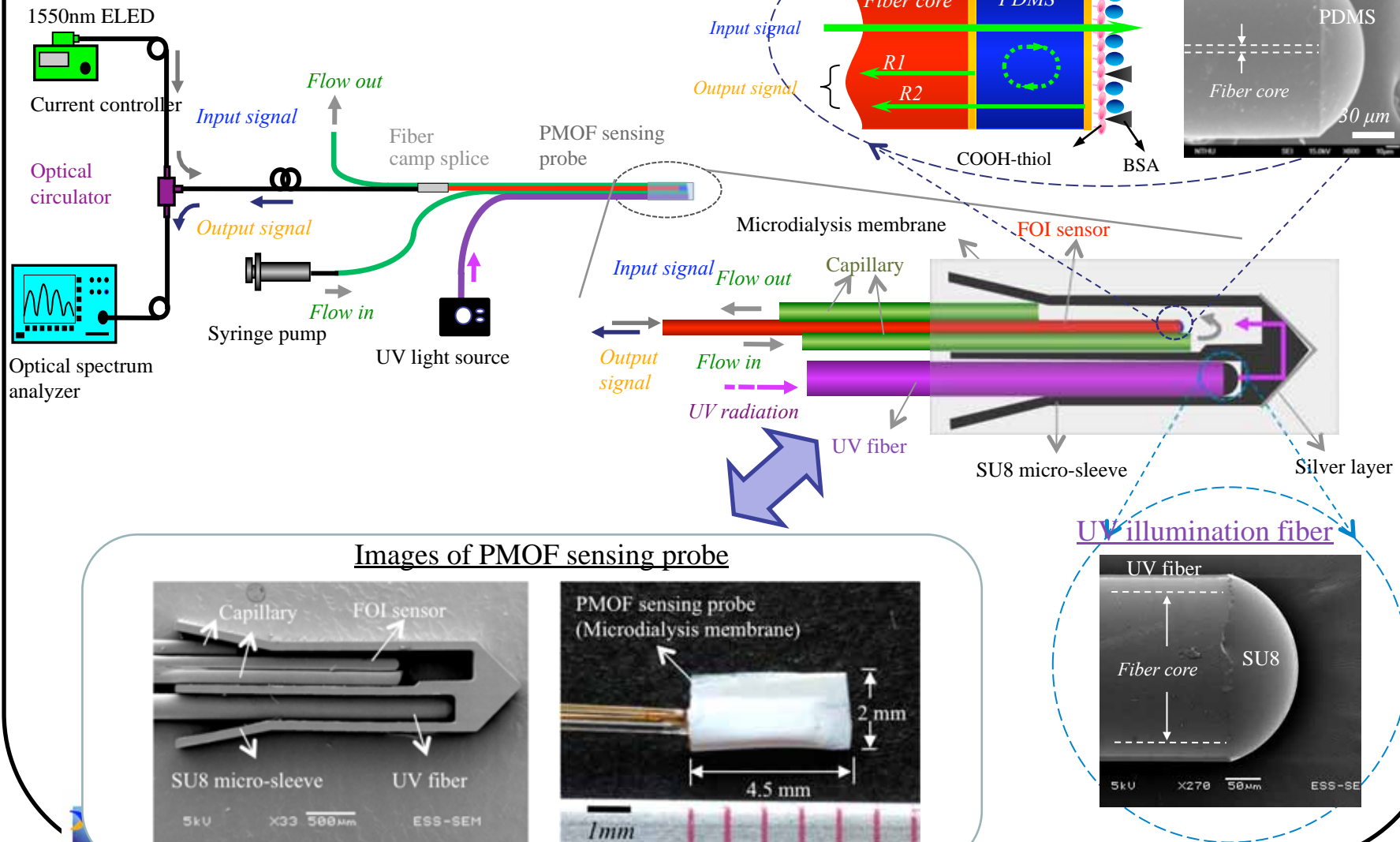
☑ Regeneration





Experimental Setup and fabrication

• Perfusion-based Micro Opto-Fluidic System (PMOFS)



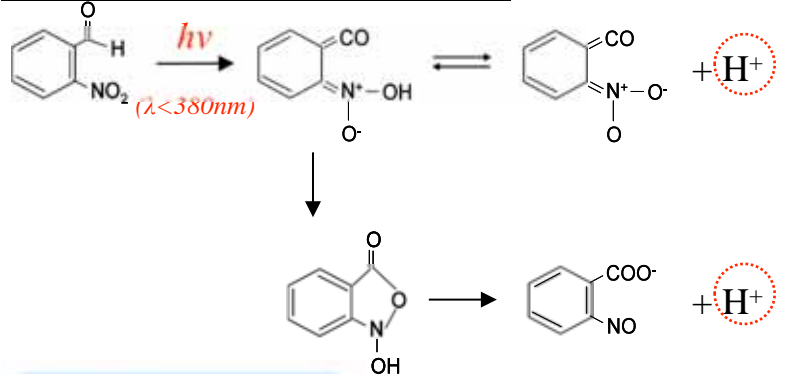


o-NBA elution method

Preparation of o-NBA Solution:

0.1g o-NBA powder mixed with 1ml poly(ethylene glycol) diacrylate (PEG), then diluted in 10^{-4} M PBS

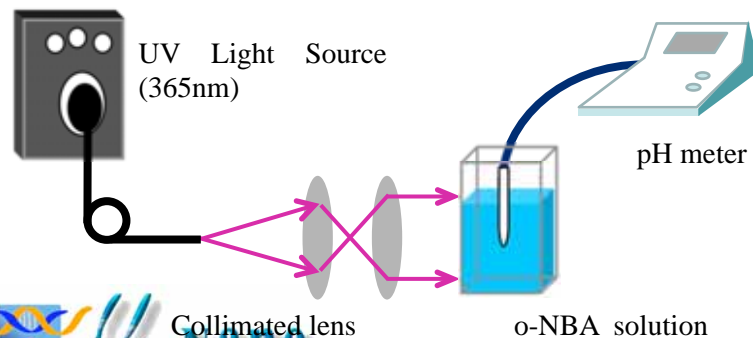
Photochemical reaction of o-NBA



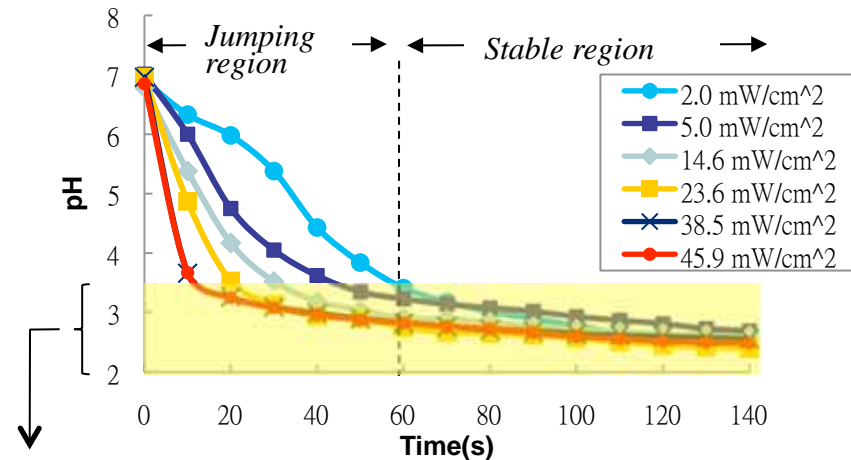
Quantum yield ~ 0.5
pKa ~ 2.1

Producing large amount of protons rapidly

Experimental setup to monitor pH variation

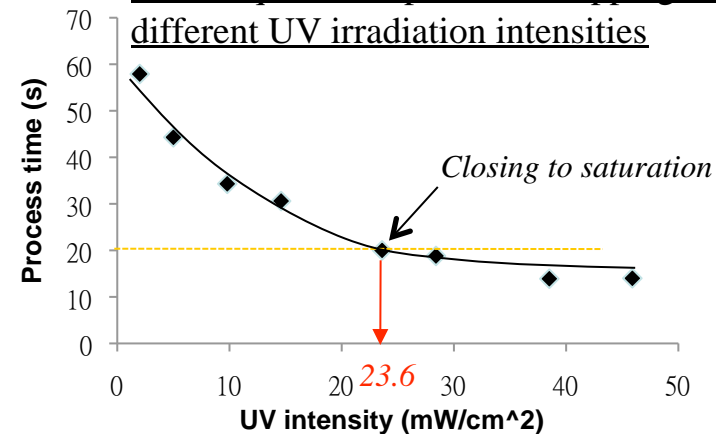


Dynamic decreases in the pH level as a consequence of the o-NBA irradiated by different intensities of UV light



Conventional pH level for elution ranges: 2.0 ~ 3.5

Time required for pH level dropping to 3.5 at different UV irradiation intensities

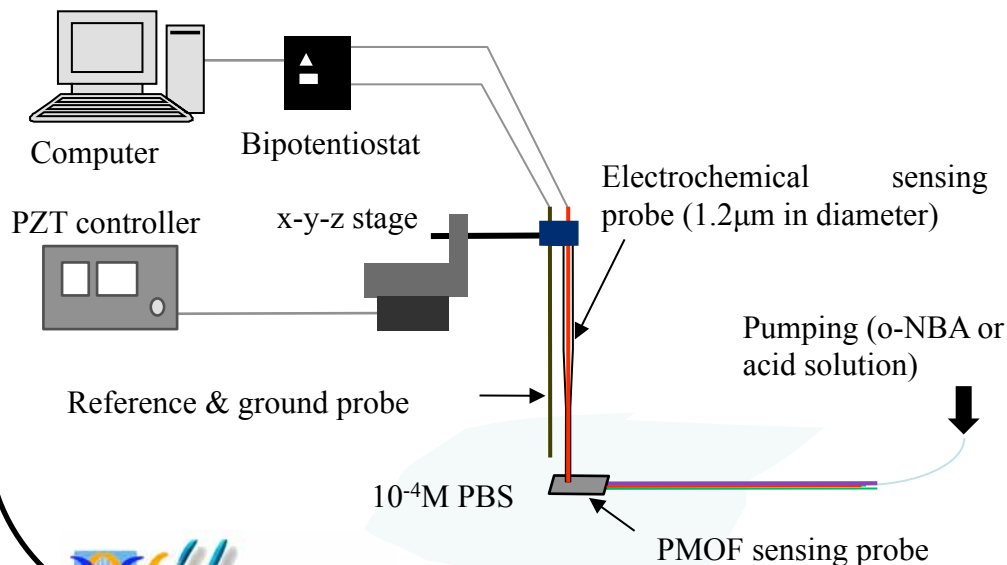




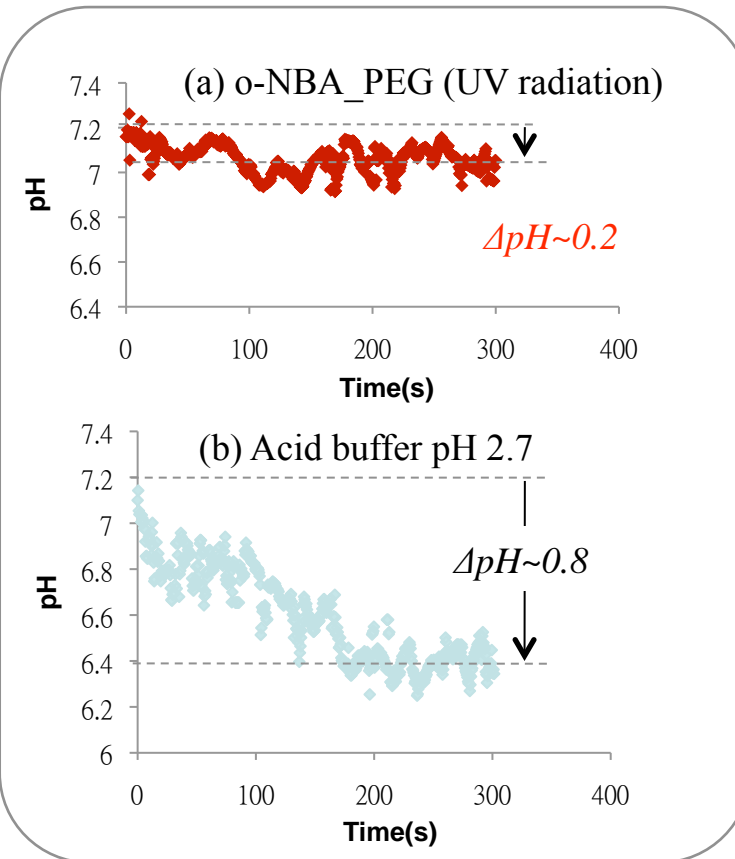
Local pH measurement

- Verify the extent of proton leakage by **measuring the pH of the 10^{-4} M PBS solution outside of the sensing probe.** (1.5 mm away from the tip of the FOI sensor)
- Comparison of local pH variation for:
 - (a) o-NBA elution method
 - (b) conventional acid elution method (steady flow of pH 2.7 acid buffer at 1 μ L/min)

Experimental setup to local pH monitoring



Results of real time pH variation

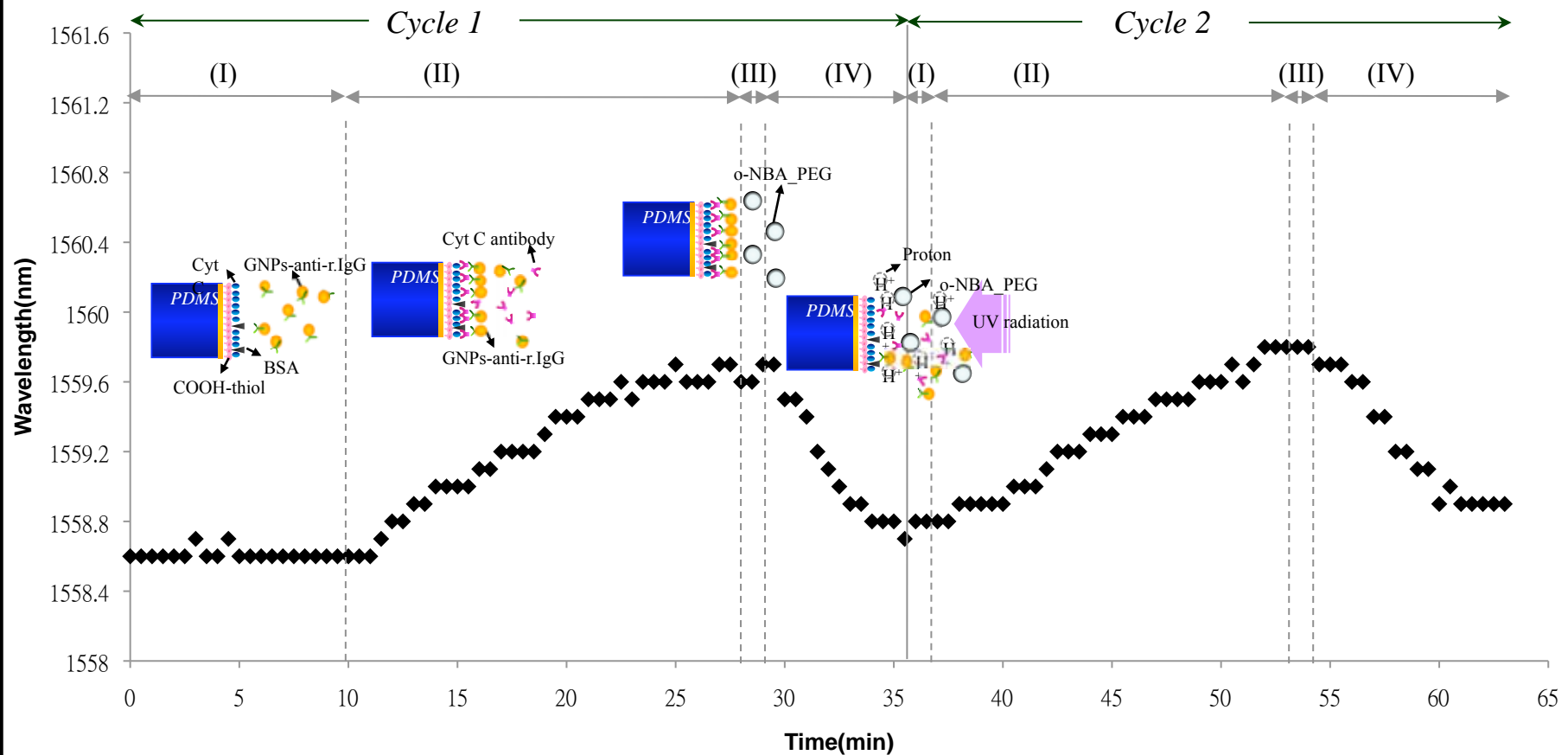


Self-contained o-NBA scheme almost no influence of pH level variation to the environment.



Results of continuous measurement (I)

- Repeated real-time immune detections for 1 $\mu\text{g/ml}$ anti-cyt C with surface regeneration process

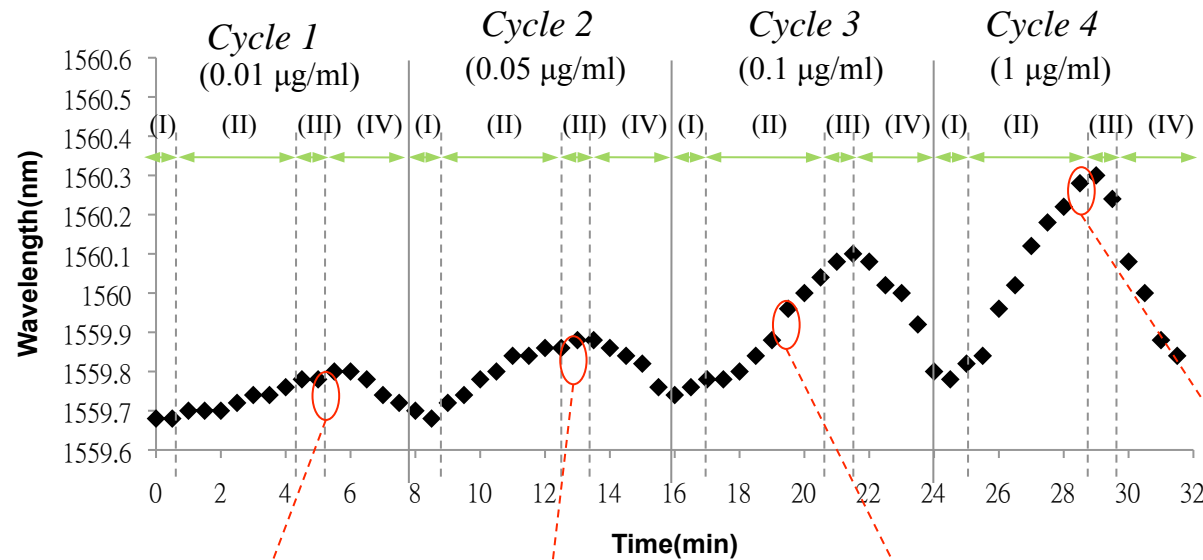


The shifts in the interference fringes for both cycles are very similar, except that the baseline slightly increases because of imperfect elution.

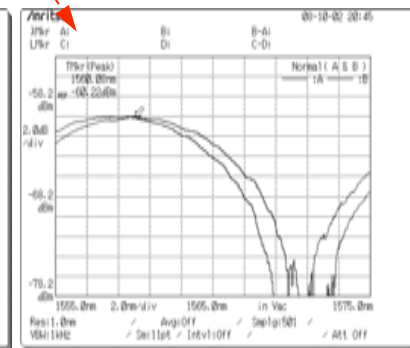
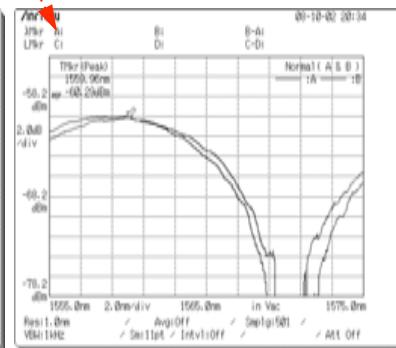
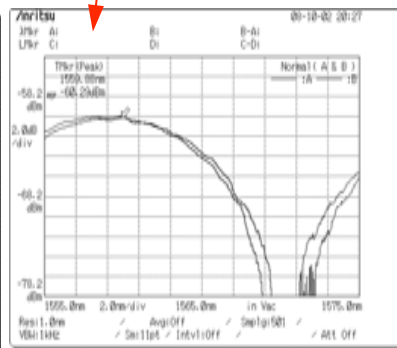
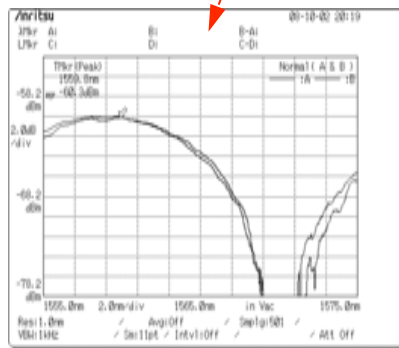
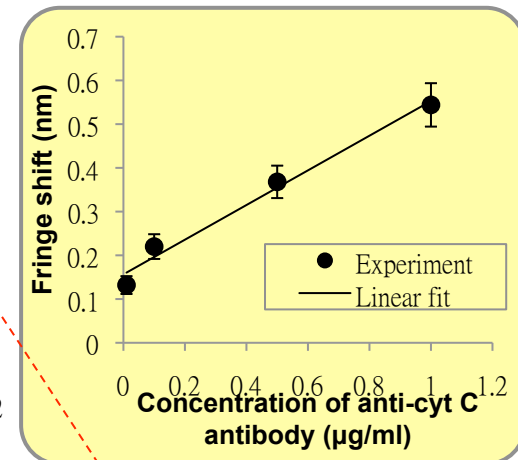


Results of continuous measurement (II)

- Sequential detection for anti-cyt C antibody solutions of different concentrations (0.01, 0.1, 0.5, and 1 $\mu\text{g/ml}$)



Relationship between fringe shift and anti-cyt C antibody of different concentrations



Y.T. Tseng and FG Tseng et al., *Lab on a Chip*, 2009

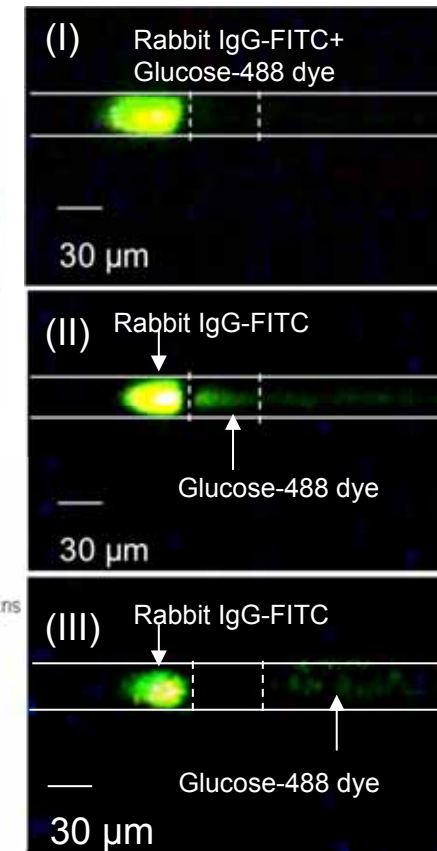
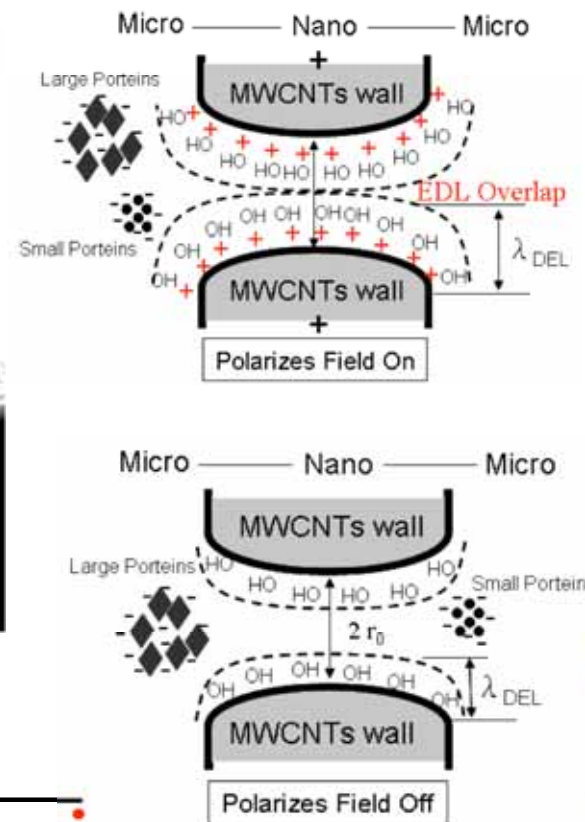
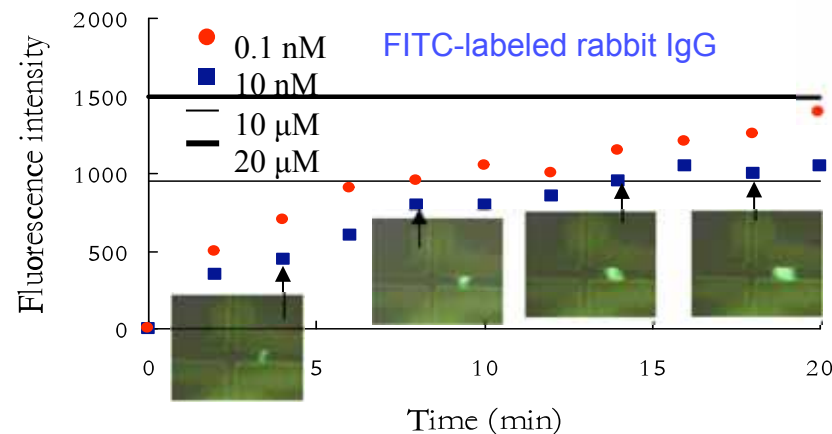
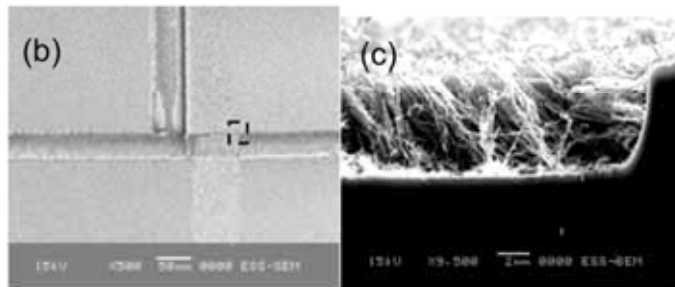
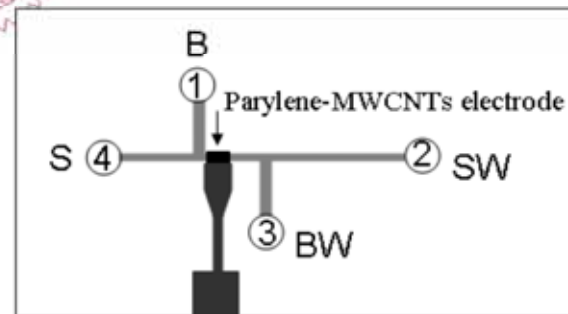


F. 利用奈米碳管與奈米流體技術 濃縮蛋白質

曾繁根 潘榮隆



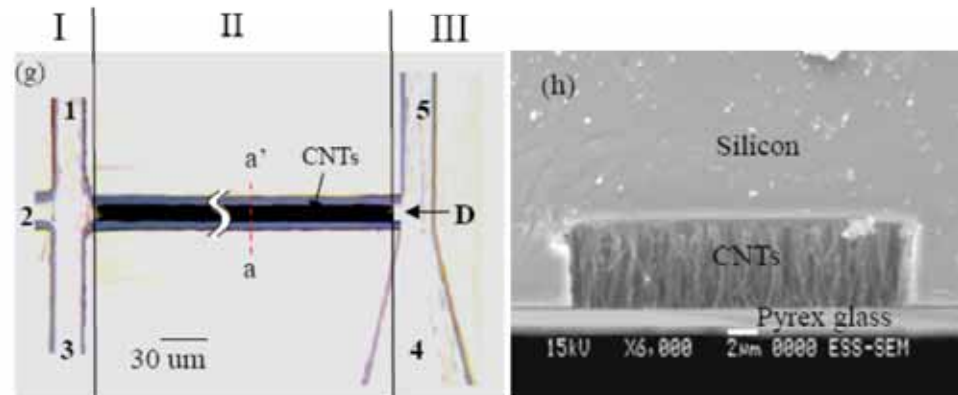
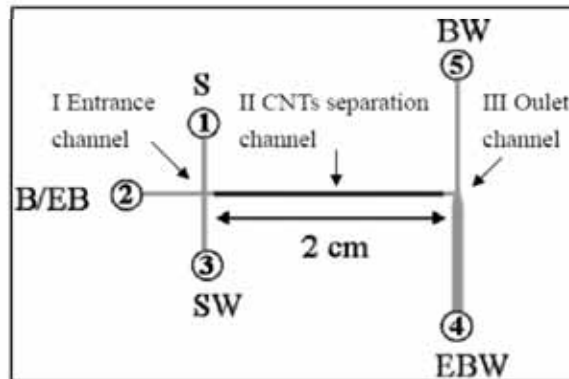
A. Electrostatic Sieving Control for Biomolecular Preconcentration



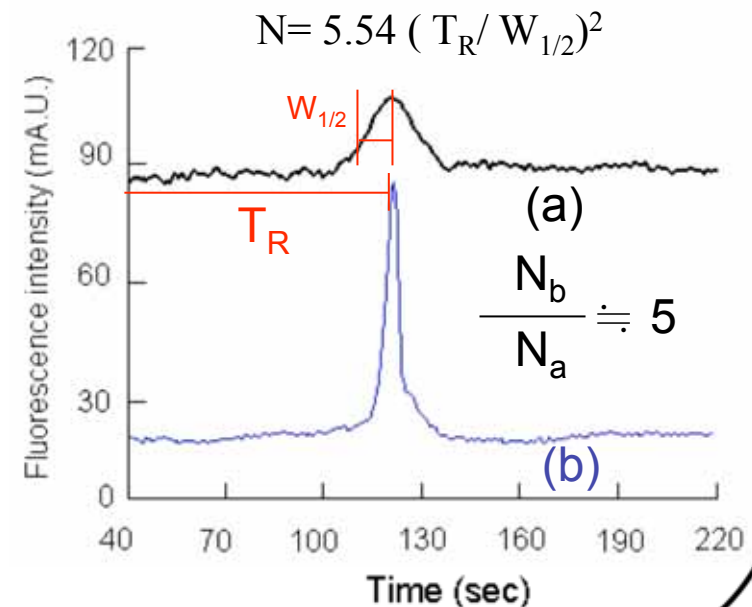
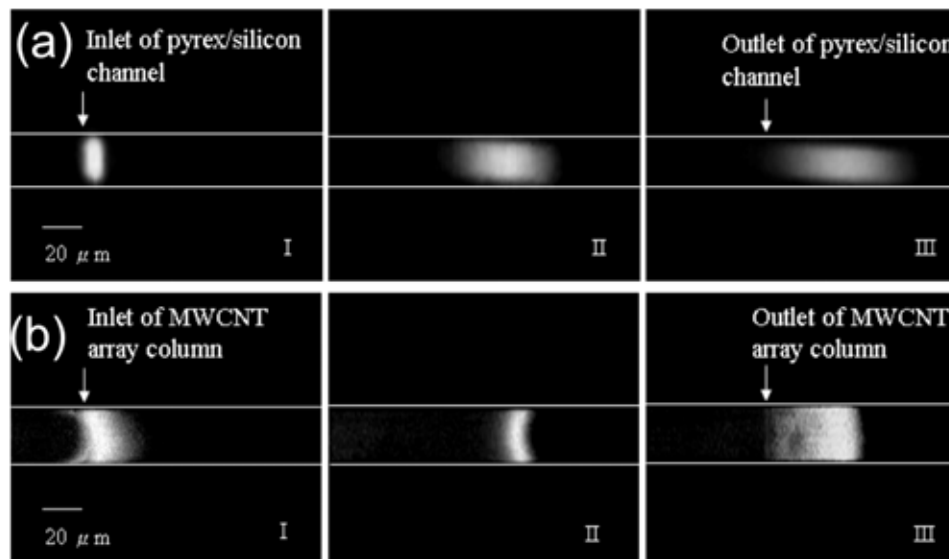
The chip design and electro-preconcentration mechanism of induced charge-selective nanochannel of MWCNTs pillars. Parylene-MWCNTs array electrodes were applied a critical voltage for anode is 30V, for cathode is 15V. (I) Polarizes Field On, (II-III) Polarizes Field Off. SEM image of (a) Top view of the electro-preconcentration channel, (b) Side view of the parylene-MWCNTS growth in microchannel



B. Nanostructured Pillars as a Stationary Phase in Microcapillary Electrochromatography (μ CEC)



Photographic top view of the μ CEC chip (dark area in the central channel consisting of MWCNTs array, 1: sample reservoir, 2: eluent buffer/running buffer reservoir, 3: sample waste, 4: eluent buffer waste, 5: running buffer waste, D: detector), (h) the SEM image of a cross section (a-a' plane) of the μ CEC channel.

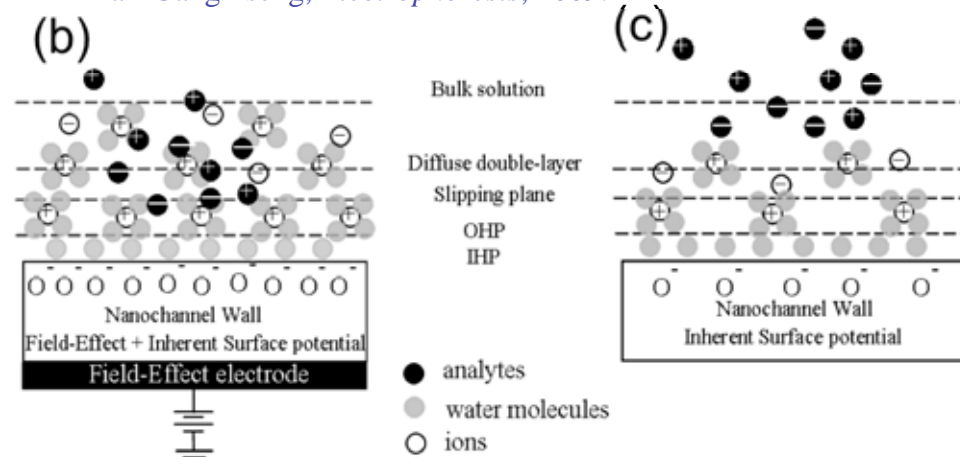
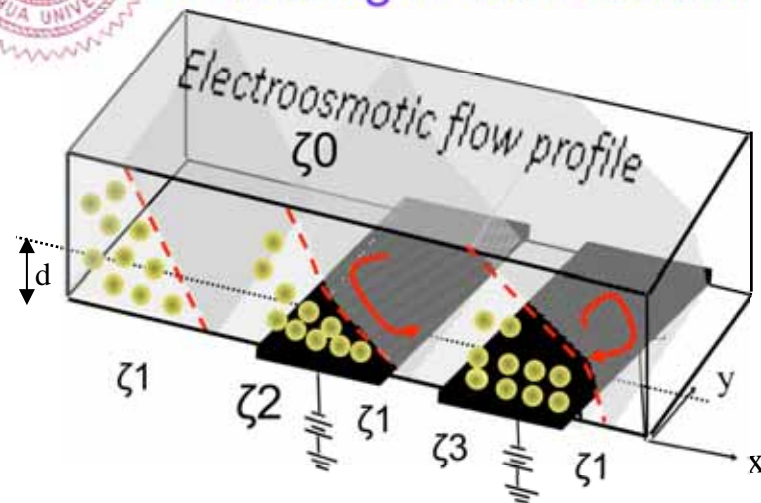


MWCNTs column - μ CEC for Rhodamine B band dispersion reduced



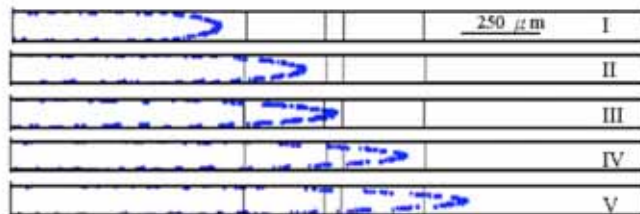
C. Dual-Asymmetry Electrokinetic Flow Focusing in NanoChannel

Fan-Gang Tseng, *Electrophoresis*, 2009.

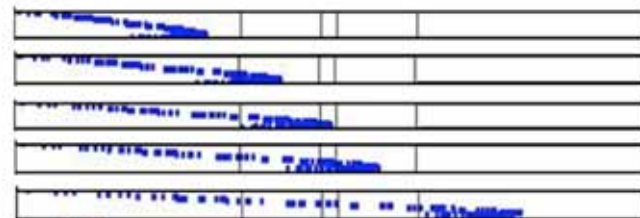


The schematics of (a) flow field evolution for **DAEF** in a capillary electrophoresis nanochannel (solid red arrows represent analyte flow direction, and $\zeta_2 > \zeta_1 > \zeta_3 > \zeta_0$), and the distribution of analytes in (b) the CE nanochannel with DAEKF, and in (c) the traditional CE nanochannel.

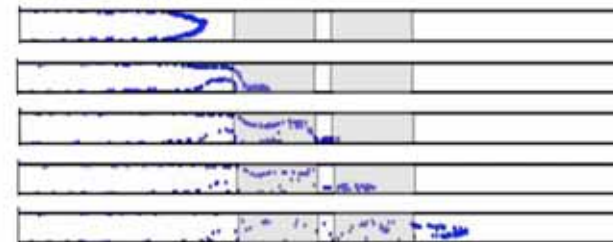
(a) Traditional EOF



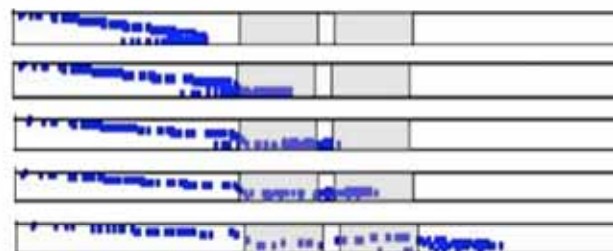
(b) Asymmetry EOF

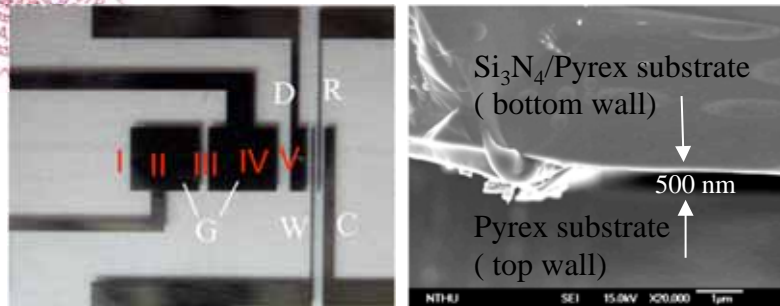


(c) Traditional EOF + Field-Effect control

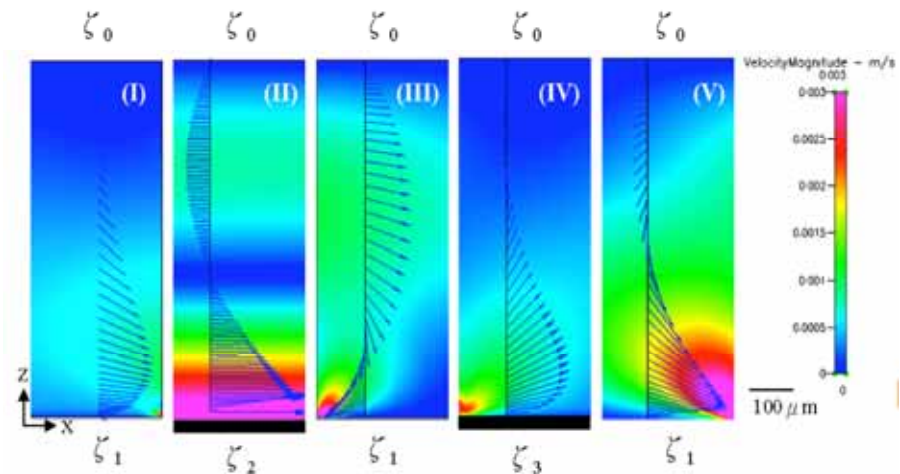


(d) Asymmetry EOF + Field-Effect control (or DAEKF)

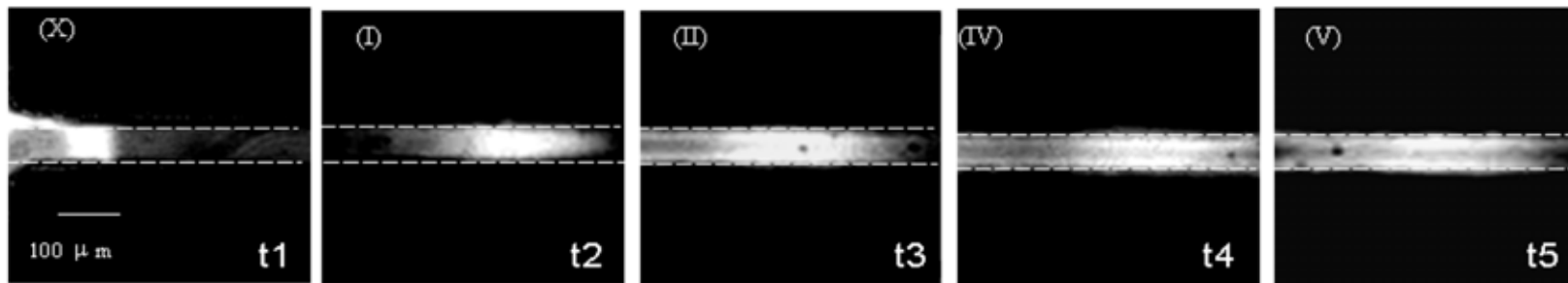




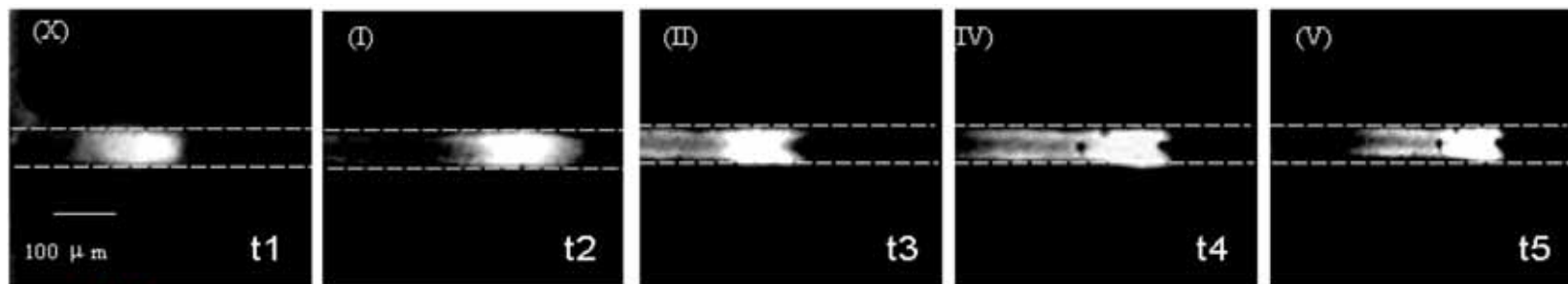
Detail flow fields of five different regions (a) are revealed in (b) for DAEKF system in nanochannel.



(a) traditional EOF pumping in a nanochannel



(b) restacking effect by the DAEKF system in a nanochannel





Summary

1. First **true** single molecule event based on **non-ambiguous** single molecule interaction
2. **High possibility** of single molecule event (**~100%**, depending on the yield of single molecule immobilization, large array)
3. **High efficient Statistics** of Single Molecule event -- enzyme kinetics and dynamics
4. **High dynamic range** for **at least 6** orders of magnitude, (**fM- μ M**, or $60-6 \times 10^8 / (100 \mu\text{m})^3$, nanofluidic molecule concentration + high density array $\sim 10^6 / (100 \mu\text{m})^2$)
5. **Very high signal/noise ratio** (atto-liter excitation $\sim (20-50 \text{nm})^3$ for $1 \mu\text{M}$, $\sim 0.1 \text{molecules} / (50 \text{nm})^3$)



Acknowledgements

- **The works were/are supported by National Science Council, Taiwan, through:**
 1. National Nanotechnology project, NSC
 2. Biomedical and Pharmaceutical National Project Program, NSC
 3. NSC Research Program
 4. 榮台聯大跨領域計劃

- **Collaborators:**

Prof. C. C. Chieng(錢景常), ESS Dept., NTHU

Prof. P. K. Wei(魏培坤), Applied Science, Academia Sinica

Prof. C. C. Yang(楊重熙), Director/Nanomedicine Center, NHRI

Prof. M. J. Lin(林茂榮), NYMU

Prof. R. L. Pan(潘榮隆), H. M. Huang(黃海美), Life Science Dept., NTHU